ISSN 1173-5996

A COMPARISON OF DATA REDUCTION TECHNIQUES FOR ZONE MODEL VALIDATION

BY

Simon Weaver

Supervised by
Dr C M Fleischmann

Fire Engineering Research Report 00/12

March 2000

This report was presented as a project report
as part of the M.E. (Fire) degree at the University of Canterbury

School of Engineering
University of Canterbury
Private Bag 4800
Christchurch, New Zealand

Phone 643 364-2250
Fax 643 364-2758

Abstract

To validate zone models from experimental data, the experimental data needs to be reduced to a form which is compatible with the zone model. Two parameters in zone modelling which experimental data needs to be reduced to before comparison, are interface height and the upper and lower zone temperatures.

Fire experiments of three different fire sizes were housed in a full sized double room enclosure. Thermocouple trees were located in the corner and centreline of each compartment.

During the analysis of the experimental data three interface height prediction methods were used. A commonly used empirical method known as the N% method did not perform well in the fire compartment. The maximum slope method which estimates the interface height as the point where the temperature change is maximal over height, worked very well for the data reduction as did Quintiere's method, which used two integral identities to solve for the interface height. The interface height determination for these methods could be used successfully with temperature averaging techniques however would not be sufficient to validate the zone models interface height calculation. The interface height does not represent any physical occurrence, rather a layer of mixed gases appears in the room between the zones. To be compared conservatively to a zone model the height at the bottom of this interface layer should be used. To determine average temperatures the interface height directly in the middle of the interface layer would be best.

Six temperature averaging techniques were investigated. All predicted the lower zone temperature accurately. Quintiere's method was the most successful in accurately predicting the upper layer temperature, as it was not affected by thermocouple readings in the interface layer. Emmon's method ranged from slightly over predicting the upper zone

temperature to greatly over predicting it. Spatial averaging, Averaging based on the equation of state and Janssens and Trans method all slightly underestimated the upper layer temperature. These methods work more successfully if averaging takes place not from the boundary specified at the interface height but from the height above and below the interface layer.

Acknowledgments

I would like firstly to thank my research supervisor, Dr Charley Fleischmann. Without his guidance, foresight, and experiences this project would not have been possible.

A special thanks to Tony Parkes for proof reading this report.

All the people who helped set up the experimental apparatus at McLeans Island deserve praise including Christian Nelson, Jason Clements, Tony Parkes, Grant Dunlop, Ian Sheperd and anyone else I have forgot to name.

Thanks go to Andy Buchanan, the other lecturer in Fire Engineering for making the year interesting and exciting.

Thanks to Mum and Dad, for financially supporting my University studies and enabling me to stay here much longer than I thought possible.

Table of contents

List of Figures

List of Tables

List of Photos

Nomenclature

A	area (m^2)
c_p	heat capacity at constant pressure (J /kg K)
E	enthalpy transport rate (W)
EOS	equation of state
H	height above floor (m)
H_d	height from floor to top of doorway (m)
H_i	interface height (m)
H_n	neutral plane height
H_r	ceiling height (m)
L	number of measurements points in thermocouple tree
m	mass flow rate (kg/s)
M	mass of gases in compartment (kg)
N	number of percentage in N% rule
P	pressure (Pa)
R	gas constant (J/kg K)
s	area of vent (m^2)
T	temperature (°C)
T_{avl}	average temperature in lower layer (°C)
T_{avu}	average temperature in upper layer (°C)
T_k	temperature at first thermocouple directly below interface height (°C)
T_{k+1}	temperature of first thermocouple directly above interface height (°C)
T_{ref}	temperature at interface height (°C)
V	compartment volume (m^3)
v	volume variable
ρ	density (kg/m^3)

1 Introduction

1.1 Aim of Research

Use of zone models is well established within the fire engineering profession to predict fire growth and smoke movement [1]. Zone models are a mathematical extension of the visual observation in a compartment fire where a room is divided into a smoky upper layer and a clear lower layer. The models work by solving conservation equations for mass, energy and momentum at the plume, surrounding vents and upper and lower zones. These conservation equations allow for calculation of temperature, pressure, and species concentrations within each zone. Many studies have been previously done [2,3] looking at the validation of zone models using experimental data. However to validate a zone model the experimental data needs to be reduced to a form compatible with the model. This research examines various techniques for reducing experimental data so it can be used for zone model validation and will attempt to determine the best method.

To collect data for the analysis of the data reduction methods an extensive experimental program was completed at the University of Canterbury's McLeans's Island field site. A full-scale double compartment separated via a doorway was built as outlined in chapter 3. 7 Experiments were run with three different fire sizes. In 6 of these runs the fire was located in the centre of the room while in the last run it was located in the corner of the room.

Three methods were used to estimate the interface height and 5 methods were used to determine the average temperature in each of the layers in the room. An additional method for calculating the average upper layer temperature based on gas velocities in the door well was included to check on the validity of the other methods. Each method was also compared with the zone model "C-Fast".

2 Overview of zone modelling

2.1 Background

The zone model concept is derived from fluid dynamics and combustion chemistry of the fire plume. When a fire occurs in a compartment it induces a fire plume. This then rises to the ceiling where it is deflected creating a ceiling jet. The ceiling jet propagates to the vertical walls where it is deflected and moves downwards. This smoke is then re-entrained in the plume and is sent back to the ceiling jet. Through this process a stratified smoke layer is formed in the room giving rise to a smoke filled hot upper layer and a clear cold lower layer. Figure 2-1 shows a typical compartment fire exhibiting zonal behaviour.

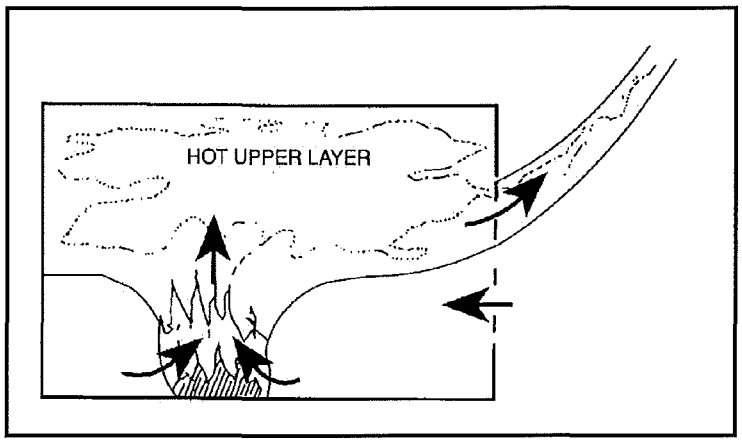

Figure 2-1 Compartment fire with visible upper and lower layers (Reproduced from Walton, 1995 [4])

The visual observation of two distinct layers with fairly uniform appearance within the compartment leads to the assumption that the density is uniform in both the upper and lower layer. The assumption is then made for zone models that temperature, pressure and species concentration are also uniform. In reality the temperature (and therefore pressure) of each layer is not constant and the zone model is at best an approximation to the real

fire situation. However, even though the temperature and pressure is not constant within each layer the differences are usually small compared to the difference between layers.

Zone models divide the room into a number of set volumes, which act as zones where the properties of temperature, density, and species concentration are constant. Usually in a zone model the room is divided into an upper and lower zone. In the room of fire origin additional zones representing the fire plume and ceiling jet are often included too [5]. Zone models work through the principles of conservation of mass, momentum, and energy applied to each zone. Differential equations for these factors then describe the underlying physics of the zone model, which allow the predictions of temperature, species concentrations and other parameters. Quintiere describes in detail these conservation equations [6].

When an object burns, a fire plume forms above it. Most zone models will consider this plume to be a separate zone within itself [5]. The zone model views the plume as the transportation mechanism for moving enthalpy and mass from the lower layer to the upper layer. The fire plume entrains and heats the surrounding cool air, which supplies oxygen to the burning process allowing the fuel to burn

Two fundamental processes exist causing flow out of vents in compartment fires which are taken into account by zone models. In the initial stages of a fire most of the air exits the vent via expansion. Air in the room is heated up and in doing so expands, pushing mainly cool air out of the compartment. When the upper layer descends past the top of the vent, hot gases will flow through the vent. After a brief period of fire growth the flow driven by buoyancy will far exceed the flow from expansion and become the primary transport mechanism for gases flowing out through the vent. The buoyant flow of gases out through the vent causes the pressure at the bottom of the room to fall below atmospheric pressure. Outside air is then drawn into the bottom of the compartment due to the pressure differentials.

2.2 Problems with zone model assumptions

The conservation equations used in zone models are based on the laws of physics and are not a source for error in zone model. However errors arise from the simplified assumptions that are used in constructing the model. Any large departure from these assumptions can radically effect the accuracy and validity of the zone model.

The following assumptions are used when applying the laws of conservation to each zone [6].

1. A distinctive upper and lower zone occurs in the enclosure with uniform density and temperature.
2. The volume of the fire plume is small compared to the gas layer and as such its effect is ignored.
3. The molecular weight of the gas and specific heat are constant. The gas is treated as an ideal gas.
4. Mass and heat transfer between the upper and lower zones is due to pressure differences between the zones and shear mixing effects, which are usually caused by convection and entrainment.
5. Horizontal and vertical transport times of gases in the plume reaching the ceiling are ignored.
6. The contribution to heat capacity from the contents of a room is ignored. Only the heat capacity of the enclosure is taken into account.
7. The horizontal cross sectional area of the compartment is constant. This is achieved by the compartment being rectangular parallelepiped in shape.
8. The pressure in an enclosure is assumed uniform however hydrostatic variations account for pressure differences at the vents of the compartment.
9. Mass flow in the plume is caused by turbulent entrainment.
10. Fluid frictional effects at solid boundaries are ignored.

Various situations can arise whereby the integrity of the zonal assumptions can break down. For example a zone model assumes that the compartment is rectangular in shape. If this is not the case and a horizontal cross sectional area is not maintained then it will be difficult to maintain a steady interface height and the distinction between upper and lower layers will be blurred.

The assumption that the volume of the fire plume is small compared to the volume of the hot gas layer can be unmerited in the case of an ultra fast fire occurring in a relatively small enclosure. In this situation the effects of the plume will cause extra strong buoyant forces leading to rapid turbulent flow in the compartment resulting in the layers in the room being well mixed. Wall fires have difficulty being modelled as two zones as the entrainment of hot gases in the plume is effectively halved (or quartered if the fire is put in the corner). Therefore the fire size is much taller in the room as it searches for more oxygen to burn.

2.3 Mixing between the two layers

Mass and heat transfer in a compartment fire is primarily due to the buoyant effects of the fire plume. A secondary transportation effect can arise through expansion of gases. These processes cause some degree of mixing which can be significant in some parts of the fire compartment such as very near the plume or vent. Other processes can also cause mixing in a compartment and reduce the overall stratification between the upper and lower layer thus breaking down the zone model. These are described in the following paragraphs. Figure 2-2 outlines the secondary flows in a compartment which induce mixing effects.

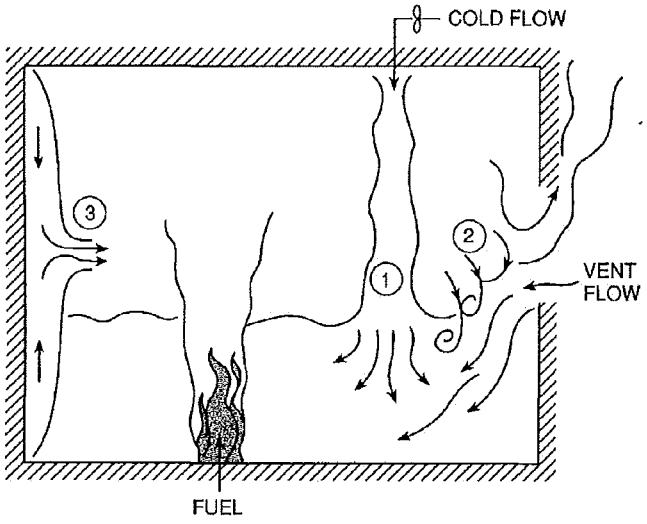

Figure 2-2 Secondary flows - mixing phenomena. 1. A cold plume descending from the upper layer into the lower layer. 2. Shear mixing of an entering vent flow stream. 3. Wall flows due to local buoyancy effects. (Reproduced from Quintiere, 1995 [6])

The inverse of a buoyant hot plume entering the upper layer can occur when a cold plume descends from the upper layer and penetrates the lower layer. Mixing occurs when the descending cold gas in the upper layer is not quite cool enough to penetrate into the lower layer. This is comparable to a hot plume, which is not quite buoyant enough to penetrate into the upper layer.

Hydrostatic pressure difference at ventilation boundaries can cause shear-mixing effects. This creates eddies in the mixed area between the upper and lower layers in the compartment. Although little research has been done in this area, McCaffrey and Quintiere [5] suggest that the flow rate of the mixed stream is proportional to the vent flow rate.

The temperature of the walls in a compartment is different than the gas temperature. This tends to heat up cool air exposed to the walls near the bottom of the compartment causing it to rise and cool down hot air at the top of the compartment causing it to fall. These two streams flowing in opposite directions can cause a horizontal flow when they meet in the centre of the compartment as shown in figure 2-2.

Mixing may also be present due to uneven combustion in the room and heating and cooling due to the plume and localised heating.

2.4 C-Fast

C-Fast is one of the worlds most widely used zone models that can predict the distribution of smoke and heat in a building during a fire [5]. It also allows predictions for multi-enclosure, multi-level buildings.

C-Fast uses an empirical correlation to determine the amount of mass and enthalpy moved between the layers by the plume. It starts the simulation with effectively a non-existent upper layer, which then gets larger as more mass and heat are pumped into the upper layer. This expansion of the upper layer causes a coinciding reduction in volume of the lower layer and the interface height or boundary between the two layers moves downwards. In the early stages of the fire the flow through the vent is all due to expansion until the interface height reaches the soffit height and C-fast establishes the door plume.

C-Fast takes account for the thermal properties of up to three layers of materials. It assumes the thermal properties of these materials are constant throughout the experiment.

The validation of the computer model C-fast was examined using reduced data from the various employed methods. C-Fast outputs the interface height and average upper and lower temperatures for a compartment fire and these are used to establish how long an enclosure is tenable. A check needs to be made to ensure that the conditions specified by C-Fast used to verify tenability conditions are conservative.

3 Methods of analysis

As zone models are only an approximation to reality it is necessary to process experimental data before it can be used for comparison and validation of a zone model. Data needs to be reduced to calculate the height in the room where the upper and lower zones meets. This "interface line" does not actually occur in reality and is most likely to be seen as an intermediate layer consisting of various degrees of mixed smoky and clear air. Once the interface height is determined the temperatures can be averaged for both the upper and lower layers. Many previous studies have used a mathematical average of the temperature readings above and below the interface line to determine the upper and lower zone temperatures respectively [2,3]. However Janssens and Trans, and He [7,8] have both pointed out that direct spatial averaging has no physically meaning when applied to a zone model. In this research 3 methods of calculating the interface height and 6 methods of calculating the zonal temperatures will be examined.

The data reduction methods will be judged on the accuracy of their fit to experimental data and how well they compare to visual observations. A further comparison can then be made between these reduced values and the results from the computer zone model C-fast.

3.1 Interface height

3 methods have been used in previous study's (7,8,11 and 12) to determine the interface height between the upper and lower layers in compartment fires. These are shown in the following sections

3.1.1 N% method

Cooper. [11] established the N% method for predicting the interface height in a compartment. This empirical rule determines the interface at the time as being the height where the temperature rising over the ambient temperature is equal to N% of the maximum rise at the time over the ambient temperature. This can be quantified as shown below.

Firstly a reference temperature is calculated from the upper layer temperature difference

$$\Delta T_{ref} = T_{max}(h_{top},t) - T_{\alpha}(h_{top}) \qquad \text{Equation 1}$$

where ΔT_{ref} = upper layer reference temperature

$T_{max}(h_{top},t)$ = maximum temperature at the maximum height in the time period between t = 0 and t =t.

$T_{\alpha}(h_{top})$ = ambient temperature at maximum height.

Then by the N% rule the temperature of the interface height is defined as

$$T(h_i,t) - T_{amb}(h_i) = N\Delta T_{ref}(t)/100 \qquad \text{Equation 2}$$

Where $T(h_i,t)$ = temperature at interface height, h_i

$T_{amb}(h_i)$ = temperature of interface height at ambient temperature

Cooper used values for N of 10, 15 and 20 for 25kW, 100kW and 225kW sized fires in various compartments. From experimental observations Cooper concluded that a N value of 10 provided the most accurate results. He [8] used 15 for the value of N for the data reduction. Both these studies involved single room compartment fires with vents (windows) to outside.

3.1.2 Maximum slope/inflection point method

The boundary between the top smoke layer and the bottom clear layer experiences sharp changes in density and as the governing mechanisms for heat transfer are similar (though not identical) to mass transfer, a similar steep change in temperature should result. This increase is assumed to be much greater than any temperature increase within each layer. By measuring the temperature at fairly regular intervals the interface height can be determined when the increase of temperature over the increase of height is maximised or when the graph of temperature versus height reaches an inflection point. Emmons [13] and Janssens and Tran [7] used the maximum slope method in their analyses of data reduction techniques. The predictive power of this method decreases when the uniformity of the layers decreases. However it is expected that the non-uniformity will never be as large as the difference between layers and should not be an issue.

3.1.3 Quintiere's method

Quintiere [12] used a method for determining interface height by solving two integral identities of the integration of temperature and the reciprocal of temperature over the volume of the compartment to estimate the interface height and lower layer temperature. This is described in the next section as the interface height calculation is inclusive of the zonal temperature calculations.

3.2 Data reduction methods for averaging temperatures

3.2.1 Mathematically/Spatially averaged temperature

The most common technique for averaging zonal temperatures is using a mathematical average. As shown in equation 3, this method gives a direct spatial average of the temperature over the total volume. This requires that the thermocouple readings inside the control volume are extrapolated to the floor and ceiling.

$$T_{av} = \frac{1}{V}\int_{V} T dv \qquad \text{Equation 3}$$

where V = total volume

For zonal averages this can be broken into an upper and lower zone as shown in equations 4 and 5. Assuming that the horizontal temperature gradient at any point in the control volume is constant and the interface height is constant, the temperatures can be integrated over the height of the compartment.

$$T_{avu} = \frac{\int_{H_i}^{H_r} T dy}{H_r - H_i} \qquad \text{Equation 4}$$

$$T_{avl} = \frac{\int_{0}^{H_i} T dy}{H_i} \qquad \text{Equation 5}$$

Where T_{avu} = average temperature of upper zone

T_{avl} = average temperature of lower zone

H_r = ceiling height

H_i = interface height

When integrating to obtain the temperature of the compartment over the volume for Spatial averaging it is assumed the temperature difference between thermocouples is linear. To obtain an average for the total compartment height of the room, the ceiling and floor temperatures were extrapolated from the top two and bottom two thermocouples respectively. Numerically the integrals needed for spatial averaging are expressed below.

$$\int_{H_i}^{H_r} T dy = \frac{1}{2}\left(\sum_{j=k+1}^{L} (T_{j+1} + T_j)(h_{j+1} - h_j) + (T_{k+1} + T_{ref})(h_{k+1} - H_i) \right) \qquad \text{Equation 6}$$

$$\int_{0}^{Hi} T dy = \frac{1}{2}\left(\sum_{j=0}^{k-1} (T_{j+1} + T_j)(h_{j+1} - h_j) + (T_k + T_{ref})(H_i - h_k) \right) \qquad \text{Equation 7}$$

Where T_j= temperature at point j, j= 0(floor),…,L+1(ceiling)

L = number of thermocouples in tree

T_k= temperature at the thermocouple which is right below the estimated interface height

T_{k+1}=temperature at the thermocouple which is right above the estimated interface height.

Janssens and Tran [7] pointed out that using a direct spatial average does not have any physical meaning as integrating temperature over the entire volume yields a physically meaningless quantity. He [8] further elaborated on this suggesting that if reducing experimental data to be compared with zone model it would be essential that the reduced parameters have the same meaning as the rest of the model. As mathematical models of thermal-fluid systems are based on fundamental laws of conservation and equations of state, all the parameters in a zone model would have physical meanings. Therefore it would be appropriate for the reduced temperatures to have real physical meaning too.

3.2.2 Average based on equation of state (EOS)

Although integrating temperature over total volume does not yield a physically meaningful quantity, integrating density over of the total volume does yield a physically meaningful quantity as shown in equation 8.

$$M = \int_V \rho dv \qquad \text{Equation 8}$$

Equation 8 combined with the equation of state (PV =RT) yields equation 9.

$$T_{av} = \frac{V}{\int_V \frac{1}{T} dv} \qquad \text{Equation 9}$$

This can be split into an upper and lower zone as shown in equations 10 and 11

$$T_{avu} = \frac{H_r - H_i}{\int_{H_i}^{H_r} \frac{1}{T} dy} \qquad \text{Equation 10}$$

$$T_{avu} = \frac{H_i}{\int_0^{H_i} \frac{1}{T} dy} \qquad \text{Equation 11}$$

He [8], using the N% method for determining the interface height compared temperatures calculated from Spatial averaging and Averaging based on the equation of state. It was found that for a rise of 100°C in the upper layer level a 5% difference in the temperature of the upper layer existed between the two methods. It was also found that the predicted lower layer temperature was almost identical for each method. This was expected, as the

lower zone temperatures in He's data were very uniform. If the temperature is uniform within a zone then equation 9 becomes the same as equation 3.

The integrals needed for Averaging based on the equation of state are expressed numerically below in equation 12 and 13. Like Spatial averaging it is assumed the temperature gradient between each thermocouple is linear.

$$\int_0^{H_i} \sum_{j=0}^{k-1} \frac{h_{j+1}-h_j}{T_{j+1}-T_j} \ln\left(1+\frac{T_{j+1}-T_j}{T_j}\right) + \frac{H_i-h_k}{T_{ref}-T_k} \ln\left(1+\frac{T_{ref}-T_k}{T_k}\right) \qquad \text{Equation 12}$$

$$\int_0^{H_i} \sum_{j=0}^{k-1} \frac{h_{j+1}-h_j}{T_{j+1}-T_j} \ln\left(1+\frac{T_{j+1}-T_j}{T_j}\right) + \frac{h_{k+1}-H_i}{T_{k+1}-T_j} \ln\left(1+\frac{T_{k+1}-T_{ref}}{T_{ref}}\right) \qquad \text{Equation 13}$$

3.2.3 Average based on Emmons' methods

Emmons [13] suggested the following method for determining the upper and lower zone temperatures. Emmons assumed that the lower zone temperature did not deviate significantly from the bottom thermocouple reading.

1. The method of maximum slope was used to determine the interface height
2. The bottom thermocouple reading was used for the value of the lower zone temperature, T_{avl}.
3. The upper zone temperature was calculated by the integral identity as shown in equation 14, which is a requirement for mass equivalency.

$$\int_0^{z_r} \frac{1}{T_r} \frac{1}{H} dH = \frac{H_r - H_i}{T_{avu}} + \frac{H_i}{T_{avl}}$$ Equation 14

3.2.4 Average based on Janssens and Tran's Method

Janssens and Tran [7] suggested the following method for determining the upper and lower zone temperatures.

1. The method of maximum slope was used to determine the interface height
2. The upper zone temperature, T_{avu} was estimated from a mathematical average of the upper layer thermocouples above the estimated interface height.
3. T_{avl} was calculated from equation 14.

Janssens and Tran found this method to yield 2-layer temperature profiles that fitted the measured profiles. They found that these techniques allowed estimations of vent flow rates that were within 10% of those measured.

3.2.5 Average based on Quintiere's method

Quintiere [12] suggested the following method for determining the upper and lower zone temperatures.

1. The upper layer temperature was calculated from an average of temperatures including points that did not deviate largely from the top thermocouple. For the analysis in this research a deviation of less than 10% from the top thermocouple reading was used as the criteria for including a temperature reading in the upper layer.

2. Equation 14 and equation 15 were solved simultaneously to compute the interface height and lower zone temperatures.

$$\int_0^{z_r} T_r \, H \, dH = (H_r - H_i) T_u + H_i T_l \qquad \text{Equation 15}$$

While equation 14 does have physical meaning and is a requirement for mass equivalency, equation 15 does not have any physical meaning, but retains the same mean temperature as the data.

3.2.6 Average based on transport terms

An alternative approach for determining the upper layer temperature in a fire room is by using the temperatures and velocities of the exhaust stream in the door exiting the room of fire origin. This method requires extensive instrumentation to measure the temperatures and velocities at numerous points in the door, This experimentation is specified in detail in the next chapter.

The total enthalpy of the exhaust flow can be defined as the sum of the average temperature of the exhaust flow multiplied by the specific heat at constant pressure and the mass flow. This is shown in equation 16.

$$c_p m T_{av} = E \qquad \text{Equation 16}$$

The total enthalpy exiting the system is equal to the thermal and kinetic energies of the exiting gas. As the kinetic energy component is relatively small we can ignore this component hence

$$E = c_p \int_A \rho u T ds$$ Equation 17

where s = the vertical cross sectional area of the of the vent (m^2)

u = gas velocity (m/s)

Using the ideal gas law PV = RT this can be changed to

$$E = c_p \frac{P}{R} \int_A u T ds$$ Equation 18

Using the ideal law again the mass flow can be described as

$$m = \int_A \rho u ds = \frac{P}{R} \int_A u ds$$ Equation 19

By substituting equations 18 and 19 into equation 16 the average temperature can be obtained using local velocities and temperatures in the door as shown in equation 20.

$$T_{av} = \frac{\int_A u ds}{\int_A \frac{u}{T} ds}$$ Equation 20

Unlike many of the other methods, which have used physically meaningless spatial averaging, equation 21 provides a physically meaningful average temperature of the gases exiting the room of fire origin. In a door well equation 20 becomes

$$T_{av} = \frac{\int_{H_n}^{H_d} u dy}{\int_{H_n}^{H_d} \frac{u}{T} dy}$$ Equation 21

where H_d = height at the top of the doorwell

H_n = neutral plane height

At the neutral plan height the pressure difference and velocity in the vent is equal to zero. He [8] used this method to validate upper layer averages for Averaging based on the equation of state. This method offers a suitable comparison, as it is not dependent on the interface height for its accuracy.

The Averaging based on transport terms also assumes a linear relationship between each bidirectional probe and temperature reading. The integrals needed for the averaging are shown in equation 22.

$$\int_{H_n}^{H_d} \frac{u}{T} dy = \frac{1}{2}\left(\sum_{j=m+1}^{d} \left(\frac{u_{j+1}}{T_{j+1}} + \frac{u_j}{T_j} \right)(h_{j+1} - h_j) + \left(\frac{u_{m+1}}{T_{m+1}} + \frac{u_n}{T_n} \right)(h_{m+1} - H_n) \right)$$ Equation 22

where T_{m+1} =temperature at point right above neutral plane height

4 Experimental set up

4.1 Overview of site

A full sized double compartment enclosure built to ISO-9705 standard [14] was constructed at the University of Canterbury's McLeans Island field site. The enclosure was constructed inside of a building to ensure stable ambient conditions during the experimental runs. A hood was built into the building to exhaust smoke from the fire experiments taking place within the double compartment enclosure. Figure 4-1 gives a schematic site plan of the McLeans Island Field site.

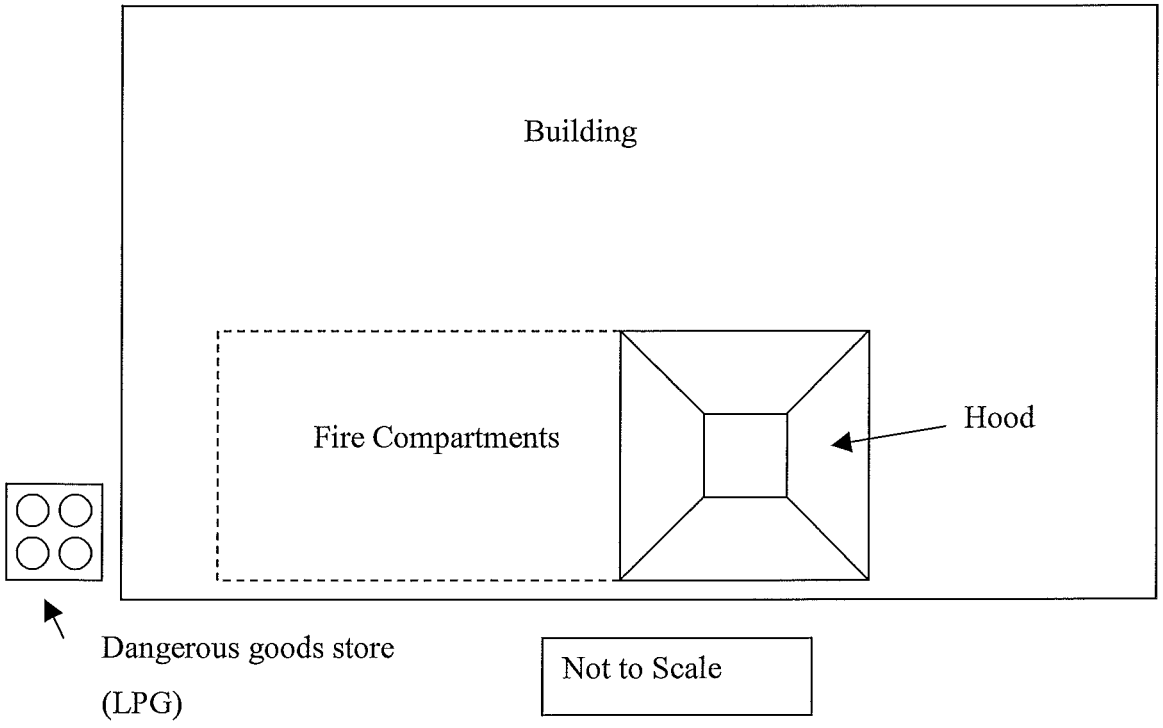

Figure 4-1 Schematic Site Plan

4.2 Fire rooms construction

The rooms' dimensions were in accordance with ISO 9705[14] standard full size room, which are 2.4 metres wide, by 2.4 metres higher and 3.6 metres long. A door area, 1.985 metres high and 0.76 metres wide separated the enclosure into two rooms. For the descriptive purposes of this report, the room where the fire was located will be known as the fire compartment and the other room shall be known as the adjacent compartment. The ISO dimensions of the fire compartment are shown in figures 4-1, 4-2 and 4-3 below. Figure 4-1 shows a vertical plan of the fire compartments, figure 4-2 shows a horizontal plan of the fire compartments and figure 4-3 shows a horizontal plan of the door area.

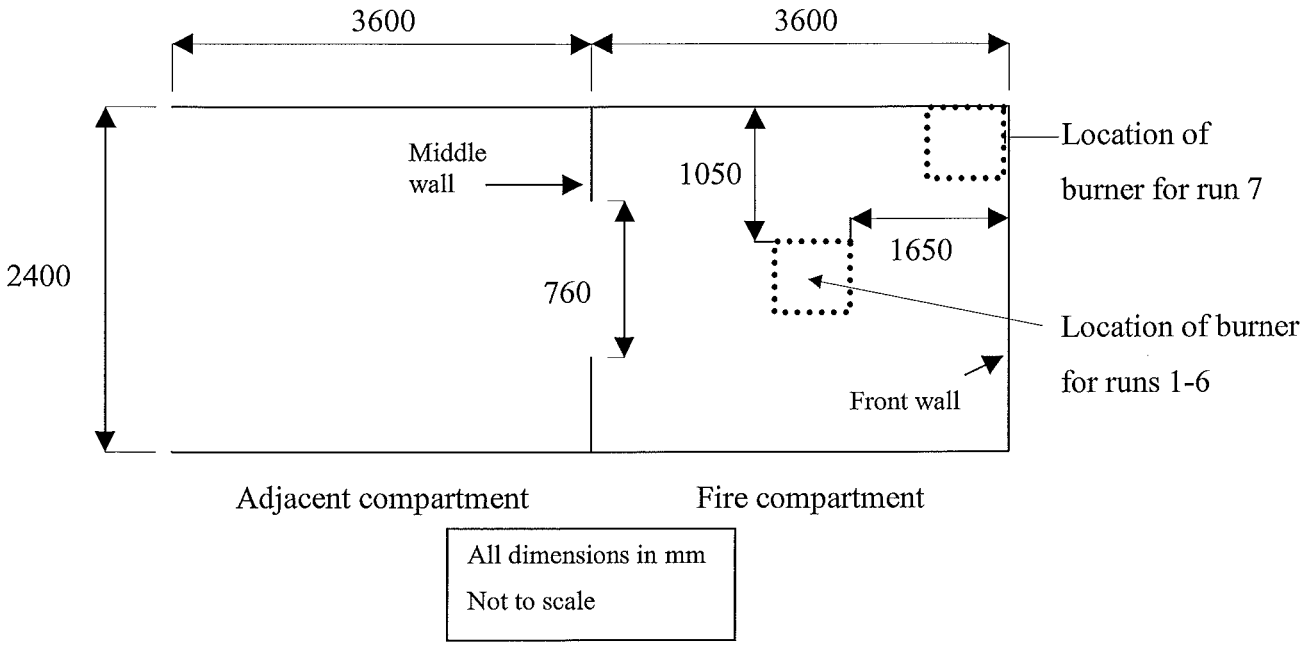

Figure 4-2 Dimensions of compartment in vertical plan

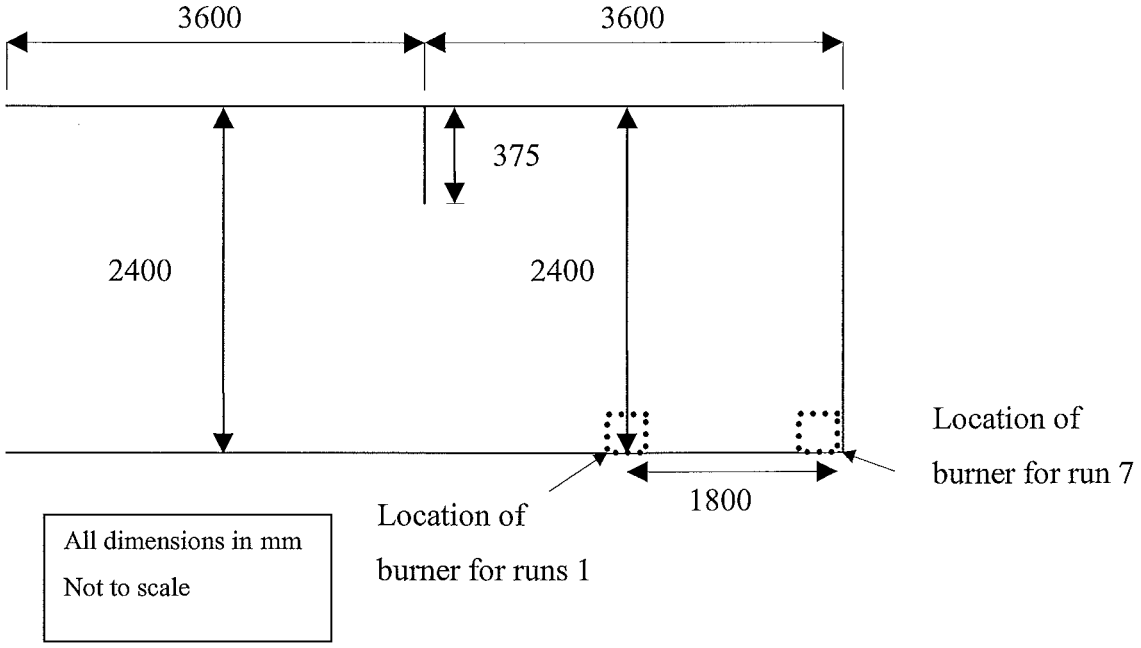

Figure 4-3 Dimensions of compartment in horizontal plan

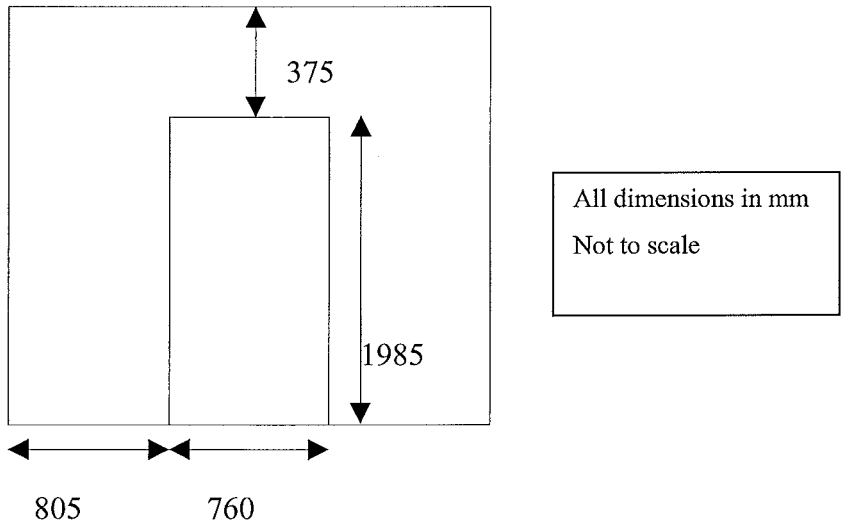

Figure 4-4 Dimensions of middle wall/door area of compartment.

The compartment was constructed on a box section steel frame. Steel studs were attached to the steel frame to form the base of the walls. A 12.5mm thick sheet of Plywood was laid on the bottom of the compartment. The inside of the compartment was completely lined with Gib fireline board 12.5mm in width. This was screwed into the steel studs in the walls and ceiling of the compartment. The walls were plastered with Gib Paste to ensure the compartment was sealed preventing smoke leaks once the experiment began. To enable the compartment to be used for multiple runs without the Gib disintegrating thermal insulation was screwed on with 30mm washers to the all surfaces of Gib board in the compartment. The insulation was of type I.S.B (Intermediate Service Board - Inzco) and was 25mm thick. It is a glass wool, lightweight, semi-rigid insulation used for surface temperatures up to 450°C. To protect the ends of the Gib the insulation was extended around the front opening of the compartment. The finished dimensions of the fire compartment were 2.37 metres wide by 2.36 metres high and 3.6 metres long. The finished dimensions of the adjacent compartment was 2.37 metres wide, by 2.36 metres high by 3.6 metres long. Photo 4-1 shows a front view of the compartment during an experimental run.

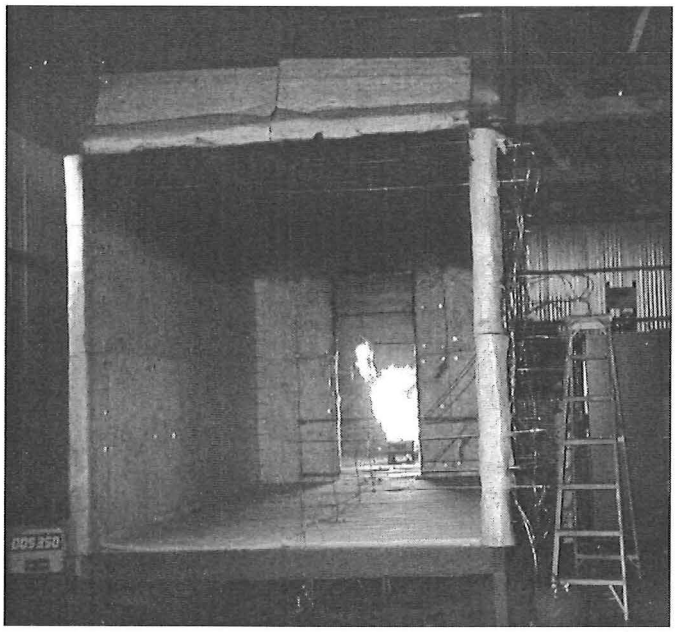

Photo 4-1 Front view of the compartment

A steel hood was built to exhaust the hot gases from the fire out of the building into the air. The exterior view of the hood is shown in photo 4-2.

Photo 4-2 Exterior view of hood

4.3 Gas Burner

A LPG gas burner was used as the fire source for the experiments. The burner was 0.3m high and had square sides of 0.3m giving a total fire area of 0.09m^2. The burner was initially filled with sand however this was later replaced with gravel as some of the sand was blown out of the burner due to the mass flow of the gas. An automatic ignition source located 350mm off the floor was used to ignite the burner. Photo 4-3 shows the automatic igniter and the sand filled burner.

For the first 6 runs the burner was located in the direct centre of the fire compartment, 1800mm from the ends of the compartment, and 1185mm from finished sides of the compartment. The location is shown in figures 4-1 and 4-2. For the final experimental run the burner was placed in the corner of the fire compartment as shown in figures 4-1, and 4-2.

.

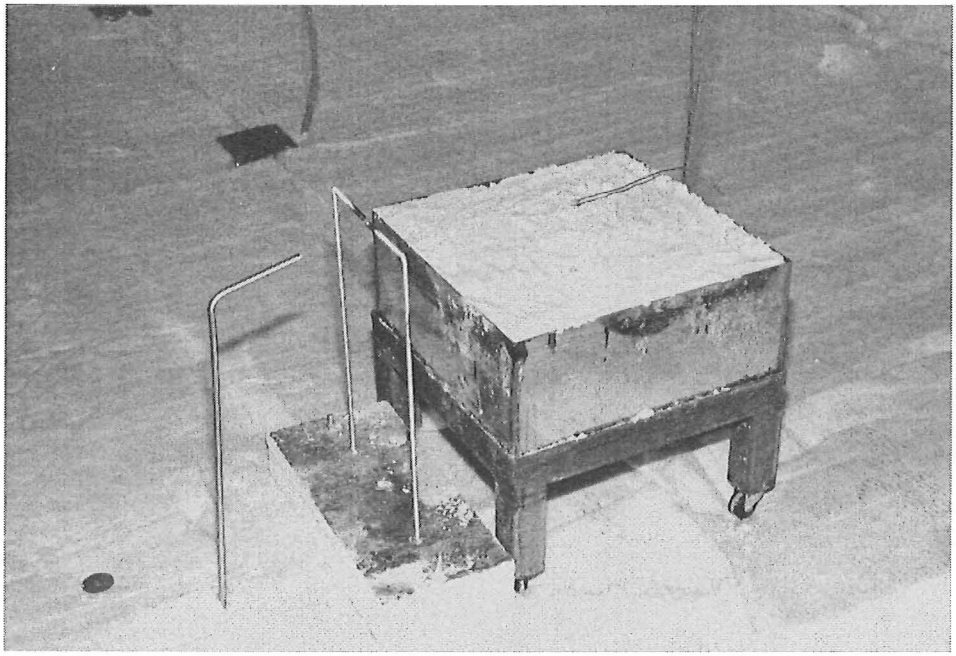

Photo 4-3 The LPG gas burner used in the experiments

4.4 Mass flow controller

The Brooks Model 5853 Flow Controller was used to control and measure the flow of the LPG gas. The mass flow controller contains a sensor which produces an electrical output signal linear with flow rate, used for measuring and control purposes. The model contains a control valve, flow sensor and an integral electronic control system. This allows a stable gas flow, without the need to continuously re-monitor and adjust gas pressures. The flow controller has an accuracy of ± 1%. Photo 4-4 shows the mass flow controller, with the LPG isolation valve and the ignition source valve.

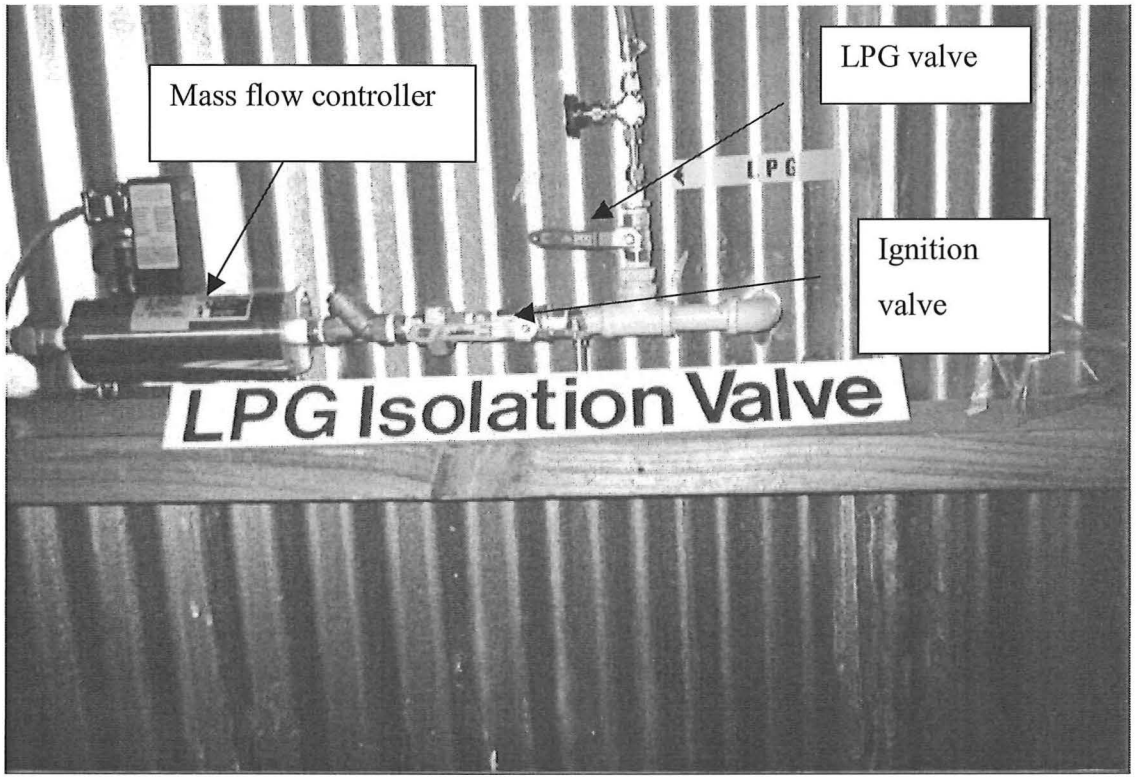

Photo 4-4 Mass flow controller, LPG isolation valve, and ignition source valve.

4.5 Thermocouple arrangement

The research undertaken by this author involves analysing compartment fires for purposes pertaining to zone models however the experimental set-up, was also designed to allow detailed analysis of field modelling. Therefore more trees are inserted in the compartment than will be required in the analyses pertaining to zone modelling.

For the base zone model analysis the thermocouple trees were place in the corner space in each compartment. In the corners it is assumed that velocities are very small and thus mixing effects will be minimised. The thermocouples were located 150mm horizontally from both the corner walls at vertical spacings of 150mm. The fire compartment had 14

thermocouples and began 150mm of the ground and finished 75mm from the top of the room. The adjacent room had 15 thermocouples and began 35mm of the ground and finished 75mm from the top of the room. This difference in the number of thermocouples was due to the slight difference in the finished height of the front and back rooms. Figure 4-4 shows the vertical plan of the fire and adjacent compartments with the locations of the corner and centreline thermocouples. Figure 4-5 shows the detailed layout of a corner thermocouple tree and a centreline tree. Photo 5-5 shows a section of the corner thermocouples in the adjacent room.

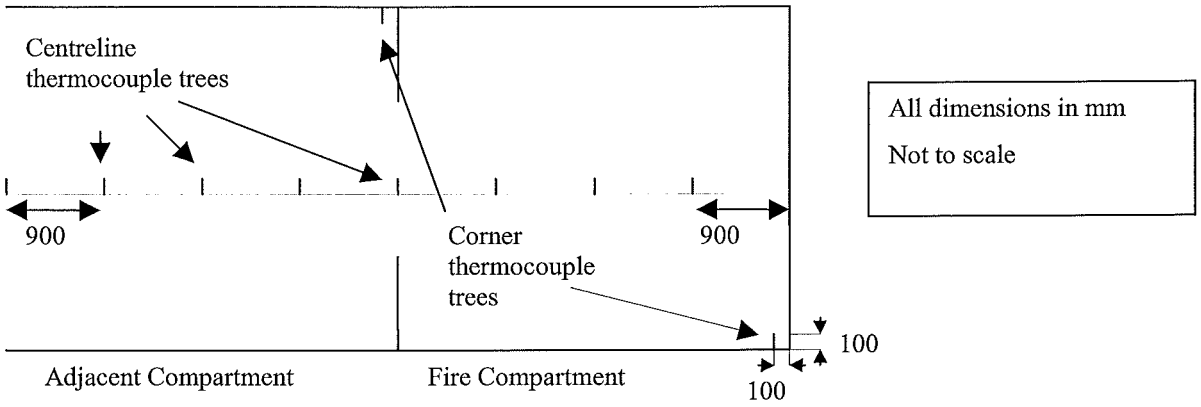

Figure 4-5 Horizontal locations of thermocouple trees in enclosure.

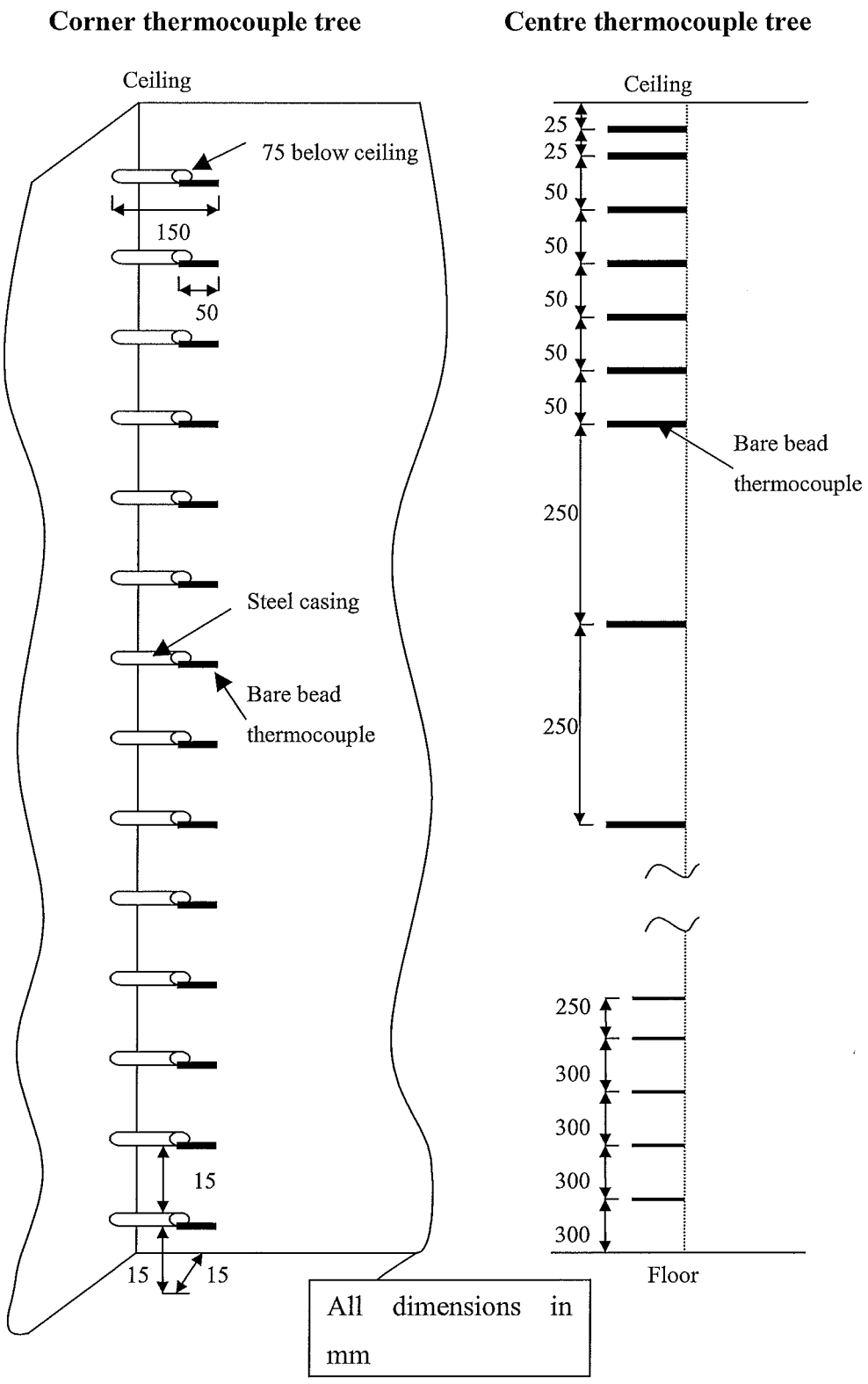

Figure 4-6 Layout of corner thermocouple tree in fire compartment and standard centreline thermocouple tree

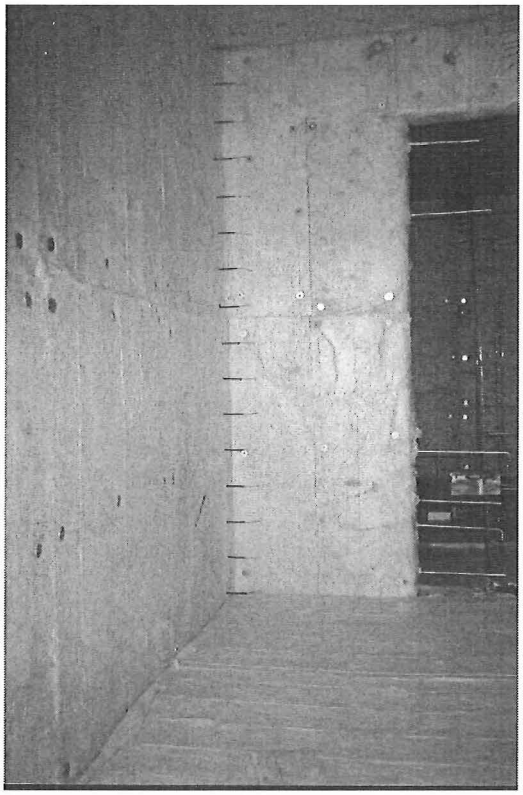

Photo 4-5 Corner thermocouple tree in the adjacent compartment

Thermocouple trees were also placed to read temperatures along the centreline of both compartments. Each room had 4 centreline thermocouple trees as shown in figure 4-4 and another thermocouple tree was placed directly under the soffit in the door space. While these were primarily inserted for field modelling analysis they will also be used in determining the effectiveness of zone models. Previous studies in validating zone models [7,8] have only used a corner thermocouple tree where the air is assumed dormant. Whether the readings in the centre thermocouple tree are conservative when compared with readings in the corner thermocouple trees could influence the criteria for validating zone models.

Each thermocouple tree had 14 thermocouples along its length plus a surface plate thermocouple on the ceiling and on the floor. A typical tree is shown in figure 4-6. Thermocouples were located 300mm, 600mm, 900mm, 1100mm, and 1350mm above the

floor and 25mm, 50mm, 100mm 150mm, 200mm, 250mm, 300, 550mm and 800m below the ceiling. These thermocouples were attached to a spring tightened wire located 100mm from the centreline of the room on the right hand side. They were then vertically protruded 100mm to measure at the centreline of the room. The top eight thermocouples of each tree were feed in through the ceiling while the remaining 7 were feed in through the floor. The thermocouple leads were attached to serial boxes, (usually one box for the upper thermocouples and one for the lower thermocouples) the information was then relayed to the computer system where the data was collected and stored.

The thermocouples used were standard glass insulated Type K Bare Bead 24 gauge. High temperature glass insulated thermocouples were used for the upper regions of the thermocouple trees while thermocouples with a lower tolerance from heat were used for the lower regions of the compartment. For the corner thermocouple trees only low temperature thermocouples were used as the thermocouples were housed in a protective steel casings 6mm in diameter. These protruded 100mm from the wall as shown in figure 4-6 with the thermocouple bead protruding another 50mm out of the steel

Thermocouples are designed to measure the temperature of the surroundings gas through convective heat flows. In actuality it is the temperature of the thermocouple itself that is being measured not the gas. Excess radiation can cause thermocouples to give a reading that is inconsistent with the actual gas temperature. To estimate the effects of radiation on thermocouples, aspirated thermocouples were set up 150 mm below the ceiling and 300 mm below the ceiling for each thermocouple tree and were aligned with the corresponding normal bare wire thermocouple at that height. Aspirated thermocouples were also located 300mm and 600mm above the floor corresponding to each thermocouple tree. Aspirated thermocouples are thermocouples located inside a steel tube. Air is sucked through the steel tube passing over the thermocouple. By doing this, ideally only the air temperature is measured and the radiated flux absorbed from the fire is significantly reduced.

4.6 Pressure readings

To determine the average upper and lower zone temperatures based on transport terms the velocity of the gases leaving the compartment need to be directly or indirectly measured. For this reason and for other field model analyses beyond the scope of the report 7 bi-directional probes were installed in the door space to measure the changes in pressure between the fire and adjacent compartment. The probes were located 100mm, 400mm, 700mm, 1000mm, 1300mm, 1600mm, 1900mm below the soffit Each probe lining up with the centreline of the room at 380mm from the side of the door area.

The field modelling analysis required detailed investigation into the ceiling jet exiting the adjacent room. Thus, bi-directional probes were also located to measure the pressure difference in the ceiling jet. Three probes were used each located 25mm off the ceiling at 900, 1800, and 2700mm from the middle wall/door area. Bi-directional probes were also located in the front opening. These were attached 100mm and 300mm below the soffit height and 600mm and 300mm above the floor level. All the bi-directional probes were connected to pressure transducer of modal "sebra 264". These were located on the outside of the compartment and then relayed to the computer for data collection. The data collection was performed along side the fire compartments. Photo 4-6 shows the data collection apparatus along the side of the fire compartment.

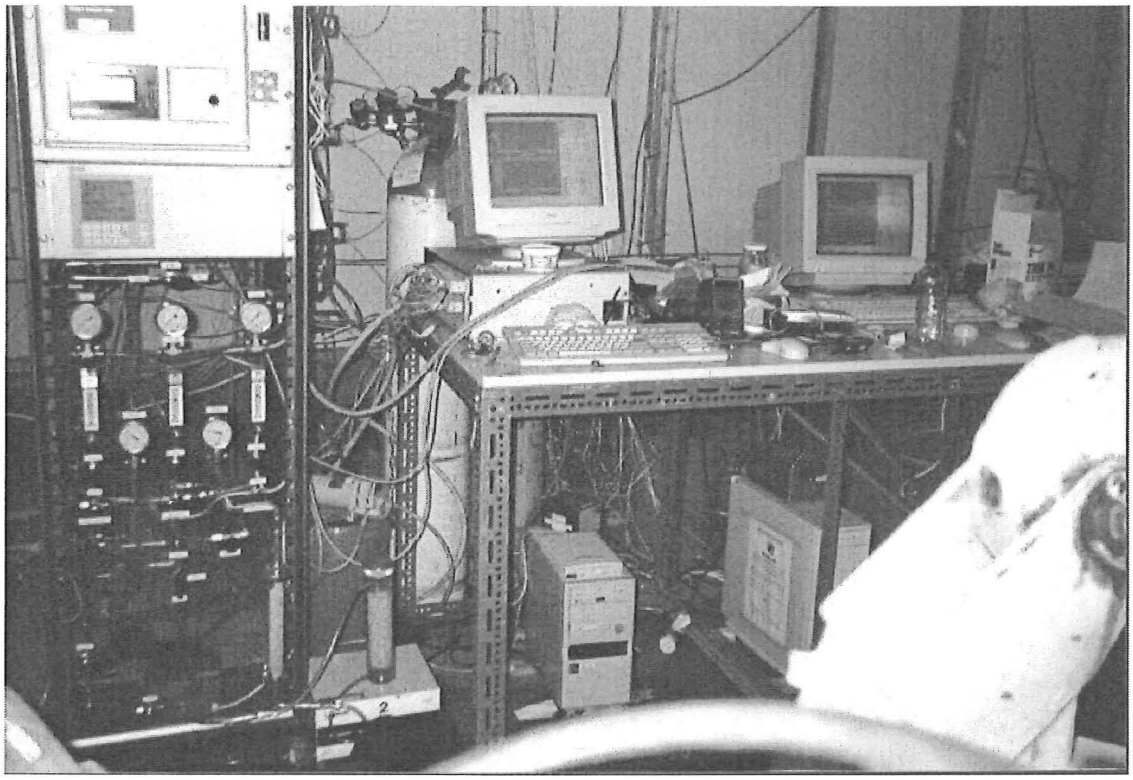

Photo 4-6 Data collection equipment set-up.

4.7 Video equipment

A video camera was set up to provide a view of the front of the compartment. Ideally a visible difference between the upper and lower layers in the room could be seen and this would be recorded by the camera for validating interface height prediction methods.

5 Experimental Procedure

A test run was initially performed to determine if any of the thermocouples were malfunctioning. 7 real runs were performed in the compartment. Three estimated fire sizes of 60kW, 120kW and 180 kW were used for each run. Table 5.1 shows the actual fire sizes as recorded via the mass flow controller.

Table 5-1 Average heat output for runs 1-7.

Run	Average Heat output (kW)	Standard deviation (kW)
1	112	0.29
2	168	0.31
3	168	0.33
4	55	0.28
5	55	0.27
6	168	0.25
7	112	0.32

Throughout runs 1 and 2 the larger gas flow would cause the burner to bubble considerable amounts of sand out thereby decreasing the consistency of the flame from the burner and blowing sand all over the floor. Heavier gravel was used for the 3rd and subsequent runs, which was not bubbled out by the mass flow of the gas.

For runs 1 to 4 the main doors into the building that housed the compartments were open. For runs 5 and 6 the main doors were closed to check how this affected the changes in ambient conditions during the course of the experiment.

As mentioned above in run 7 the burner was placed in the corner of the room to determine what effects this had on the zone/field modelling. Photo 5.1 shows fire experiment 7 where the burner was located in the corner of the room. The close

proximity of the burner to the corner of the room caused the surrounding insulation to melt exposing the Gib board. As the insulation melted away the Gib board slowly began a process of decomposition. This was mostly due to 2 screws, which were protruding into the naked flame of the fire and conducted sufficient heat to cause a very localised area of decomposition, which grew rapidly with the addition of convective heat. It should be noted however that the Gib structure did remain intact for the entire duration of the experiment. Photo 5-2 shows the decomposition in the Gib board 40.5 minutes after the fire was initiated.

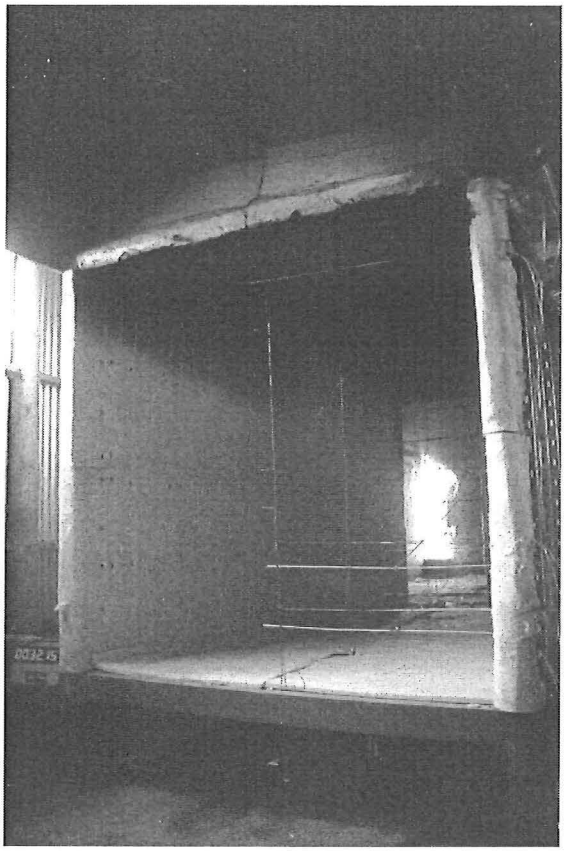

Photo 5-1 Fire experiment, run 7 with burner place in the corner of the room..

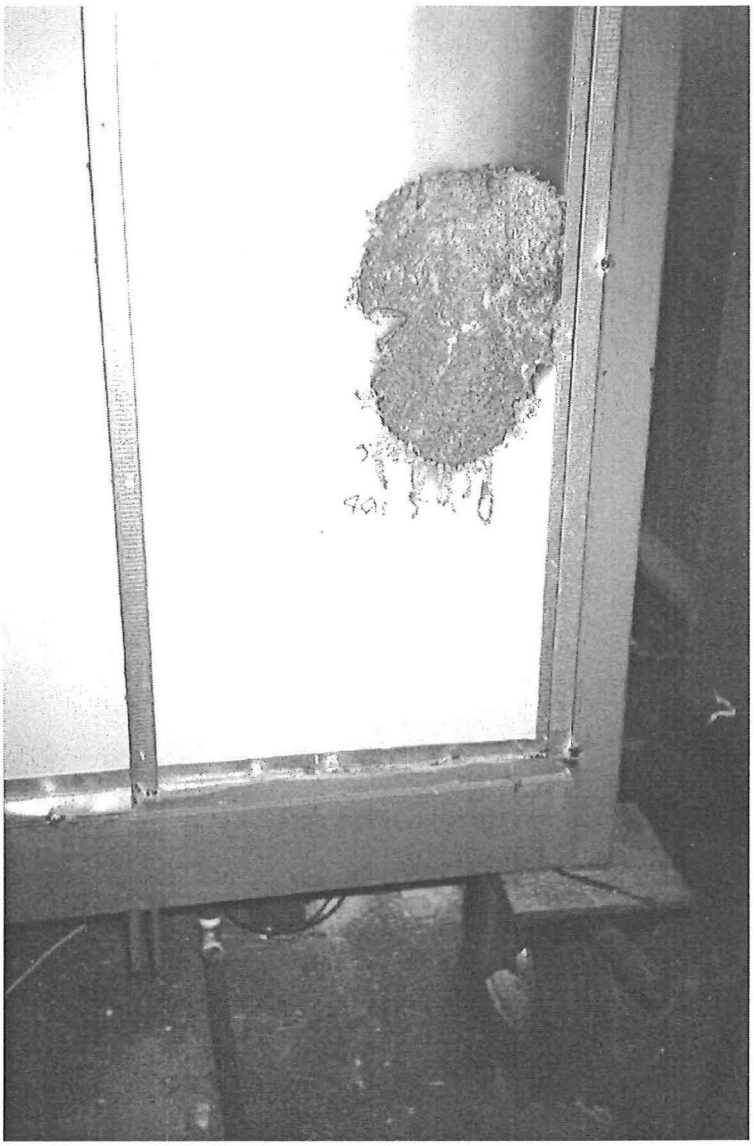

Photo 5-2 Damages to Gib board after 40.5 minutes for run 7

6 Results/Discussion

6.1 Interface height predictions

6.1.1 Interface height predictions using corner thermocouple trees

The interface height predictions determined through Quintiere's method, the maximum slope method, and the N% method are shown in figures 6-1 to 6-6. Figures 6-1 to 6-3 show the interface height predictions and measured profiles in the fire compartment for 55kW, 112kW, and 168kW fire sizes respectively. Figures 6-4 to 6-6 show the interface height predictions and measured profiles in the adjacent compartment for 55kW, 112kW, and 168kW fire sizes respectively. The N% method uses N values of 10, 15 and 20. The experimental data was taken from run 4 for the 55kW fire, run 1 for the 112kW fire and run 6 for the 168kW fire. For these runs the fire was located in the centre of the fire compartment. The thermocouple trees, which recorded the temperature, were located in the corner of both compartments as specified in chapter 4. The interface height predicted by C-Fast is also shown on the graphs.

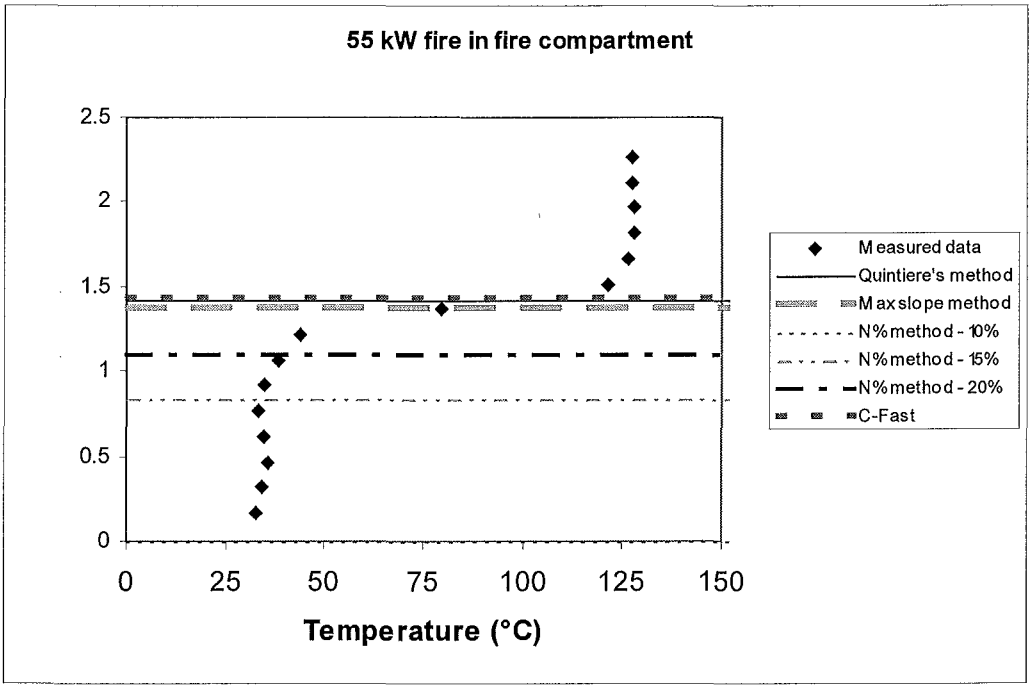

Figure 6-1 Interface height predictions in fire compartment for 55kW fire

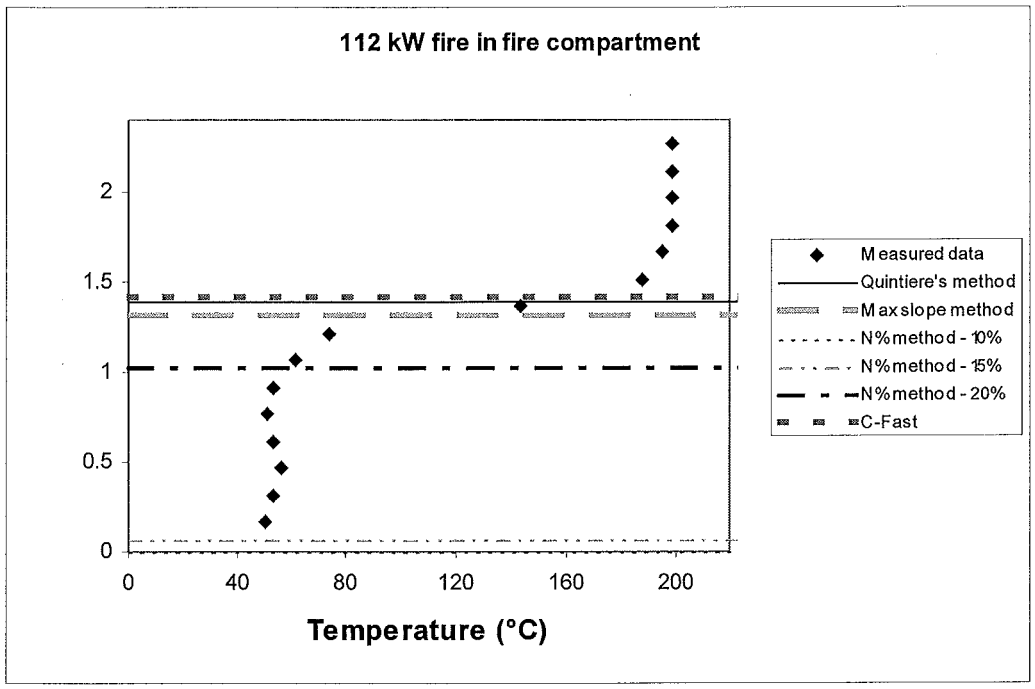

Figure 6-2 Interface height predictions in fire compartment for 112 kW fire

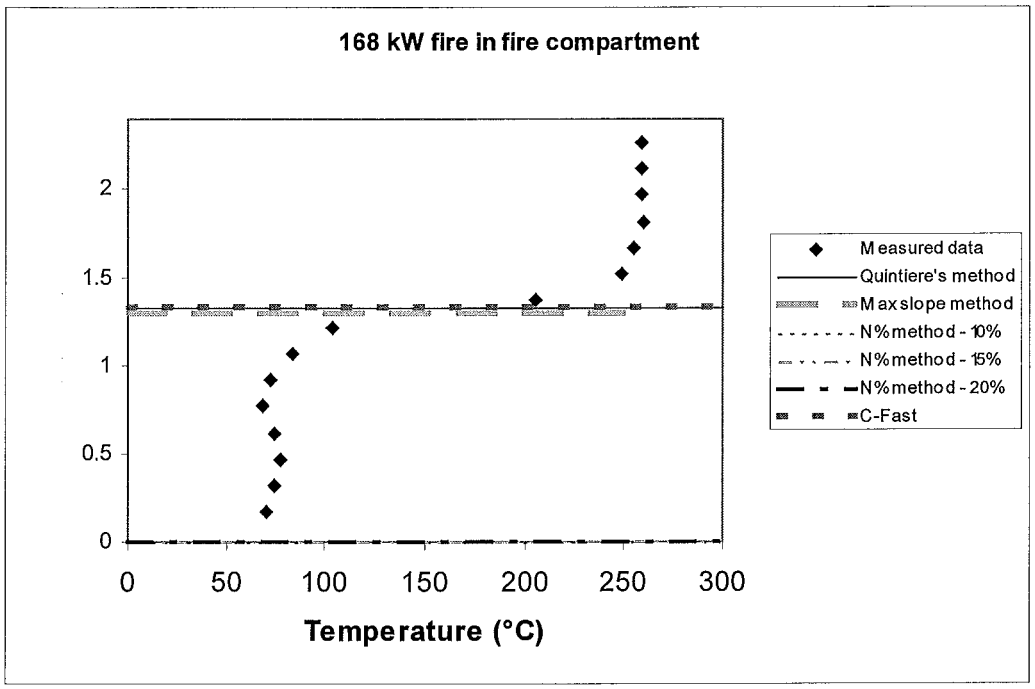

Figure 6-3 Interface height predictions in fire compartment for 168 kW fire

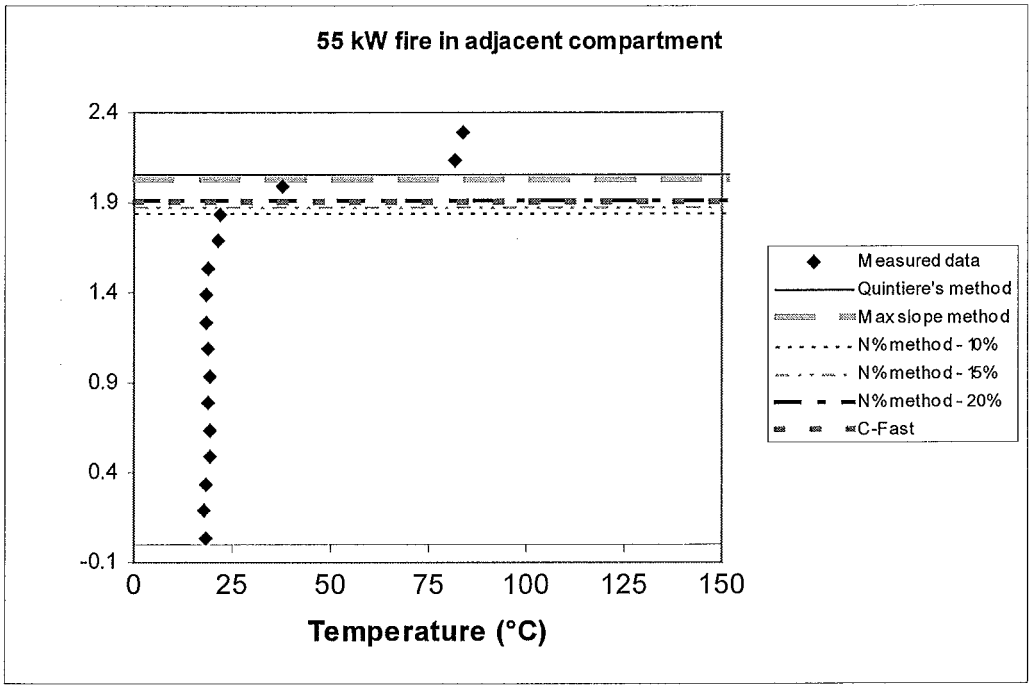

Figure 6-4 Interface height predictions in adjacent compartment for 55kW fire

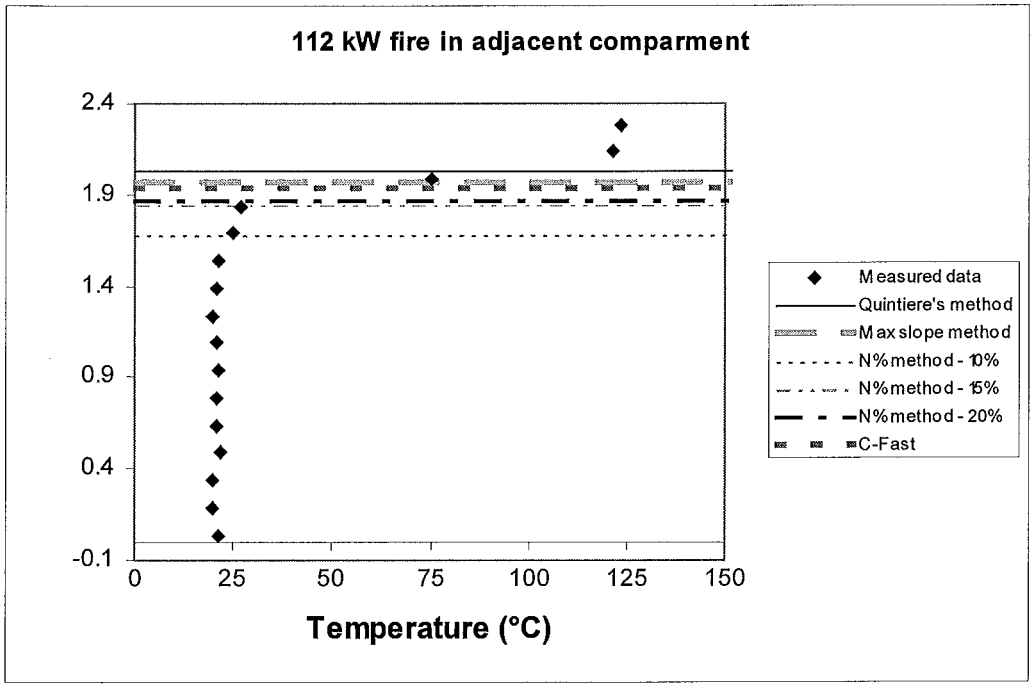

Figure 6-5 Interface height predictions in adjacent compartment for 112kW fire.

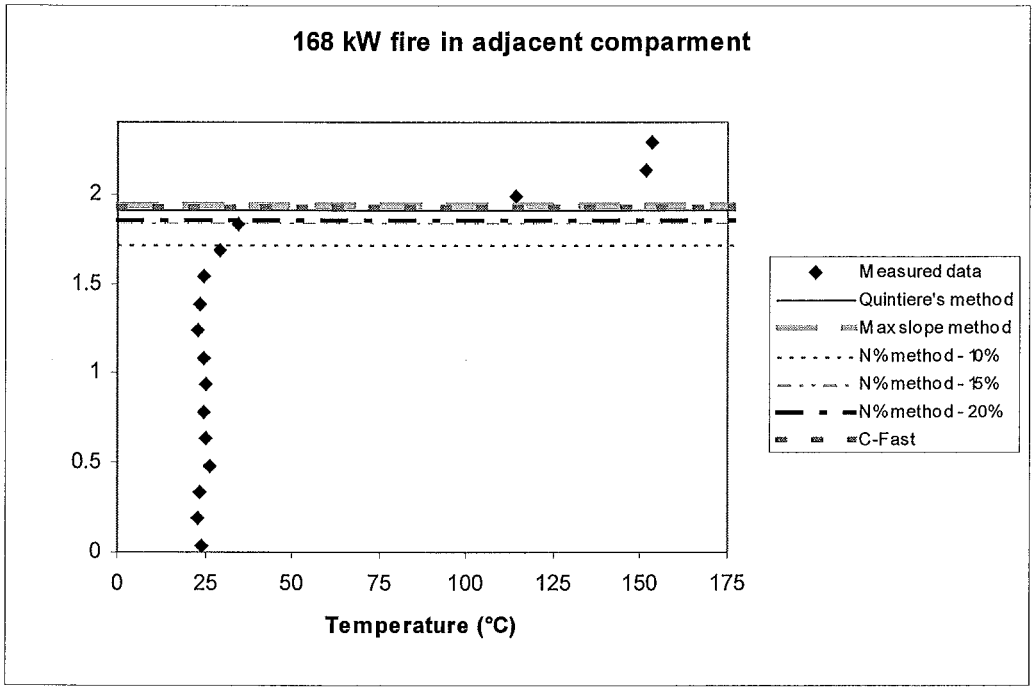

Figure 6-6 Interface height predictions for adjacent compartment for 168 kW fire

The assumption of a relatively quiescent zone in the corner of each room appears justified from the shape of the measured temperature profiles in figures 6.1 to 6.6. Each graph shows clear stratification with a bottom cooler layer and a top hot layer. Previous research has often used visual observations to verify predictions of interface height [8,11]. For these experiments the visual observation of a smoky upper layer separated from a clear lower layer was difficult to see due to lack of light in the fire compartment and a low smoke density in the adjacent compartment.

When viewing the temperature profiles there is a clear separation between the upper and lower thermocouples. This separation, however, is not a line but an area approximately 0.3m high. For the purposes of this report this intermediate layer between the upper and lower regions of fairly constant temperature will be referred to as the "interface layer". When assessing temperature-averaging techniques it is necessary to locate the interface height, which best separates the upper and lower. This would lie directly in the middle of

the interface layer. With this criterion, Quintiere's method and the maximum slope method give the best prediction of interface height.

The N% method was much less successful in predicting the interface height. In the fire compartment (figures 6-1 to 6-3) the N% method using values of 10, 15 and 20, under-predicted the interface height for all fire sizes. In many cases the predicted interface height was zero thereby making the entire room an upper hot zone. Previous study's using the N% method [3, 8, 11] have all been with rooms which have direct venting to the ambient conditions (outside) for the duration of the experiment. This has allowed temperatures in the lower regions of the compartment to be quite close to ambient. In this situation, all the air being transported into the fire compartment comes from the adjacent compartment, which contains much higher enthalpy comparative to ambient air. Thus the temperatures in the lower regions of the fire compartment are significantly higher than ambient and the interface height is under predicted. The empirical nature of the method makes it susceptible to flaws such as this, and if this method were to be used for further data reduction, these flaws would have to be taken into account. Previous studies [8, 11] have found different values of N to give the best results, however in these studies the vent sizes have been different. Therefore if a vent to the outside were present in the fire compartment, the value of N would be dependent on the vent size.

Unlike the fire compartment, the adjacent compartment has vents directly to the outside. Figures 6-4 to 6-6 show that the interface height predictions in the adjacent compartment are much more accurate than those predicted in the fire compartment. This method still tends to underestimate the interface height using N values of 10, 15 and 20 with 20 giving the closest prediction to the other two methods. The N % for all values of N tested, tended to predict the interface height around the point where the lower temperatures started increasing significantly from the uniform bottom temperatures. This would be in agreement with previous research, which verified the N% method based on visual observations [8, 11]. Visual observations would determine the interface height from the point where the lower clear layer ended and the intermediate layer of mixed clear air and smoke began, not where the upper layer actually began.

Figures 6-1 to 6-3, 6-5, and 6-6 shows that C-Fast's prediction of the interface height is in close proximity to the interface height predicted with Quintiere's method and the maximum slope methods. Only in figure 6-4 for the adjacent compartment with a 55kW fire does it predict the interface height lower, more close to the N% method. C-Fast's prediction would seem accurate if it were going to be used to calculate zonal temperatures within the model.

One of the recommended tenability limits for a fire where life-threatening conditions may occur is that the visibility in the relevant layer should not fall to less than 2m. [14]. If the interface height from C-Fast was used for verifying these tenability conditions in the fire safety design of a building, the calculated interface height would be too high and would need to be conservatively estimated as the height at the bottom of the interface layer. In this case the N% method in a room with vent(s) to ambient conditions would be a good method of validating the zone models interface height calculation. Therefore in data reducing experimental data to determine the interface height, 2 estimates need to be given. One interface height is located in the middle of the interface layer to determine the upper and lower layer temperatures and another height prediction is required at the bottom of the interface layer for determining a conservative value of it's height for validating a zone model's interface height. Another approach could be to use only the first interface height but add a large margin of safety if this was to be compared with the zone models interface height output.

6.1.2 Interface height predictions using centreline trees

The thermocouple readings in the corner of each room were located in an area where the gas velocities would be significantly less than in the centre of the room. Measuring just in the corner however assumes that the interface layer is constant throughout the room. By analysing the thermocouple trees at various points along the centreline of the compartment the variation of interface height with horizontal location can be studied.

Also the ability of the interface height prediction techniques to work in non-ideal, well mixed conditions can also be seen. Figures 6-7 and 6-8 show the measured temperature profile and predicted interface heights for thermocouple trees located on the centreline of the fire compartment 900mm and 2700mm from the front wall during a 112kW fire. Figure 6-9 shows the measured profile and interface height estimates for the thermocouples located on the centreline of the adjacent compartment 1800mm away from the middle wall (or directly in the centre of the room) during a 112kW fire.

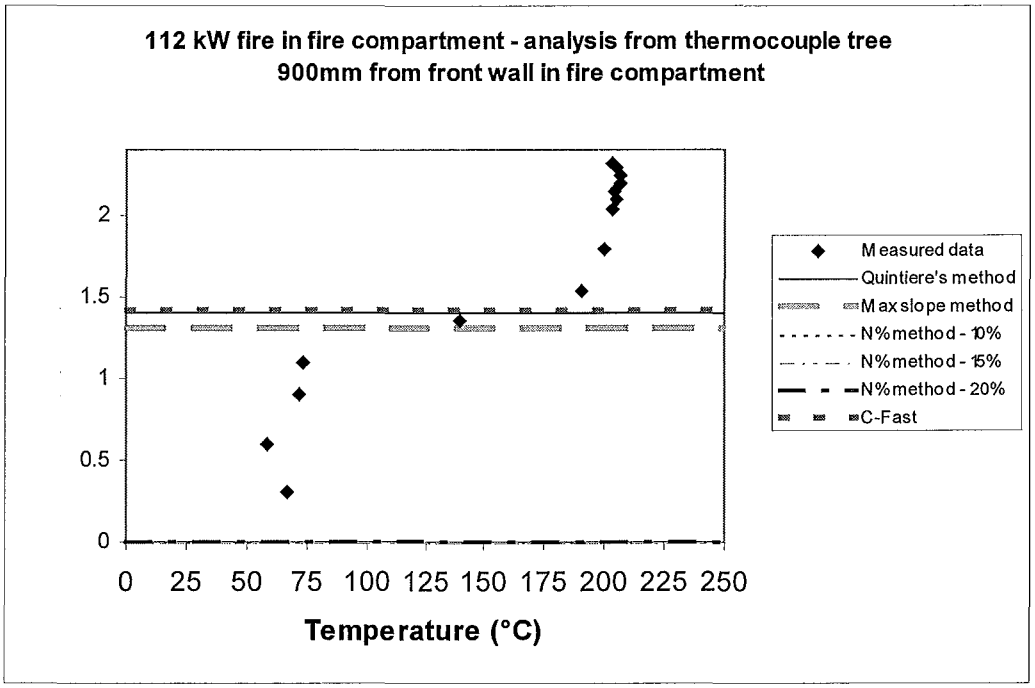

Figure 6-7 Interface height predictions using centreline thermocouple tree located in fire compartment 900mm from front wall for 112kW fire

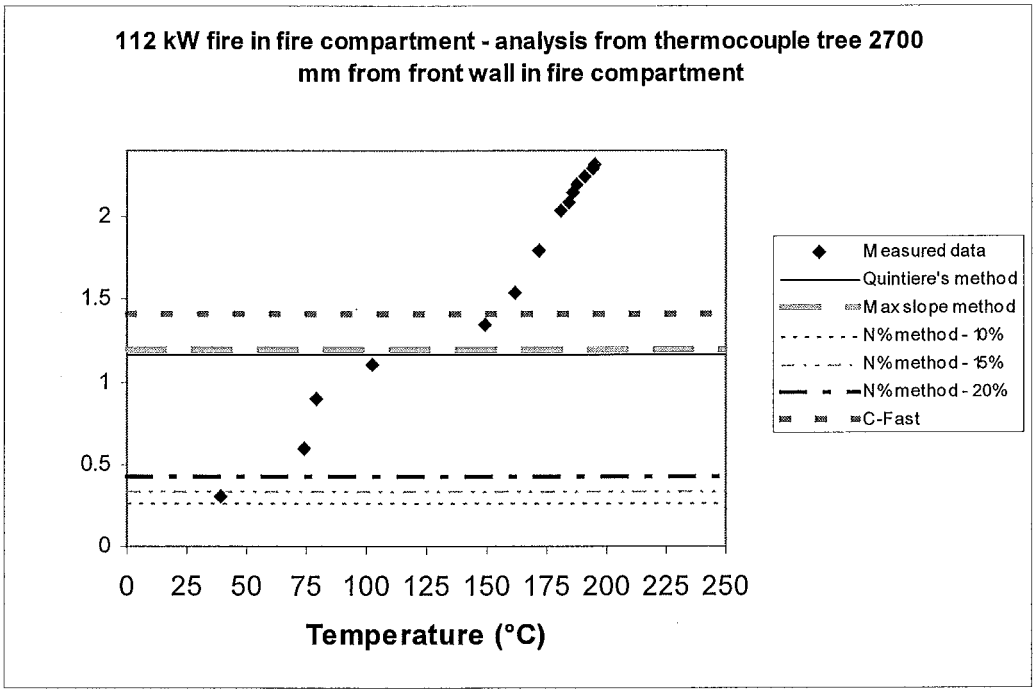

Figure 6-8 Interface height predictions using centreline thermocouple tree located in fire compartment 2700mm from front wall for 112kW fire.

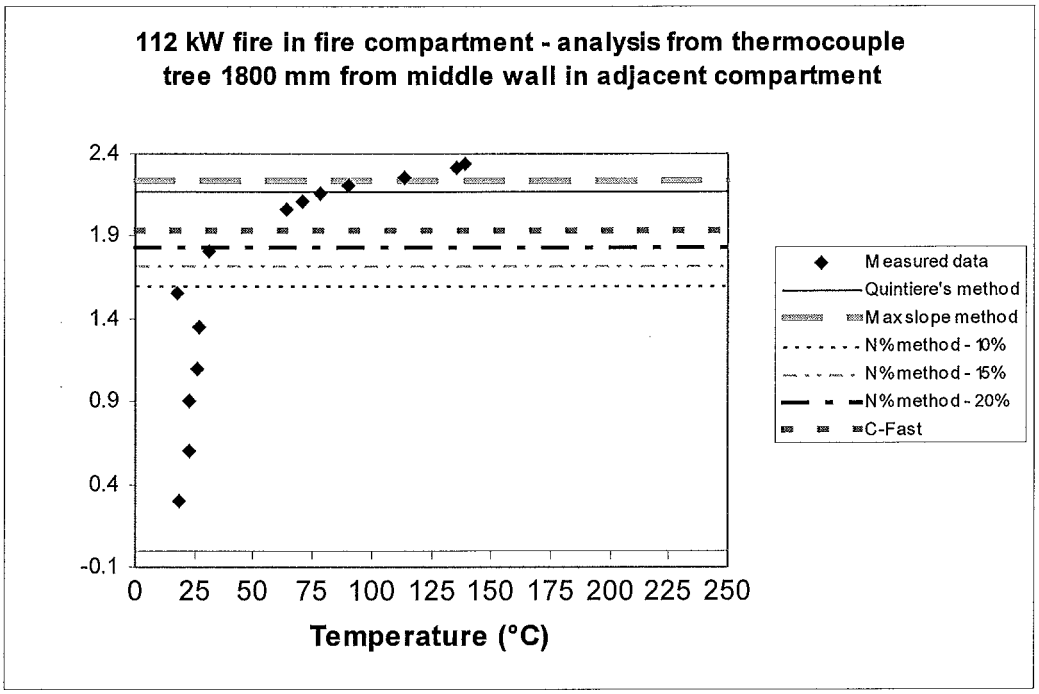

Figure 6-9 Interface height predictions using centreline thermocouple tree located in adjacent compartment 1800mm from middle wall (door area) for 112kW fire.

Table 6-1 shows the discrepancy between the interface height predicted at the corner thermocouple tree in the fire compartment and the centreline thermocouple trees located 900mm and 2700mm from the front of the fire compartment. It also shows a comparison between the corner thermocouple tree in the adjacent compartment and the centreline thermocouple located 1800mm from middle wall in the adjacent compartment.

Table 6-1 Comparison between corner and centreline interface height predictions

Tree Location	Fire Size	Discrepancy between corner and centre predictions				
		Maximum slope method	Quintiere's	N% method 10	N% method 15	N% method 20
900 mm	55	1%	0%	100	54%	-43%*
from front	112	-1%	1%	N/A	N/A	N/A
(fire comp)	168	-2%	4%	N/A	N/A	N/A
2700 mm	55	8%	14%	N/A	52%	56%
from front	112	14%	16%	N/A	-399%	59%
(fire comp)	168	19%	8%	N/A	N/A	605%
1800 mm	55	-13%	-7%	5%	6%	2%
from middle	112	-11%	-2%	13%	6%	4%
(adjacent comp)	168	-16%	-12%	46%	11%	6%

*A negative difference indicates that the centre layer was higher than the corner layer

Figure 6-7 shows that for interface height predictions of the thermocouple tree located 900 mm from the front of the fire compartment, the effects of mixing due to flow from the fire plume, do not appear to significantly disturb the stratification between the layers. Table 6-1 indicates that for Quintiere's method and the maximum slope method the differences between this centreline thermocouple is very small, ranging 1% to 4%. Most comparisons with the N% method were not available as either the corner and/or the centreline prediction was at floor level.

Figure 6-8 shows the interface height predictions for the thermocouple trees located 2700 mm from the front of the fire compartment. The measured profile shows much less stratification than what occurs in the corner thermocouples, and the apparent upper and lower layers are less clear as the temperature in each zone increases over the height of the

compartment. The effects of turbulent flow generated by the fire plume are probably not too significant as the tree located 900mm from the front does appear to be effected by the plume (the effect should be similar for both trees). The de-stratification of the layers would be mainly due to mixing effects at the cold/hot interface of the outgoing and incoming gas streams. Although there is much de-stratification in the compartment, the separation between the two layers can still be seen and is aptly calculated from the maximum slope and Quintiere's method. The assumption that the increase in temperature over height between the two zones will be significantly greater than the differences within each zone is still valid for this highly mixed scenario. The N% method again failed to adequately predict the interface height, largely underestimating it. For this tree the predicted heights were above floor level due to the thermocouples being exposed to cooler air being sucked in from the adjacent compartment before it had time to be heated in the room.

Table 6-1 shows that the predicted interface height for Quintiere's method and the maximum slope method for the tree located 2700mm from the front of the fire compartment were significantly less than in the corner compartment for all fire sizes with the differences ranging from 8% to 19%. This would be expected near the vent, however as the thermocouple tree located 900mm from the front wall did not differ significantly in predicted interface height from the corner tree's, it can be assumed the interface height is fairly constant in the room in all areas except those between the fire and the door. The N% method showed no correlation between the corner and centreline predictions.

Figure 6-9 presents the interface height predictions for the thermocouple tree located directly in the centre of the adjacent compartment. The experimental data shows a fairly constant lower layer, however the upper layer is very non-uniform and increases significantly over the height of the compartment. The measured temperature points in the top of the compartment are indicative of a ceiling jet exiting the compartment. As there is no soffit at the exhaust end of the adjacent compartment, it is difficult for a layer of fairly constant properties to form. More research needs to be done on how the height of the ceiling jet varies over the length of the compartment.

The N% method (at N=20) predicts the interface height as being close to the bottom of the interface layer, Quintiere's method and the maximum slope method predict the interface layer very high up in the compartment. Quintiere's method is an iterative method, which depends on the average temperature of upper layer thermocouples, not deviating more than 10% from the top thermocouple reading. As the temperatures in the adjacent compartment vary considerable with height, the interface height has to be inflated to very high levels to have the thermocouple readings above it deviating no more than 10%. However this should not be an issue for averaging the temperatures, as it will only predict higher more conservative upper and lower layer temperatures. The maximum slope method predicts the interface height due to the dramatic increase in temperature in the last few thermocouples in the room. This may actually be the difference between the ceiling jet and the upper zone. For these types of data it may be necessary to divide the room into three zones, a lower zone, ceiling jet and upper zone.

As shown in table 6.1 the difference in the interface height prediction between the corner and centreline thermocouple tree located 1800mm from the middle wall for the maximum slope method and Quintiere's method ranges from 13 to 16% and 7% to 12% respectively. This difference would be somewhat expected due to the presence of the ceiling jet. The N% reading gives a more consistent correlation with the corner thermocouple indicating that the bottom of the interface layer may not vary as much as the predicted interface height for different locations in the room. This further illustrates that the N% rule could be used to verify the interface height in zone models, if the interface height is going to be used for tenability criteria (providing the compartment has ambient venting).

6.2 Temperature averaging methods

6.2.1 Radiation effect

Various measurements were taken in the fire compartment with aspirated thermocouples to determine the effects of radiation on the normal, bare bead thermocouples. These however failed to give consistent readings and subsequently have been left out of the analysis. The suction of air through many of the thermocouples was smaller than it should have been indicating that they might have been blocked by soot from the fire.

6.2.2 Determination of the average temperature using the N% rule for interface height

The N% method of predicting interface height was shown in the previous section to range from slightly under predicting the interface height to suggesting the interface height layer was at floor level and the whole room was just one hot upper layer. With a too low interface height prediction the value for averaging the upper layer would subsequently be overly large. This would cause some temperature measurement points that were not in the upper layer (and some even in the lower layer) to be included in the averaging resulting in an under prediction of the upper layer temperature. Figures 6-10 and 6-11 show the average calculated temperatures (using the N% to calculate interface height) for a 112kW fire in the fire compartment and adjacent compartment respectively. Figure 6-12 shows the zonal averages for a 168kW fire in the fire compartment. Spatial averaging and Averaging based on the equation of state (EOS) are shown. A value of 20 for N is used as this gave the best prediction of the interface height.

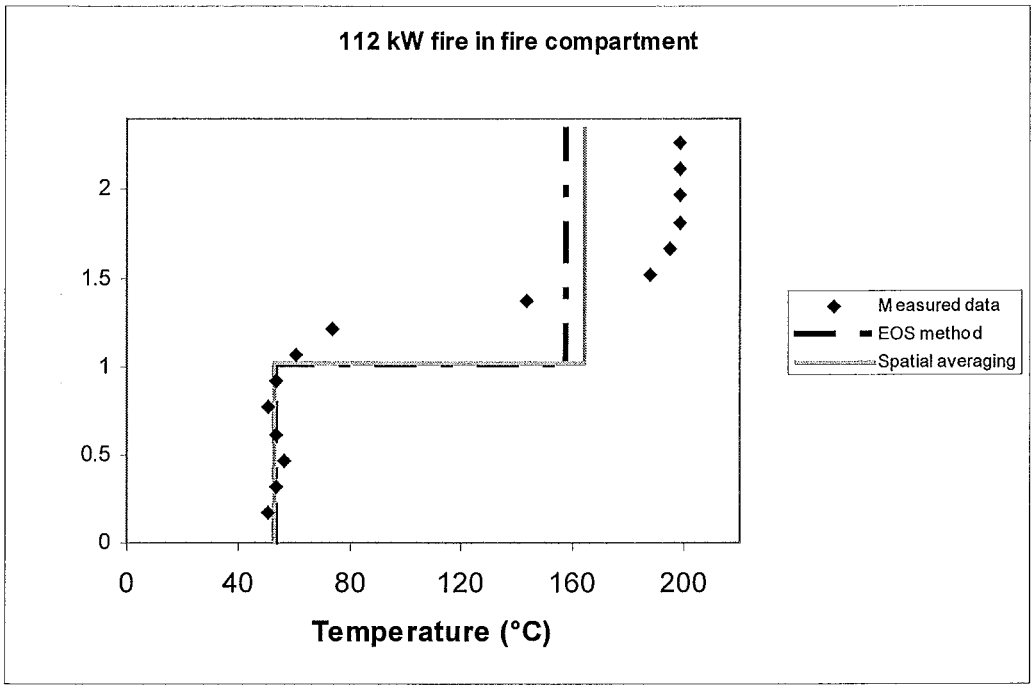

Figure 6-10 Zonal temperature predictions using the N% rule for N =20 in fire room for 112kW fire.

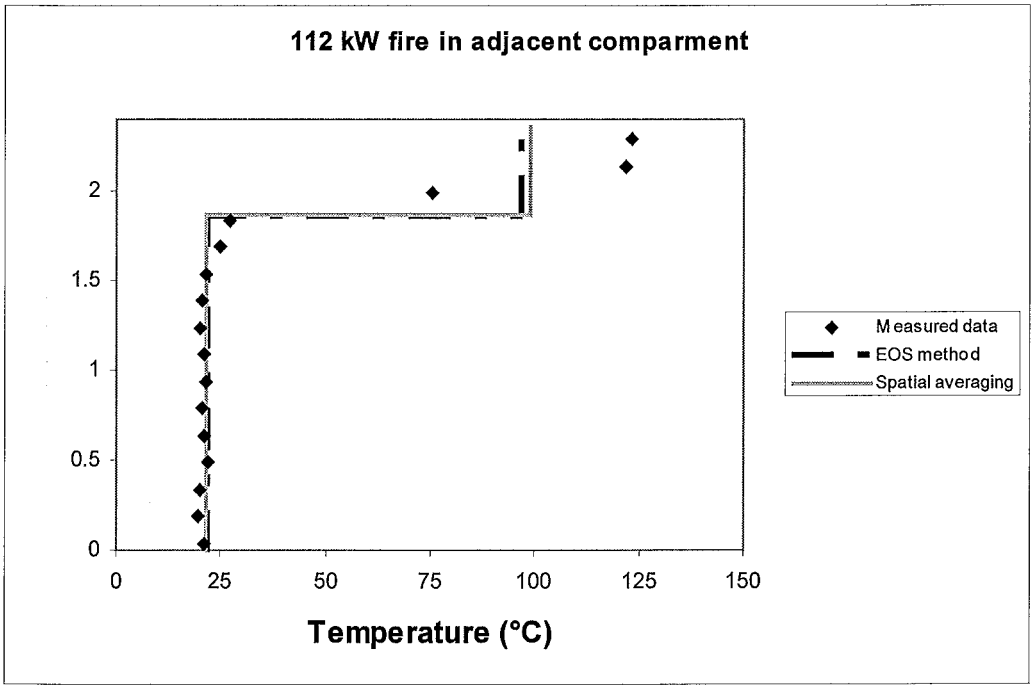

Figure 6-11 Zonal temperature predictions using the N% rule for N = 20 in adjacent compartment for 112kW fire.

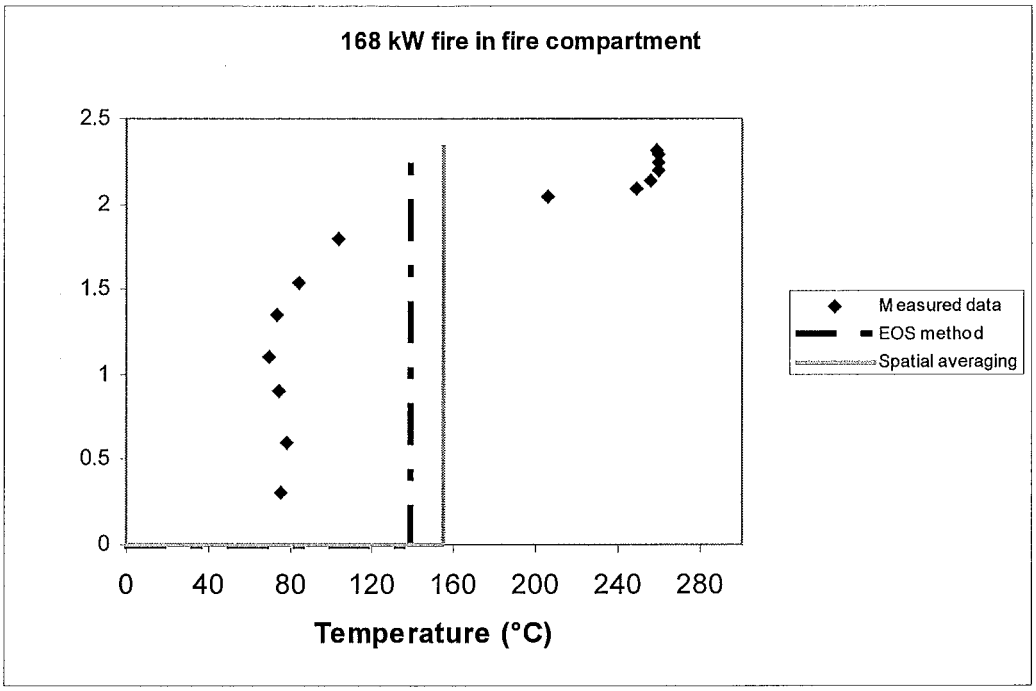

Figure 6-12 Zonal temperature predictions using the N% rule for N = 20 in fire compartment for 168kW fire.

The plot of measured experimental data for each graph illustrates that the assumption that gas velocities were relatively small in the corner of each room with little mixing occurring between each layer was justified. Two clearly stratified zones of nearly uniform temperature are apparent from the experimental data in the plot. The bottom 7 thermocouples in the front room and bottom 13 in the back room are all very close in temperature and do not deviate more than 10°C for either room. The top 5 thermocouples in the front room and top 2 thermocouples in the back room are also very close and do not deviate more than 10°C. Based on this observation from the graphs, the criteria for judging how well the zonal temperatures are estimated, is based on how well the estimated temperatures compare to the bottom 7 and top 5 thermocouples in the fire compartment and bottom 12 and top 2 in the adjacent compartment.

The lower zone temperature predictions for all runs in the back and front of the room are very accurate. The interface height prediction is at the point where the temperatures in the thermocouple tree, just starts to deviate from uniform. Therefore only the bottom 7 thermocouples in the fire compartment and bottom 13 in the adjacent compartment are

used in the averaging. As these thermocouples are approximately constant in temperature and are the criteria for the lower layer (as mentioned in the previous paragraph) a good average is obtained.

The upper zone prediction is severely underestimated in all cases. This underestimation is proportional to the underestimation of the interface height with a worst case scenario being where the interface height was estimated at floor level as shown in figure 6-12 for the 168kW fire in the fire compartment. In this case the average temperature for the upper layer is really an average temperature for the entire room. To determine a better method for estimating zonal temperatures a better method of determining interface height has to be used. The next section will investigate this.

6.2.3 Comparison of averaging techniques

Quintiere's method and the maximum slope method were superior to the N% method in predicting the interface height for averaging temperatures as shown in the previous section. Quintiere's method of calculating zonal temperatures is inclusive with the calculation of interface height. The other methods of predicting temperature in this analysis all use the maximum slope method to predict interface height. Previous studies have used different interface height prediction methods with different temperature averaging methods. Therefore temperature-averaging methods between studies cannot be truly compared, as differences in interface height prediction will radically change the temperature averages. Therefore in the analysis of temperature averaging schemes, the interface height predictions needs to kept constant. Figures 6-13 to 6-18 show the zonal temperature predictions for fires sizes of 55kW, 112kW, and 168kW for both the fire compartment and the adjacent compartment using the maximum slope method to predict interface height (except for Quintiere's method which is interface height inclusive). Results from the simulation of the zone model "C-Fast" are also shown in each figure to see how well it compares with the reduced experimental data.

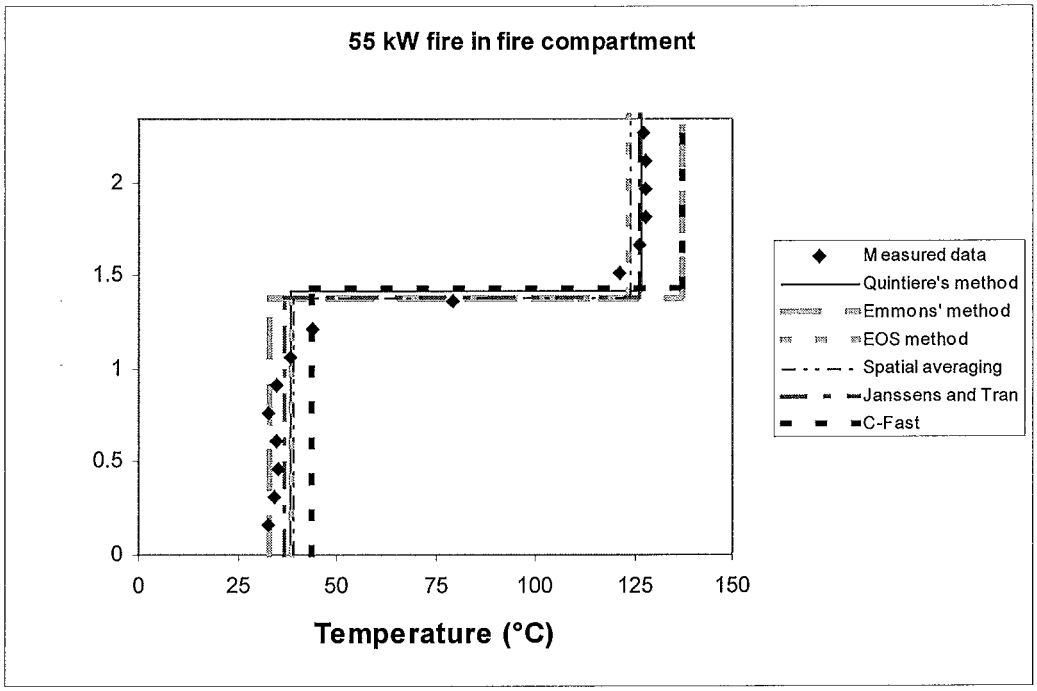

Figure 6-13 Comparison of averaging methods in fire compartment for 55kW fire.

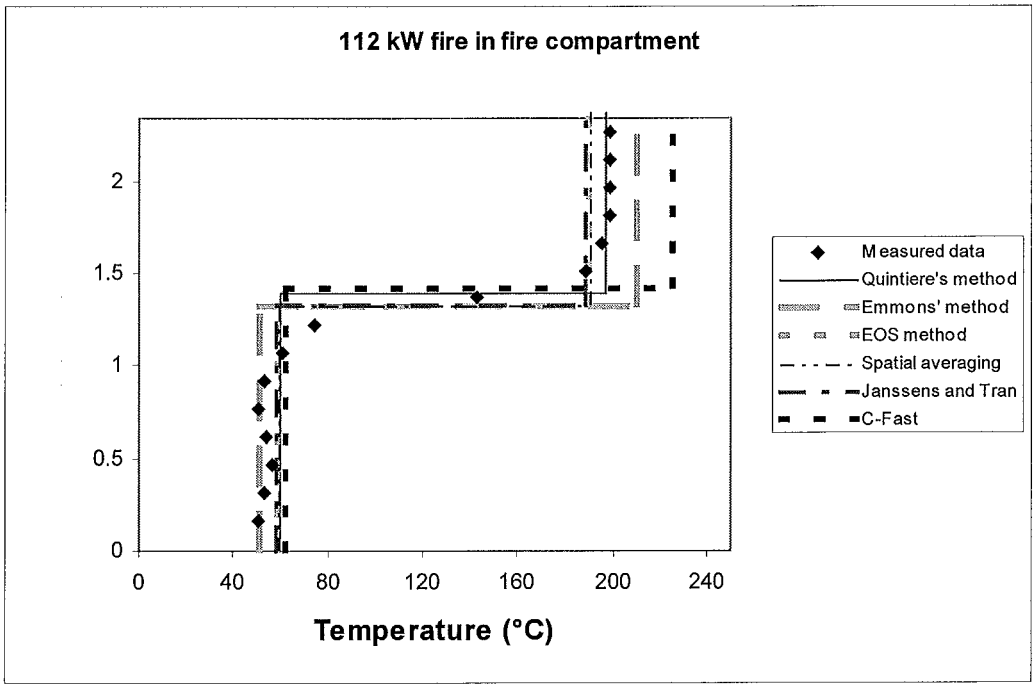

Figure 6-14 Comparison of averaging methods in fire compartment for 112kW fire

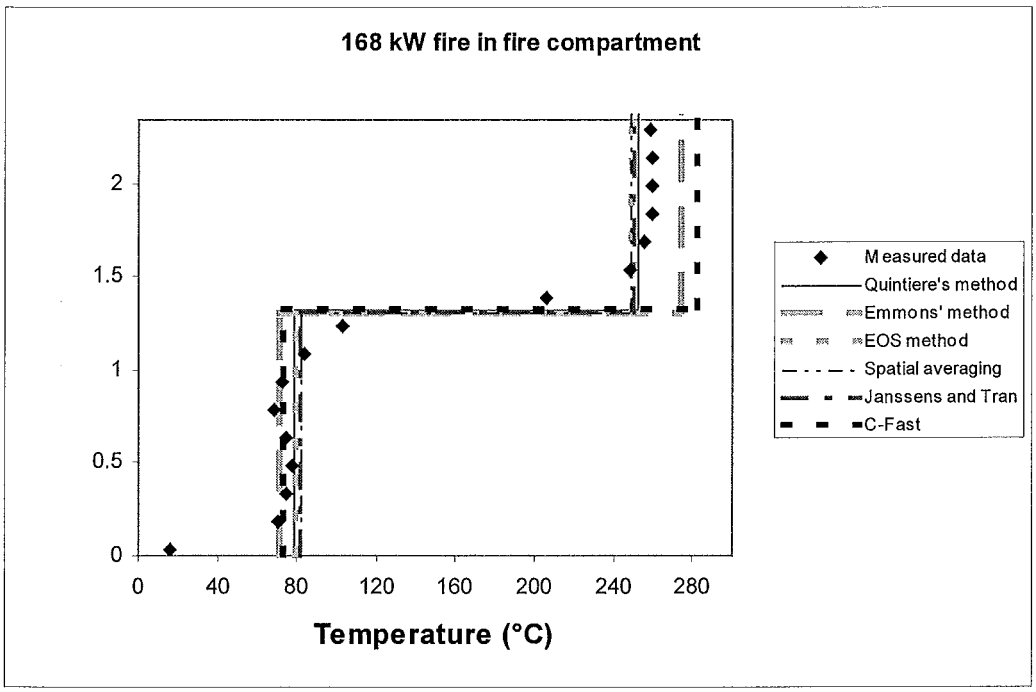

Figure 6-15 Comparison of averaging methods in fire compartment for 168kW fire

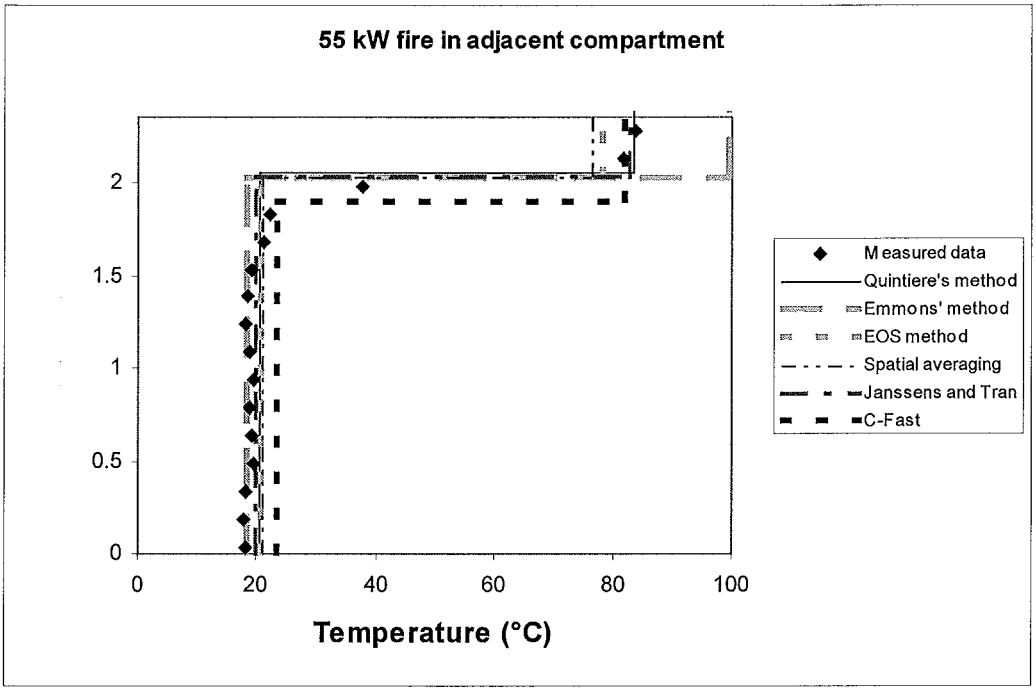

Figure 6-16 Comparison of averaging methods in adjacent compartment for 55kW fire

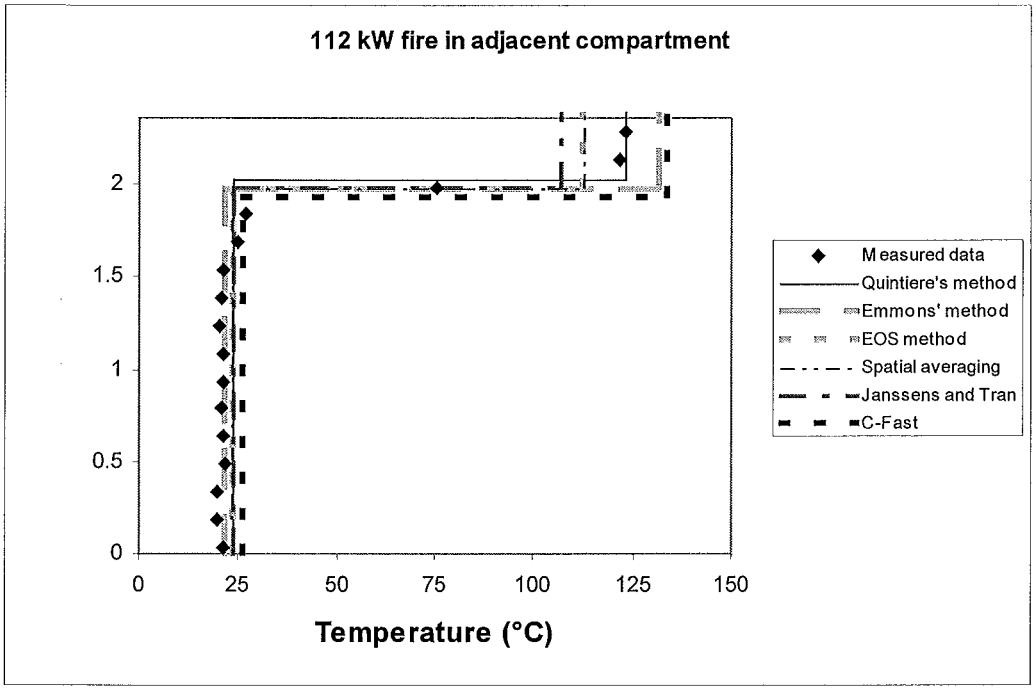

Figure 6-17 Comparison of averaging methods in adjacent compartment for 112kW fire.

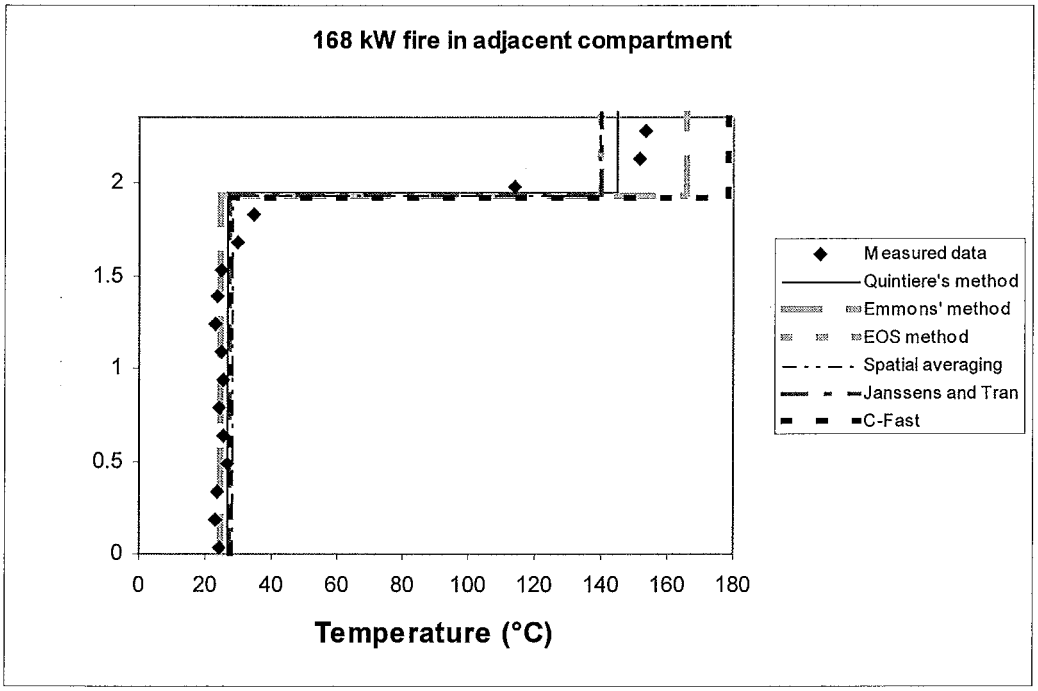

Figure 6-18 Comparison of averaging methods in adjacent compartment for 168kW fire.

The criteria for determining how accurately the data is reduced is the same as mentioned earlier where the accuracy of the method is judged by the closeness of the data to the top and bottom thermocouples (where the temperatures are almost constant). Although this criteria was only specified for the 112kW fire it can be seen in figures 6.13 to 6.18 that the uniformity in the upper and lower thermocouples does not vary with fire size. The top 5 and bottom 7 thermocouples in the fire compartment are approximately uniform and the top 2 and bottom 13 thermocouples in adjacent compartment are approximately uniform.

Emmon's method estimated the lower zone temperature, as the temperature reading of the bottom thermocouple. This proved successful with estimates being fairly close to the thermocouple which forms the lower zone. There was a slight under prediction due to the temperature of the bottom thermocouple being a little lower than the other lower zone thermocouples, however this was not significant in estimating the lower zone temperature with the results being fairly close to the other averaging methods. All the other methods predicted the lower thermocouple temperature satisfactorily, as was the case when the N% method was used for the interface height prediction method.

Unlike the N% method the predicted interface height was not directly above the uniform bottom thermocouples in each compartment. The interface height was located in the middle of the interface layer thus some of the temperatures included in the averaging methods using direct Spatial averaging and Averaging based on equation of state were significantly higher than the readings from the uniform bottom thermocouples. These methods use an integral of temperature or the reciprocal of temperature over the entire lower volume to determine the lower layer temperature. However as most of the temperature readings in the lower zone occurred in the uniform region, readings that were in the mixed interface layer had little influence on the total average calculated in the lower zone. The fire compartment had a lower interface height than the adjacent compartment resulting in proportionately less uniform temperature readings being taken for lower zone averaging. This meant that the thermocouple readings in the interface layer for the fire compartment had slightly more influence than the adjacent compartment causing a very small overestimation of temperature.

Emmon's method was the only method to constantly over predict the upper layer temperature in each run. Emmon's method solved the upper layer temperature from an integral identity using lower zone temperature and predicted interface height. Although a slight under prediction in the lower layer did not significantly effect the lower layer temperature estimation, it did result in a large over-prediction of the upper layer. This shows the weakness of combining an integral identity to determine an average with the very simplified assumption such as using the bottom thermocouple reading to determine the lower zone temperature.

Direct Spatial averaging and Averaging based on equations of state gave very similar results. The similarity in the methods should be expected due to the uniformity of the temperatures in the upper and lower layers. To evaluate the difference between these two methods it would be necessary to analysis data that was less uniform. The upper zone temperature prediction was always under predicted. Both methods directly find the upper average from integrating the temperature over volume or the reciprocal of temperature over volume from the interface height upwards. As the interface height is located in the middle of the interface layer, some of the temperatures included in the averaging would be located there too. Unlike the bottom thermocouple readings the amount of uniform temperature readings from thermocouples in the upper layer is quite small thus thermocouple readings in the interface layer that are included in the averaging can impart significant effects. Therefore for this set of data in all runs these two methods have always underestimated the upper zone temperature. The amount of under-prediction is more significant in the adjacent compartment where only the top two thermocouples are approximately constant.

Janssens and Tran's method of predicting the upper layer temperature varied from significantly underestimating the temperature in the adjacent compartment, to slightly underestimating temperatures in the fire compartment. The accuracy of the Janssens and Tran's method was again due to the location of the interface height. This method uses a mathematical average of the thermocouples above the interface height and if any of these

thermocouples lie in the interface layer region then underestimation of the upper layer temperature will ensure.

Quintiere's method had the most success in accurately predicting the upper layer temperatures. In all runs shown the upper layer profile lines up very well with the top five thermocouples for the front room and top two for the back room. For these sets of data Quintiere's model works the best because it does not attempt to mathematically average the entire upper zone. Rather it calculates the upper zone temperature, averaging the temperatures that deviate less than 10% from the top thermocouple reading. The success of Quintiere's model might not be good however if the upper layer temperatures are not constant in height as this may cause temperature in the upper layer to deviate more than 10% from the top thermocouple reading.

Figures 6-13 to 6-18 also show how the temperature averaging methods compare with the zone model C-Fast. The lower layer temperature predicted in C-Fast is very close to all of the methods while the upper layer temperature is about 4-40°C higher than the upper layer temperatures reduced from experimental data. This larger envelope of predicting upper layer temperature is closest to Emmons' method. Therefore for the corner thermocouple trees C-Fast gives a conservative prediction of the lower and upper layer temperatures.

The major problem with the averaging methods except for Quintiere's is they evaluate the temperatures directly above and below the interface height. However as mentioned in the previous section a clear-cut interface height between the upper and lower layer does not exist, there is rather an intermediate area or interface layer between the two zones. Errors are caused when some thermocouple measurements used for the overall zone averages are located within this interface layer. This could be improved if the data was effectively divided into three zones instead of two, determining an interface layer as opposed to an interface height to distinguish temperatures into an upper and lower layer. In this method the temperatures used for the upper and lower zone averaging would only be taken above or below the interface layer. This would prevent the problem of

temperatures in the mixed interface layer being used for analysis of the average temperatures.

One suggestion for an empirical method of achieving this goal is to firstly establish an interface height and then determine the interface area as the area where the slope of temperature over height between thermocouple readings is more than double the average slope between them. The temperatures would then be averaged from the next thermocouple reading above or below the interface layer. This method has been applied very successfully in the temperature averaging methods as shown in the following figures: Figures 6-19 and 6-20 show the zonal temperature predictions using the "interface layer" method for the fire compartment and adjacent compartment respectively. Using this "interface layer," method the results from spatial averaging, EOS averaging and Janssens and Trans method are virtually identical and compare very closely with Quintiere's method. Appendix 6 shows this interface layer method applied to the 55kW and 168kW fires with equally impressive results.

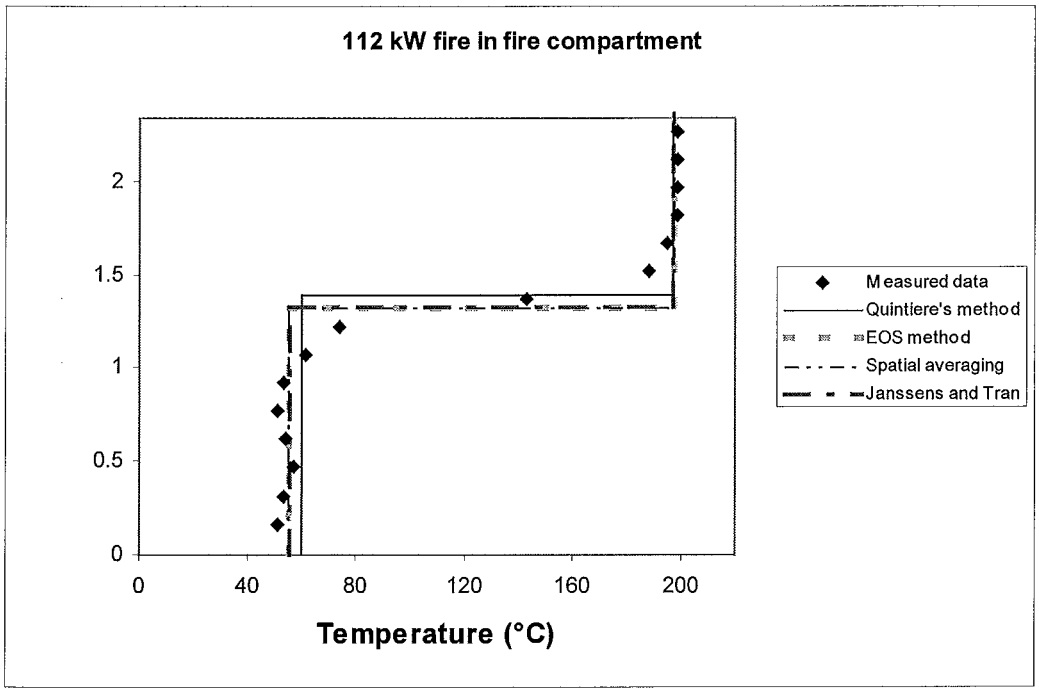

Figure 6-19 Temperature prediction based on an interface layer in fire compartment using corner thermocouple tree.

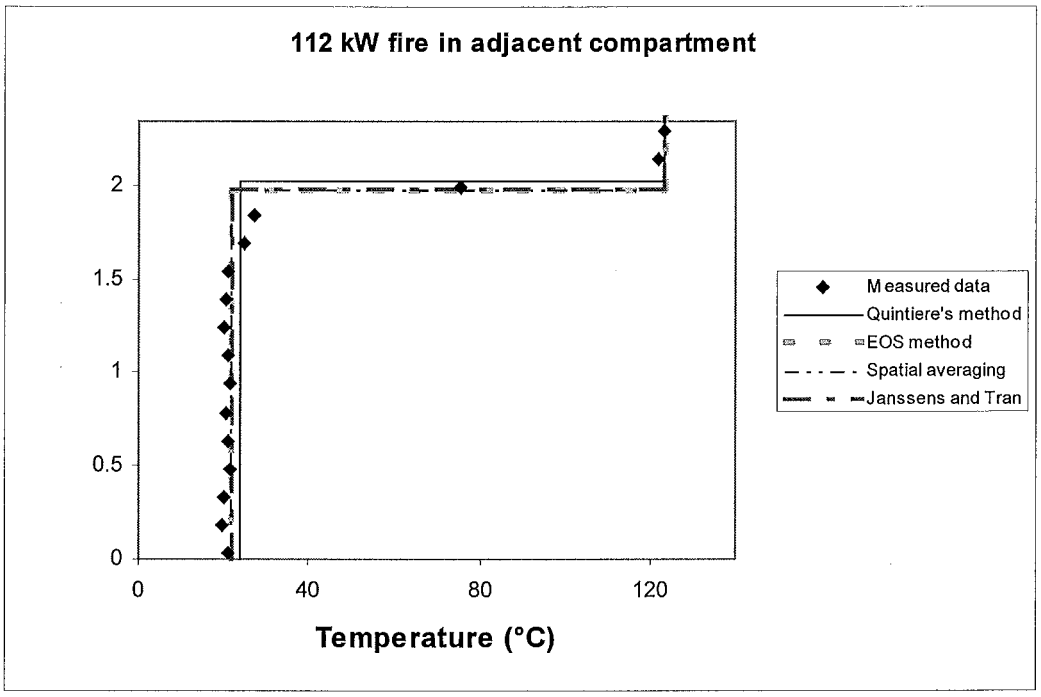

Figure 6-20 Temperature prediction based on an interface layer in adjacent compartment using corner thermocouple tree.

6.2.4 Comparison of averaging techniques using centreline thermocouple trees

Previous research in reducing data to evaluating zone models has used the corner thermocouple tree to determine the zonal temperatures. This may be misleading if we assume the interface layer being uniform is incorrect. Two centreline thermocouple trees located 900mm and 2700mm from the front wall in the fire compartment were analysed as well as one tree in the direct centre of the adjacent room. Thermocouple readings in the corner of a compartment where gas velocities are minimised may give the closest approximation of a zonal model with clear, uniform upper and lower layers. However temperature averaging methods need to be compared on how they handed non-perfect data. Figures 6-21 and 6-22 shows the two layer profiles predicted for the thermocouple trees located 900mm and 2700mm from the front of the fire compartment respectively. Figures 6-23 show the predicted two layer profiles for the centreline thermocouple trees located 1800mm from the middle wall in the adjacent compartment.

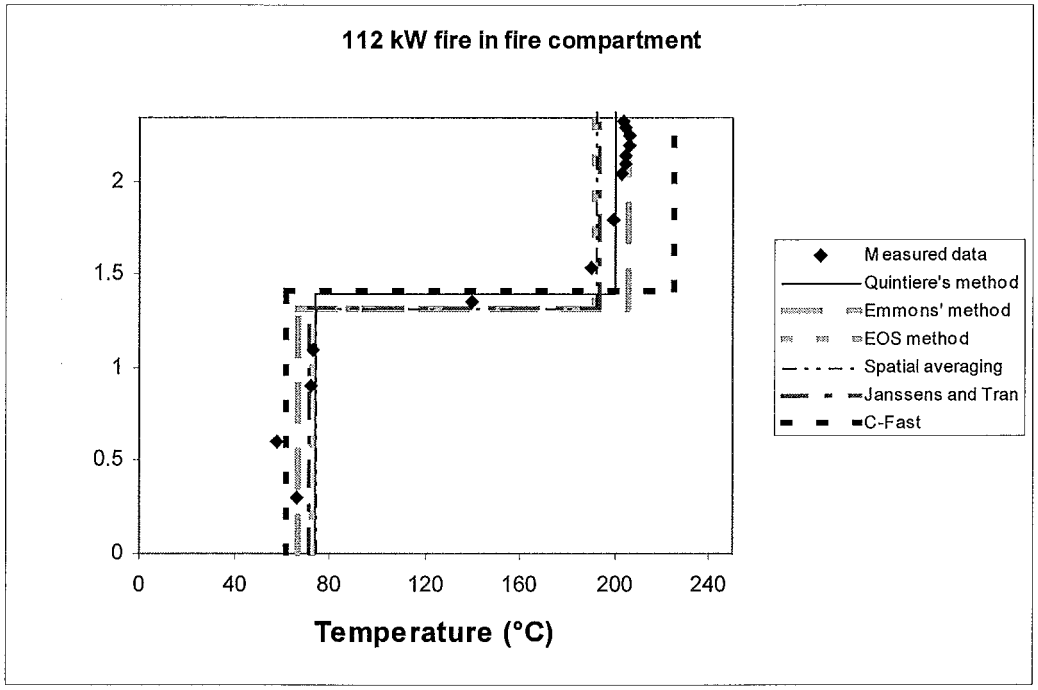

Figure 6-21 Comparison of averaging techniques using centreline thermocouple tree located 900mm from front in fire compartment during 112kW fire

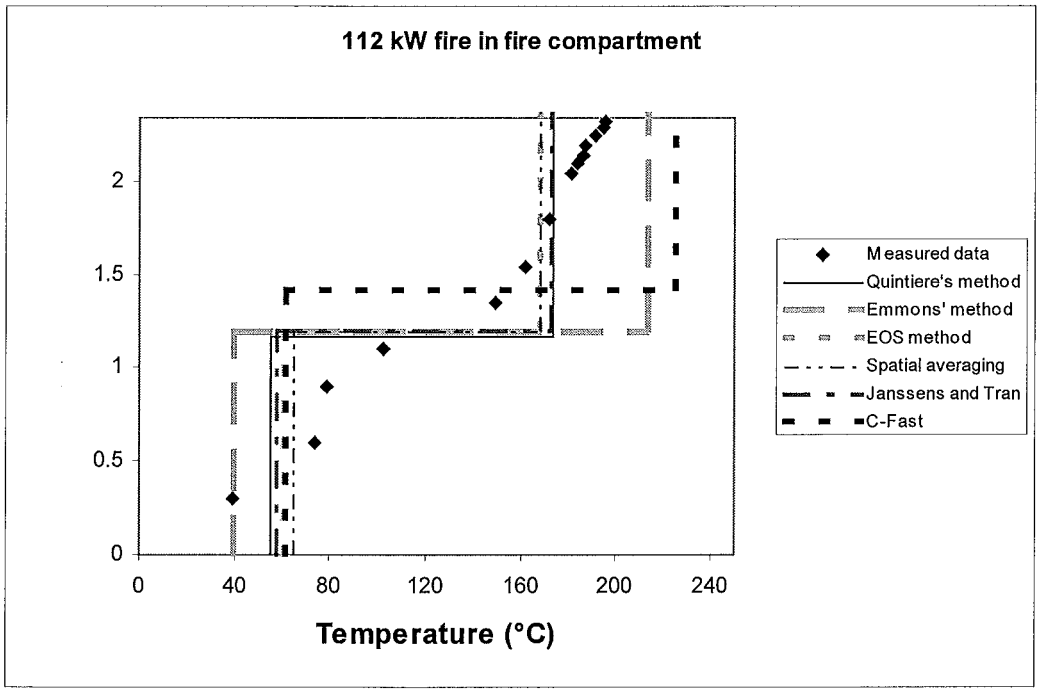

Figure 6-22 Comparison of averaging techniques using centreline thermocouple tree located 2700mm from front in fire compartment during 112kW fire

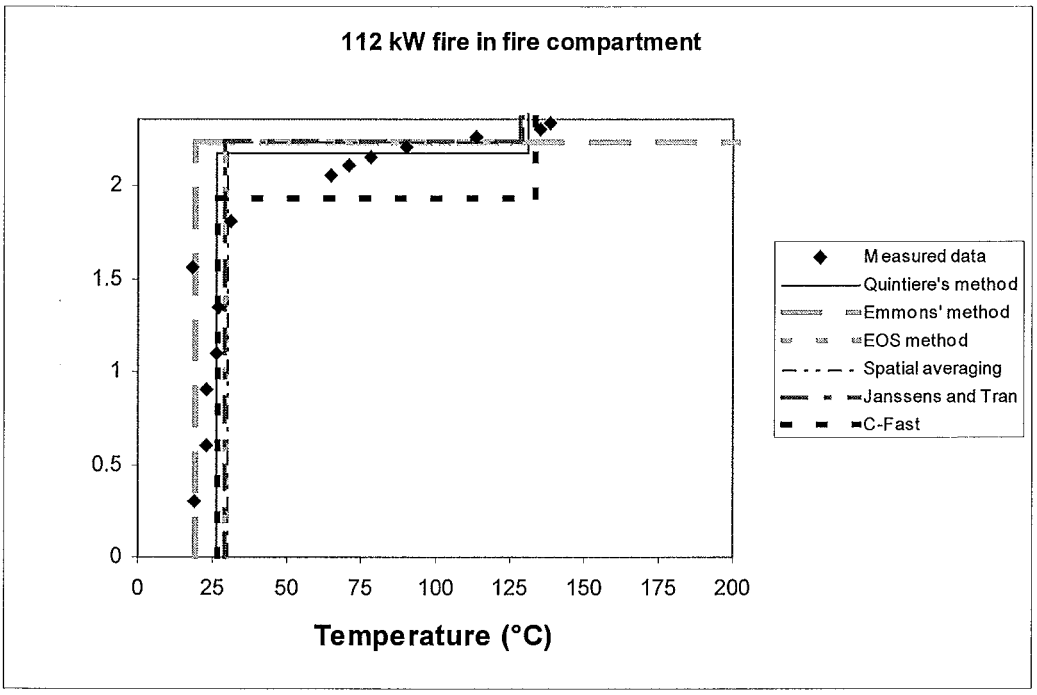

Figure 6-23 Comparison of averaging techniques using centreline thermocouple tree located 1800mm from front in fire compartment during 112kW fire

Tables 6-2 to 6-4 show a comparison between temperature predictions for the corner thermocouple and the centreline thermocouple trees. Spatial averaging and Quintiere's method are used for the comparison. Spatial averaging had very similar readings to Averaging via the equation of state and Janssens and Tran's method. Quintiere's method is shown as it provides good predictions of the interface layer in the corner, but unlike the other methods uses an iterative process for calculating interface height and zonal temperatures, not attempting to mathematically average any of the zones.

Table 6-2 Comparison of zonal temperature predictions between corner tree and centreline tree located 900mm from front wall in fire compartment.

	Fire Size (kW)	Interface height (m)			Upper layer T (°C)			Lower layer T(°C)		
		Corner	Centre	Diff	Corner	Centre	Diff	Corner	Centre	Diff
Spatial Averaging	55	1.39	1.40	1%	124	126	2%	39	52	34%
	112	1.33	1.32	1%	190	192	1%	59	74	24%
	168	1.31	1.29	2%	248	249	0%	81	98	21%
Quintieres Method	55	1.42	1.42	0%	127	129	2%	38	51	24%
	112	1.39	1.40	1%	197	201	2%	60	74	19%
	168	1.32	1.37	4%	253	260	3%	79	98	20%

Table 6-3 Comparison of zonal temperature predictions between corner tree and centreline tree located 2700mm from front wall in fire compartment..

	Fire Size (kW)	Interface height (m)			Upper layer T (°C)			Lower layer (°C)		
		Corner	Centre	Diff	Corner	Centre	Diff	Corner	Centre	Diff
Spatial Averaging	55	1.39	1.22	12%	124	129	11%	39	30	15%
	112	1.33	1.20	10%	190	168	11%	59	83	39%
	168	1.31	1.15	12%	248	220	11%	81	88	8%
Quintiere's Method	55	1.42	1.22	14%	127	113	11%	38	41	6%
	112	1.39	1.16	16%	197	174	12%	60	55	8%
	168	1.32	1.22	8%	253	233	8%	79	82	4%

Table 6-4 Comparison of zonal temperature predictions between corner tree and centreline tree located 1800mm from middle wall in adjacent compartment.

	Fire Size (kW)	Interface height (m)			Upper layer T (°C)			Lower layer (°C)		
		Corner	Centre	Diff	Corner	Centre	Diff	Corner	Centre	Diff
Spatial Averaging	55	2.04	2.27	10%	76	84	8%	21	25	15%
	112	1.98	2.25	12%	112	129	13%	24	30	21%
	168	1.94	2.24	13%	139	167	17%	28	38	26%
Quintieres Method	55	2.06	2.09	1%	83	71	15%	21	21	3%
	112	2.06	2.09	1%	83	71	15%	21	21	3%
	168	1.95	2.14	9%	145	170	15%	27	31	15%

The assumption of the thermocouple trees being fairly quiescent with minimal mixing of the relevant layers is not applicable for the readings taken from centreline thermocouple trees. Mixing as a direct result of turbulent forces generated from the fire plume, ceiling jets, gas expansion, air being sucked in from adjacent compartment, wall effects and other phenomenon will cause the temperatures to be more non-uniform within each zone than the thermocouples trees in the corner. This will also allow a better comparison to He's work, which dealt with an upper layer where the temperature increased with height.

Figure 6-21 shows the estimated data reduction techniques versus the measured profile for the thermocouple tree located 900mm off the front wall in the fire compartment. A stratifying effect between the two layers can still be easily seen in the measured data. Emmon's method predicts the upper zone temperature well in this case, as the lower zone temperature prediction is very accurate. In all methods the fit to the upper layer temperature is comparable to the fit in the corner thermocouple tree as shown in table 6-

2. The differences between them range between 0 to 4%. There is a significant difference between the estimated lower layer temperature for each run with differences ranging between 19% to 34%. This difference cannot be attributed to the predicted interface height as this changes very little between the corner and centre trees. The bottom thermocouples were probably subject to some turbulent forces arising from the buoyancy of plume gases, however this would be quite small as shown by the uniformity of the four bottom thermocouple readings. The bottom thermocouples of this centreline tree would have been subject to significant amounts of radiative due to their close proximity to the fire. The corner thermocouple tree was much further away from the fire source and would not be so significantly effected by the radiation.

The steady state zonal temperature predictions from the thermocouple tree located 2700mm from the front wall in the fire compartment is shown in figure 6-22. The measured temperature profile was very different than that measured for the thermocouple tree located 900mm from the front of the fire compartment. The profile shows that both the upper and lower thermocouples were non-uniform, increasing temperature with height although not linearly. However a distinction between the upper and lower layers is still clearly visible with the increase of temperature over height between the 4^{th} and 5^{th} thermocouple being much greater than at any other point in the graph.

Again Emmon's method over predicts the upper layer temperature. The lower layer is much less uniform than in the corner trees and increases significantly with height. This causes the predicted lower zone temperature to be much too low, resulting in a calculation of the upper zone temperature that is unrealistically high. All other methods tend to give fairly similar results in predicting the temperature of both layers. Quintiere's methods still works well despite the increase in temperature of thermocouples in the upper zone as the upper layer temperatures are still within 10% of the top temperature.

Table 6-3 compares the results from the centreline thermocouple tree located 2700mm from the front of the compartment with the corner tree in the fire compartment. Both Spatial averaging and Quintiere's method show similar correlations between the

centreline and corner thermocouples. For the centreline tree the upper zone temperature is lower than in the corner and the lower zone temperature is higher. The interface layer here is lower than the corner prediction. This thermocouple tree is half way between the door and fire so the air surrounding it is effected by mixing due to vent flows, turbulence from the buoyant gases in the plume and from the hot/cold interface between the two compartments.

Although there are considerable difference in the temperatures and interface height predictions at this tree compared to the corner tree, this does not indicate these differences would occur in other parts of the compartment. The thermocouple tree located 900mm from the front wall in the fire compartment gave fairly consistent results with the corner thermocouple tree except for the lower zone average which was higher due to radiation. This would indicate that the effects of mixing from the plume flow is not as important as the mixing caused by vent flows and shear mixing between the incoming and outgoing streams of gases. This is mainly a problem near the vent and would not exist in most places in the room, so the temperatures in most parts of the compartment could be well approximated by the temperature in the corner.

Figure 6-23 shows the calculated two layer profiles and the measured experimental data for the centreline thermocouple trees located in the adjacent compartment 1800 mm from the door or exactly in the middle of the room. The measured data had a fairly uniform lower zone temperature, however the upper zone was non-uniform and continuously increased with height due to the ceiling jet exiting the compartment. This ceiling jet effect would be considerably different if a soffit existed at the outside vent of the adjacent compartment causing backflow, which would allow a much more significant layer to develop.

The criteria for judging how well the upper layer zone is estimated is much more ambiguous with the non-uniformity of temperature. All methods except for Emmons' predicted fairly similar temperatures for the upper zone, which was close to the temperature of the upper two thermocouples. Emmon's method completely fails in

predicting the upper layer temperature with averages up to and exceeding 500°C (not seen in graphs, see appendix 2) higher than what they should be.

Quintiere's method, Jansens and Trans, Averaging based on equations of state and Spatial averaging, all give very similar results. The interface height prediction is very high up in the compartment resulting in the methods predicting the upper layer average to be near the temperature of the second thermocouple from the ceiling. As shown in table 6-4 the upper predictions from the centreline thermocouple tree are quire similar to the corner tree predictions ranging from 8% to 17%. However, the average zonal temperatures from the centre thermocouple tree are lower than the corner tree predictions in this compartment. Therefore using data reduced from the corner thermocouple trees for validation of a zone model is sufficient for this scenario assuming the other centreline thermocouples give similar results.

This effect of the ceiling jet on the upper layer average does not significant affect the upper layer average. If the interface height were predicted using the N% method the temperature in the upper layer of the room would be significantly reduced. Although the N% method worked much better in the adjacent compartment it would fail to work here, as all the points in the ceiling jet would be included in the averaging.

6.2.5 Comparison of averaging techniques for corner fire

The previous analyses have been for a fire located in the centre of the room. An experimental run was staged where the fire was located in the front corner of the fire compartment as specified in chapter 4. Putting the burner in the corner of the room will changes the dynamics of the fire plume as entrainment is quartered due to walls being on two sides of the fire. With less entrainment the flames of the fire are significantly higher as the fire needs to search for more oxygen. The combustion will be more incomplete compared to the centre runs, as less oxygen is available. Figures 6-24 to 6-26 show the measured temperature profiles and estimated zonal temperature averages for thermocouple trees in the fire compartment located in the corner, 900mm from front wall and 2700mm from the front wall respectively.

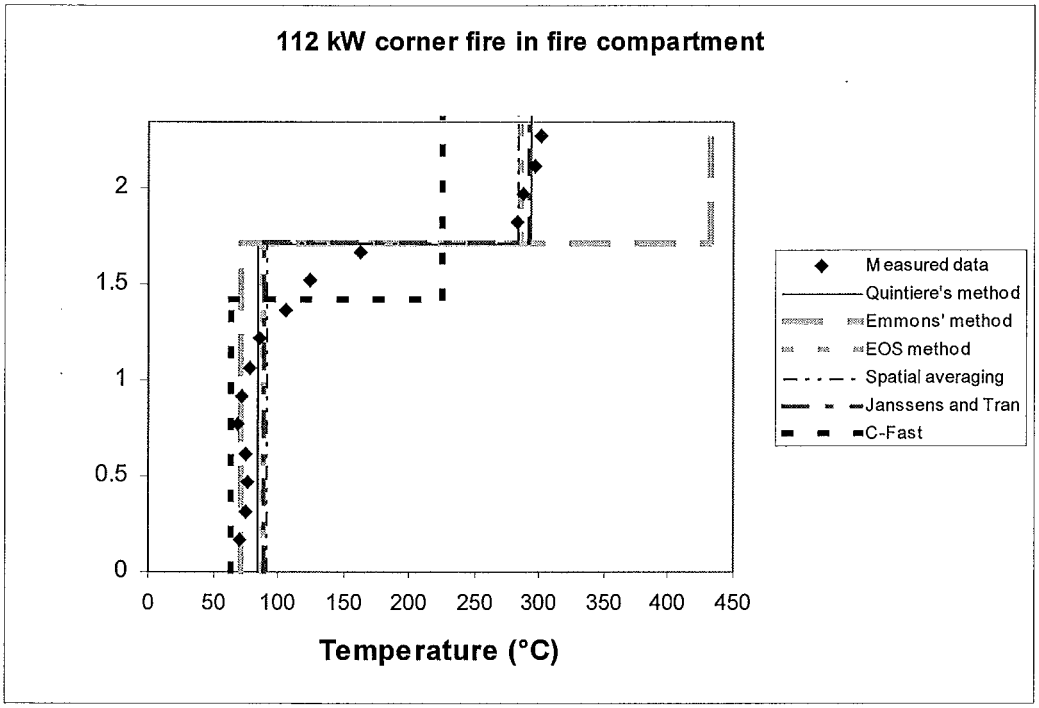

Figure 6-24 Comparison of averaging techniques in fire compartment for corner fire using corner tree thermocouples

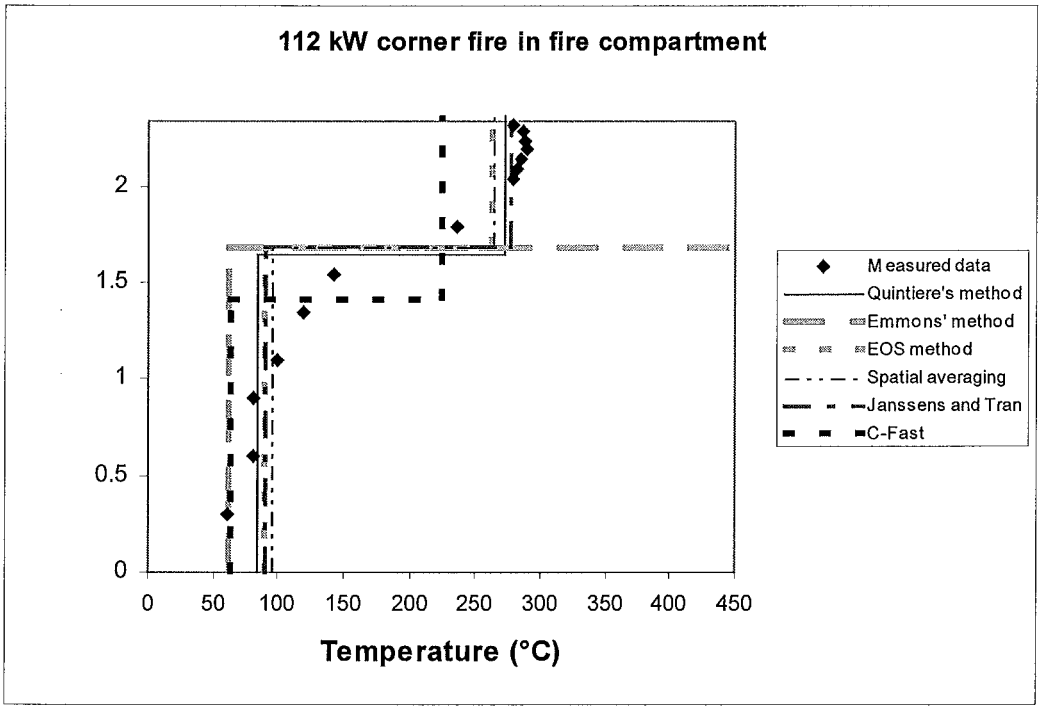

Figure 6-25 Comparison of averaging techniques in fire compartment for corner fire using centreline thermocouple tree located 900mm from front wall.

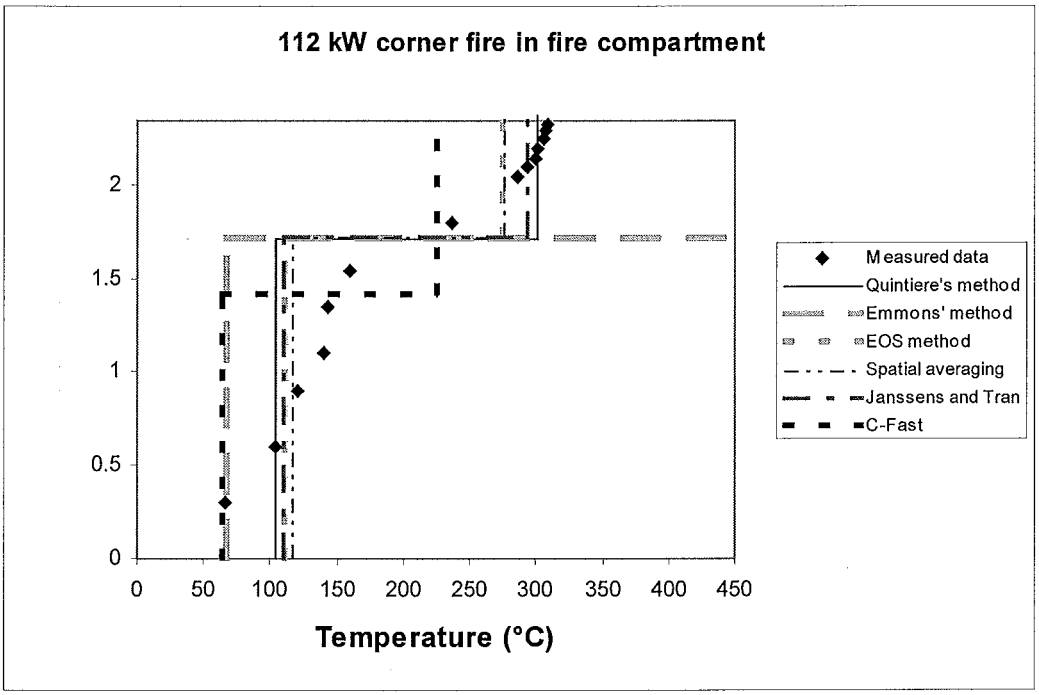

Figure 6-26 Comparison of averaging techniques in fire compartment for corner fire using centreline thermocouple tree located 2700mm from front wall

Having the fire in the corner of the room was a good test to see if the data reduction techniques would work if some of the assumptions regarding zone modelling were not valid. These included the assumption that fluid frictional effects at solid boundaries are ignored and that the plume size is insignificant compared to its surroundings. Table 6-5 shows the range of interface heights and zonal temperatures predicted from the fire compartment for the corner thermocouple tree and tree's located 900mm and 2700 mm from the front of the compartment.

Table 6-5 comparison of predicted interface height, and zonal temperatures using Quintiere's method.

	Interface height (m)	Upper layer T (°C)	Lower layer (°C)
Corner	1.71	293	85
900 from front	1.71	301	104
2700 from front	1.65	272	85
Range	0.06	29	20

The measured data from the centreline thermocouple tree located 900mm from the front wall in the fire compartment had the least distinction between the upper and lower areas, though appears to be still approximated well by all averaging techniques except for Emmon's method. The thermocouple tree located 2700mm from front wall also appears well mixed however this is to a lesser extent than when the fire was located in the centre of the room.

The range between the three trees was quite small with the corner tree being 8°C cooler in the upper layer than the tree located 900mm from the front of the compartment. This was probably due to the radiation effects of the fire as the flames were significantly higher than when the fire was located in the centre of the room. Quintiere's method was used for the comparison as all methods (except for Emmon's method) gave very similar results.

Table 6-4 shows how the zonal temperature predictions and interface heights compared between the three-thermocouple trees. The interface height did not alter significantly between methods (0.06s). The centreline thermocouple couple trees located 900mm from the front wall, exhibited upper and lower layer temperatures that were significantly higher than the other trees. Mixing in the upper layer tends to decrease the temperature, so other factors must have caused this temperature rise. As the fire had much less entrainment than the fire in the centre of the room, the flame height was significantly higher. With higher flames the radiative surface of the fire exposed to the thermocouple tree would affect the upper zone thermocouples in close proximity, though this would need to be verified however with working aspirated thermocouples. The corner tree was 19°C hotter than the tree located 2700mm from the front of the compartment due to the influx of cooler air mixing with the upper layer present at that tree.

Although C-Fast allows the fire location to be specified in its input it does not simulate corner fires well as shown in figures 6-24 to 6-26, nor does it take into account the lack of entrainment of cool air, which causes a significant increase in the temperature of the upper layer.

6.2.6 Useability of data

For the conclusions from these experiments to have any validation, the results need to be repeatable. Seven runs were performed in the experiment, although only three fire sizes were used. Graphs of corner tree temperature predictions for runs not shown in the results can be seen in Appendix 3. After the first two runs the sand in the burner was replaced and after the 5th run the doors to the outside off the compartment were closed to provide more stable ambient conditions during the run. It was assumed however that these changes did little to alter the experimental results and would not significantly affect the zone modelling of the enclosure. Two runs at 55kW and three runs at 168kW were completed. Comparisons between the predicted interface height, lower layer temperature and upper layer temperature in the fire compartment are shown below. Table 6-6 compares run 4 and 5(55kW) and table 6-7 compares run 3 and 6(112kW).

Table 6-6 Repeatability for 55 kW fire (runs 4 and 5)

Method	Discrepancy		
	Interface height	Upper layer temperature	Lower layer temperature
Emmons	3%	2%	14%
EOS	3%	1%	10%
Spatial averaging	3%	1%	10%
Janssens and Tran	3%	2%	21%
Quintiere	6%	1%	8%

Table 6-7 Repeatability for 168kW fire (runs 3 and 6)

Method	Discrepancy		
	Interface height	Upper layer temperature	Lower layer temperature
Emmons	0%	5%	3%
EOS	0%	4%	2%
Spatial averaging	0%	4%	2%
Janssens and Tran	0%	4%	2%
Quintiere	0%	4%	2%

Table 6-6 demonstrated that there were only small differences in the interface height level and the upper layer temperature. The difference in the lower layer temperature was more significant, however this would have been due to changing ambient conditions. This may have been helped by the closing of the outside doors, which increased the ambient temperature in each room from 15°C to 18°C. Table 6-7 shows that the differences in runs 3 and 6 are also very small with a minor difference between the upper layer temperatures.

6.2.7 Averaging based on transport terms

An alternative method was used for averaging the temperature of the upper layer using the velocities and temperatures of the gases exiting the front compartment. He [5] used this method to verify the results from averaging based on the equation of state. Unfortunately the bi-directional probes gave inconsistent readings from which no conclusions could be made.

7 Conclusions

Techniques were analysed that convert experimental measurements taken in a compartment fire into a reduced form that could be used for comparisons with zone models. Three interface height prediction methods and six temperature averaging methods were investigated. These methods were used to analyse a series of full scale fire experiments in two compartments separated via a door way.

The experimental data obtained from three fire sizes of 55kW, 112kW and 168kW indicated that a significant interface layer of mixed hot and cold air existed between the smoky and clear or hot and cold layers in the room. This required that two interface height predictions should be made when producing the data. One interface height prediction needs to be made specifically for the calculation of the average temperature within each zone, however this should not be used for validating the interface height determined by a zone model. This interface height would be determined as the height that is directly in the centre of the interface layer, where the change in temperature over height is maximised. A second interface height estimation should be used for validating a zone models output of interface height, which is used for assessing tenability limits for a fire simulation. As the tenability limits for interface height is based on visual obscuration, the height would have to be located at the bottom of the interface layer to be conservative.

The empirically based N% method of predicting interface height did not predict the interface height with any degree of accuracy in the main fire compartment. Previous research used the N% method successfully in rooms had had direct venting to outside ambient conditions. Having a vent to ambient conditions results in lower layer compartment temperatures that are only slightly higher than ambient, however in this research the fire compartment only had a vent leading into the adjacent compartment. This resulted in a lower layer temperature that was significantly higher than ambient temperature causing a large under prediction of the interface height, in many cases predicting the height to be at ground level. The N% method worked satisfactory in the

adjacent room (which had direct venting to ambient conditions) and predicted the interface height near the bottom of the interface layer. This would be good for validating the zone model calculation of interface height, however would cause an underestimation of the upper layer temperature when averaging techniques were used.

Quintiere's method and the maximum slope method predicted the interface height directly in the centre of the interface layer for nearly all of the thermocouple trees. This did not give a good interface height for direct comparison with a zone model, but it gives a good height for temperature averaging methods to be based on. When the upper layer consists almost solely of a ceiling jet, the interface height prediction using Quintiere's method and the Maximum slope method tend to give a very high estimate of the interface layer.

A comparison with the Zone model "C-Fast" showed that C-Fast's calculation of interface height was closer to Quintiere's method and the maximum slope method rather than the N% method. This indicated that C-Fast predicts the interface height in the middle of the interface layer and not at the bottom of it. Therefore using the interface height calculation from C-Fast to assess tenability conditions may lead to an incorrect design.

Six methods were used for averaging temperatures. Emmon's method constantly predicted the upper layer temperature to be higher than any of the temperature measurements in the thermocouple trees. This over-prediction was not too significant except for thermocouple trees that had significant mixing in the lower part of the tree. As Emmon's method assumes that the lower zone temperature does not vary from the bottom thermocouple reading, when the lower thermocouple readings increased in height the upper temperature prediction was greatly over estimated. Quintiere's method worked excellently to predict the lower and upper layers, as it did not depend on temperatures in the interface layer for the averaging. Spatial averaging through using the equation of state and Janssens and Tran's method gave very similar good results, but all slightly underestimated the upper layer temperature (though well estimated the lower layer

temperature). This was because some of the temperatures used in averaging the upper layer averaging were located in the cooler interface layer.

It is suggested that averaging schemes such as Spatial averaging, Averaging via the equation of state, and Janssens and Tran's method which involved integration of temperature or the reciprocal of temperature over volume use a different approach for determining the interface height. This alternative approach would involve determining upper and lower limits of the interface layer and integrating the temperatures to these limits not to the actual interface height (which does not exist anyway). This would also be much closer to a physical meaning of the zone concept. The bottom of the interface layer could then be used to validate the zone model calculations of the interface layer. Calculation of the zonal temperatures using this method all yielded almost identical results for all three methods, indicating that the interface height(s) used in calculating the averaging temperatures are a much more important factor in obtaining the correct average temperatures than the averaging methods themselves.

C-Fast showed favourable comparisons to the temperatures predicted by all the methods, predicting a slightly larger upper layer temperature than the models predicted (except for Emmon's method). C-Fast failed to predict the correct interface height and zonal temperatures for a corner fire, indicating that the assumptions that are broken down by putting the fire in the corner have a significant effect on the temperatures in the room.

8 Recommendations for future work

The findings from this research have indicated that when validating a zone model the interface height used in the calculation of zonal temperatures needs to be different than that calculated for validating the interface height of a zone model. The interface height used for validating that aspect of the zone model should be approximately at the bottom of the interface layer, however like the data reduction techniques current zone models such as C-Fast only output the interface height that is used for temperature calculation. It would be interesting to see a zone model that output the interface height as the estimated height at the bottom of the interface layer, not directly in the middle of it.

Further, better methods for calculating the interface layer boundaries could be looked at. The prescribed empirical method in this text works well for data that is well stratified, however may not work so well if the data is less uniform. This needs to be investigated

As mentioned earlier in the text a more thorough investigation of the ceiling jet in the adjacent compartment might prove useful to see how this varies with the length of the compartment. Adding a soffit to the end of the adjacent compartment and other different geometry's could lead to interesting results.

9 References

1. Friedman,R.1992. "An International Survey of Computer Models for fire and Smoke," *J. Fire Prot. Eng.,* 4(3):81-92
2. W.K.Chow, "Prediction of Fire Environments in Apartments Using Zone Models," *Journal of fire Sciences,* 14:263 – 311.1996
3. Luo, M., He, Y. and Back., V.," A comparison of existing fire model predictions with experimental results from real fire scenarios," *J. Applied Fire Science*, 6:357-382,1996
4. Walton, W.D.1995. "Zone computer fire models for enclosures," In the *SFPE Handbook for Fire Protection Engineering,DiNenno*, ed., Boston, MA : Society of fire protection engineers, 7:3-148-3151.
5. NIST. *A User's Guide for FAST: Engineering Tools for Estimating Fire Growth and Smoke Transport.* U.S. Department of Commerce
6. Quintiere J.G.,1995. "Compartment fire modelling," In the *SFPE Handbook for Fire Protection Engineering,DiNenno*, ed., Boston, MA : Society of fire protection engineers.
7. Janssens, M. L and H. C. Tran 1992. "Data Reduction of Room Tests for Zone Model Validation," *Journal of Fire Sciences*, 10:528-555
8. He, Y. 1997. "On Experimental Data Reduction for Zone Model Validation," *J. Fire Sciences,* 15:144-161
9. B.J. McCaffrey and J.G. Quintiere, "Buoyancy-Driven Counter-currents Flows Generated by a Fire Sources, "*Heat Transfer and Turbulent Buoyant Convection,* Vol. II, D.B. Spalding and N.Afgan, ed., Hemisphere Pub. Co., pp. 457 – 472 (1977)
10. Peacock,R. D., Forney, G. P., Reneke, P.,Portier, R. and Jones, W. W. 1993."CFAST, The Consolidated Model of Fire Growth and Smoke Transport,' NIST Technical Note 1299, National Institute of Standards and Technology, Gaithersburg, Maryland, U.S.A.
11. Cooper, L., M.Harkleroad, J.Quintiere and W. Rinkinen. 1982. "An Experimental Study of upper Hot Layer Stratification in Full-Scale Multiroom Scenarios," *J, Heat Transfer,* 104:741-749

12. Quintiere, J., K. Steckler and D. Corley. 1984. "An Assessment of Fire Induced Flows in Compartments," *Fire Science and Technology,* 4:1-14.
13. Emmons, H. 1989. "Vent Flows,"In the *SFPE Handbook for Fire Protection Engineering*, Ph. DiNenno, ed., Boston, M.A: Society of Fire Protection Engineers, Part 1,pp. 130-137
14. ISO 9705 (1993) *Full Scale Room Test for Surface Products*, International Standards Organisation, Geneva, Switzerland
15. Buchanan,A., *Fire Engineering Design Guide,* Centre for advanced Engineering, University of Canterbury 1994.

Appendix 1 – Inputs into C-Fast

Simulations were performed with C-fast for the compartment requiring the compartmental dimension, vent sizes and fire area size (burner area) as specified in chapter 4.

C-Fast also required the properties of the surrounding enclosure to estimate the enthalpy conducted through the walls, ceilings and floors.

As C-fast allows surface compositions to be made up to three materials thick, both the insulation and the Gib board could be included in the model. The thermal properties of these two surfaces are specified below. The conductivity for the insulation was estimated assuming a mean temperature of 100°C.

Table A1-1 inputs into C-Fast

Emissivity 0.9

Material	Conductivity W/mK	Specific heat J/kgK	Density kg/m^3	Thickness M
ISB insulation	0.045	720	75	0.025
Gib fyreline board	0.16	900	790	0.013

The heat release rate specified in the modelling increase from 0 kW to a constant value in 10 seconds where it remained for 3600s. Then it was reduced to zero in 3610s. This allowed more than sufficient time for the simulation to arrive at steady state values for the hot upper layer, the cool lower layer, and the smoke interface height.

Three constant heat release rates of 55kW, 112kW and 168kW were used for the run. These were taken from readings of the mass flow controller during the experimental runs. For these simulation the burner was specifies as being in the centre of the front room. A further simulation was performed with the burner located in the corner of the room and a heat release rate of 112 kW.

The results of these simulations are shown below in table A.2.

Table A1-2 Predictions of interface heights and zonal temperatures from C-Fast simulations

	Fire Size Fire Location	55kW Centre	112kW Centre	168kW Centre	112kW Corner
Interface height	Fire room	1.44	1.42	1.33	1.42
	Adjacent room	1.91	1.94	1.93	1.94
Upper zone Temperature	Fire room	137.1	224.8	282.15	223.58
	Adjacent room	81.9	133.5	178.26	132.80
Lower zone Temperature	Fire room	43.6	61.6	73.01	62.79
	Adjacent room	23.2	26.1	27.18	26.26

Appendix 2 – Steady state measured temperature profiles

The steady state measurements from corner and centreline thermocouple trees are shown in tables 9-1 to 9-5 below. The steady state measurements were averaged from measurements taken every 5 seconds for 20 minutes after the runs had been going for 30 minutes.

Table A2-1 Measured temperature readings from corner thermocouple tree in fire compartment

	Fire	Height from floor level(m)															
Run	Size(kW)	0.035	0.185	0.335	0.485	0.635	0.785	0.935	1.085	1.235	1.385	1.535	1.685	1.835	1.985	2.135	2.285
1	112.2	21.2	19.8	19.9	21.8	21.0	20.7	21.4	21.1	20.1	20.6	21.3	24.9	27.1	75.4	121.6	123.4
2	168.13	21.1	18.8	18.8	21.3	19.9	19.5	20.4	20.4	19.3	20.1	21.0	26.3	30.3	104.9	156.2	158.7
3	168.18	22.0	20.4	20.6	23.1	21.7	21.2	22.0	21.6	20.4	21.0	22.1	26.7	30.8	99.0	149.8	152.3
4	55.36	18.3	17.9	18.3	19.6	19.1	19.0	19.5	19.0	18.2	18.5	19.0	21.2	22.1	37.7	81.8	83.8
5	55.33	21.9	21.7	22.2	23.8	23.6	23.5	24.3	23.8	22.9	23.2	23.8	26.1	27.4	57.4	85.6	87.0
6	168.14	24.3	23.1	23.6	26.6	25.3	24.5	25.4	24.8	23.2	23.7	24.7	29.5	34.4	114.1	151.5	153.4
7	112.1	28.9	27.7	28.2	31.2	30.2	29.7	30.9	30.6	29.1	29.7	30.6	34.7	36.7	50.5	151.6	153.6

Table A2-2 Measured temperature readings from corner thermocouple tree in adjacent compartment

	Fire	Height from floor level(m)															
Run	Size(kW)	0.165	0.315	0.465	0.615	0.765	0.915	1.065	1.215	1.365	1.515	1.665	1.815	1.965	2.115	2.265	
1	112.2	50.7	53.5	56.5	53.7	50.9	53.4	61.1	73.9	143.0	188.1	195.2	198.7	198.5	198.7	198.5	
2	168.13	63.5	68.1	72.0	67.6	62.8	66.6	77.2	97.1	199.6	253.3	261.7	266.7	266.5	266.9	266.1	
3	168.18	65.6	70.7	73.6	69.2	63.9	68.3	78.7	96.6	195.7	243.9	251.1	255.0	255.2	255.2	254.6	
4	55.36	32.8	34.4	35.6	34.7	33.0	34.9	38.4	43.8	79.4	121.2	126.3	127.8	127.9	127.5	127.3	
5	55.33	38.0	39.5	40.8	40.0	38.3	40.1	43.9	49.4	90.3	123.7	128.3	129.9	130.0	129.7	129.5	
6	168.14	70.7	74.8	77.8	74.4	68.8	72.8	83.7	103.3	205.8	248.5	255.1	259.5	259.2	259.1	258.3	
7	112.1	70.1	75.5	77.4	75.0	68.4	71.5	77.9	85.9	106.7	123.7	163.5	282.8	286.7	296.1	300.6	

Table A2-3 Measured steady state temperature readings for centreline thermocouple tree located 900mm from the front wall in the fire compartment

Run	Fire Size(kW)	Height from floor level(m) 0.3	0.6	0.9	1.1	1.35	1.56	1.81	2.06	2.11	2.16	2.21	2.26	2.31	2.335
1	112.2	66.6	58.5	72.0	73.2	139.8	190.6	199.7	203.1	204.5	204.3	206.4	206.4	204.7	203.3
4	55.36	43.6	42.4	51.3	56.0	81.7	122.8	128.9	130.6	131.5	131.4	131.9	132.3	131.7	131.0
6	168.14	89.7	80.4	94.3	97.2	197.8	250.4	259.3	263.2	264.5	263.6	265.1	266.4	264.0	261.6
7	112.1	65.9	103.3	120.0	140.0	142.9	158.8	235.6	285.7	293.4	299.0	300.5	306.1	306.4	308.0

Table A2-4 Measured steady state temperature readings for centreline thermocouple tree located 2700 mm from the front wall in the fire compartment

Run	Fire Size(kW)	Height from floor level(m) 0.3	0.6	0.9	1.1	1.35	1.54	1.79	2.04	2.09	2.14	2.19	2.24	2.29	2.315
1	112.2	39.5	74.2	79.1	102.3	149.1	162.0	171.8	181.1	183.9	186.0	187.2	191.1	194.2	195.1
2	168.13	47.5	91.1	101.6	132.9	186.4	209.2	227.3	244.9	248.9	252.5	255.0	260.9	266.2	266.7
3	168.18	45.6	89.5	102.8	141.3	189.8	205.1	218.4	232.3	235.9	239.0	240.4	244.8	249.0	249.7
4	55.36	31.3	49.3	50.0	62.7	95.1	106.9	113.0	117.0	118.1	119.1	119.5	121.3	123.5	124.5
5	55.33	33.9	54.4	56.1	70.0	103.3	109.9	114.9	118.4	119.5	120.6	121.0	122.5	124.7	125.5
6	168.14	59.0	94.3	109.9	152.3	198.5	212.7	224.8	238.1	241.9	244.9	246.4	249.4	254.2	254.8
7	112.1	60.5	81.5	80.4	99.2	120.1	142.9	236.4	278.6	281.6	284.3	288.5	287.1	286.7	278.7

Table A2-5 Measured steady state temperature readings for centreline thermocouple tree located 1800 mm from the middle wall in the adjacent compartment

	Fire	Height from floor level(m)													
Run	Size(kW)	0.3	0.6	0.9	1.1	1.35	1.54	1.79	2.04	2.09	2.14	2.19	2.24	2.29	2.315
1	112.2	18.6	22.9	22.7	26.2	27.1	18.0	30.9	64.4	70.8	78.2	90.0	113.8	135.4	138.6
2		17.4	22.0	21.5	26.4	28.4	19.5	34.7	81.8	91.1	102.6	120.0	154.6	184.6	187.8
3		18.1	23.0	21.9	26.1	28.4	19.2	37.1	82.1	90.5	100.5	116.3	147.2	173.3	176.2
4	55.36	17.4	21.3	20.6	22.5	23.0	16.6	22.6	44.7	48.8	52.6	58.7	71.3	84.3	87.2
5		21.1	25.6	25.2	27.0	27.6	23.6	26.5	52.9	56.5	60.1	65.9	76.9	88.7	91.3
6	168.14	20.9	27.9	23.7	27.1	30.3	25.0	47.1	91.4	99.0	108.3	122.8	151.1	175.0	177.6
7	112.1	25.9	30.4	31.2	36.2	38.7	34.9	39.4	57.2	61.0	62.0	74.6	124.5	182.5	190.5

Appendix 3 – interface height predictions and temperature averages

Tables A-8 to A-12 show the reduced interface heights and upper and lower zonal temperatures for each run for the specified corner thermocouple trees.

Table A3-1 Interface height and zonal temperature predictions from corner thermocouple tree in the fire compartment

	Run	1	2	3	4	5	6	7
	Fire Size	112.2	168.13	168.18	55.36	55.33	168.14	112.11
Interface Height prediction	Quintiere's	1.39	1.37	1.37	1.42	1.33	1.32	1.71
	Maximum slope	1.33	1.31	1.31	1.39	1.34	1.31	1.72
	N% - 10	0.00	0.00	0.00	0.00	0.00	0.00	0.00
	N% - 15	0.07	0.00	0.00	0.84	0.01	0.00	0.00
	N% - 20	1.02	0.06	0.04	1.09	0.99	0.00	1.07
Neutral plane height		1.01	0.95	0.99	1.01	1.01	0.99	0.84
Upper layer temperature	Quintiere's	197.0	264.4	253.3	126.8	125.5	252.7	293.0
	Emmons	209.5	285.1	270.8	137.0	134.6	273.5	431.3
	EOS	189.2	253.8	243.7	123.4	124.3	248.1	284.4
	Spatial averaging	189.8	254.5	244.2	123.5	124.6	248.4	282.3
	Janssens and Trans method	188.7	255.8	245.6	126.5	123.8	250.4	291.5
	Transport Terms	174.6	233.5	220.8	114.5	116.3	222.3	241.3
Lower layer temperature	Quintiere's	59.7	75.2	76.3	38.5	41.7	78.8	84.9
	Emmons	50.7	63.5	65.6	32.8	38.0	70.7	70.1
	EOS	58.1	73.1	74.5	38.4	42.7	79.3	86.9
	Spatial averaging	59.4	75.3	76.5	39.0	43.2	81.4	90.0
	Janssens and Trans method	58.4	76.0	77.4	37.1	46.7	82.1	88.5

Table A3-2 Interface height and zonal temperature predictions for corner thermocouples tree in the adjacent compartment

	Run	1	2	3	4	5	6	7
	Fire Size	112.2	168.13	168.18	55.36	55.33	168.14	112.11
Interface Height prediction	Quintiere's	2.02	2.00	2.01	2.06	1.90	1.91	2.07
	Maximum slope	1.98	1.96	1.96	2.04	1.98	1.94	2.05
	N% - 10	1.68	1.80	1.72	1.84	1.84	1.72	1.86
	N% - 15	1.84	1.85	1.84	1.88	1.86	1.84	1.93
	N% - 20	1.86	1.86	1.86	1.91	1.87	1.85	1.99
Upper layer temperature	Quintiere's	123.07	158.32	151.85	83.45	80.65	145.00	153.27
	Emmons	131.06	162.74	160.34	99.34	102.58	165.25	195.91
	EOS	111.85	142.71	137.01	78.23	79.83	139.63	144.41
	Spatial averaging	112.49	143.40	137.77	76.43	80.09	139.41	139.26
	Janssens and Trans method	106.78	139.96	133.71	82.78	76.64	139.70	152.59
Lower layer temperature	Quintiere's	23.73	23.91	25.09	20.58	24.21	26.77	32.66
	Emmons	21.18	21.14	22.01	18.31	21.90	24.33	28.90
	EOS	23.26	23.12	24.35	20.50	24.81	27.06	32.55
	Spatial averaging	23.55	23.89	25.01	20.94	24.95	27.96	33.68
	Janssens and Trans method	23.85	23.41	24.71	20.00	25.26	27.05	31.91

Table A3-3 Interface height and zonal temperature predictions for centreline thermocouple tree located 2700mm from front wall in fire compartment

	Run	1	2	3	4	5	6	7
	Fire Size	112.2	168.13	168.18	55.36	55.33	168.14	112.11
Interface height prediction	Quintiere's	1.16	1.35	1.21	1.22	1.18	1.22	1.65
	Maximum slope	1.20	1.21	1.17	1.22	1.20	1.15	1.69
	N% - 10	0.26	0.27	0.25	0.31	0.27	0.14	0.16
	N% - 15	0.34	0.35	0.33	0.40	0.35	0.24	0.33
	N% - 20	0.42	0.44	0.41	0.48	0.43	0.34	0.51
Neutral plane height		1.01	0.95	0.99	1.01	1.01	0.99	0.84
Upper layer temperature	Quintiere's	173.7	247.3	227.2	112.7	115.2	233.4	271.8
	Emmons	213.3	295.1	278.0	130.0	133.3	251.8	531.8
	EOS	167.8	221.1	212.5	109.4	112.0	214.3	262.4
	Spatial averaging	168.1	222.9	213.9	109.5	111.8	216.1	262.5
	Janssens and Trans method	173.1	244.1	232.3	112.4	118.8	216.7	277.0
	Transport Terms	174.6	233.5	220.8	114.5	116.3	222.3	241.3
Lower layer temperature	Quintiere's	55.0	77.4	69.4	40.7	43.8	82.3	84.7
	Emmons	39.5	47.5	45.6	31.3	33.9	59.0	60.5
	EOS	60.6	75.2	72.8	43.0	46.7	79.3	89.5
	Spatial averaging	64.4	81.0	78.4	44.6	48.4	82.7	94.3
	Janssens and Trans method	57.7	69.0	67.2	45.5	46.6	77.9	89.9

Table A3-4 Interface height and zonal temperature predictions for centreline thermocouple tree located 1800mm from middle wall in adjacent compartment

	Run	1	2	3	4	5	6	7
	Fire Size	112.2	168.13	168.18	55.36	55.33	168.14	112.11
Interface height prediction	Quintiere's	2.17	2.17	2.16	2.09	2.04	2.14	2.25
	Maximum slope	2.25	1.92	1.91	2.27	1.94	2.24	2.27
	N% - 10	1.60	1.65	1.57	1.60	0.09	0.93	1.04
	N% - 15	1.73	1.80	1.69	1.76	0.36	1.65	1.87
	N% - 20	1.83	1.86	1.81	1.84	1.78	1.74	1.99
Upper layer temperature	Quintiere's	131.4	178.5	168.0	71.3	73.3	170.2	189.5
	Emmons*	5004.0	-1534.3*	-1803.2	809.1	1379.4	-1404.4	-1731.1
	EOS	128.6	174.1	164.1	83.1	87.7	166.6	174.4
	Spatial averaging	129.2	175.1	164.9	83.5	88.0	167.3	175.2
	Janssens and Trans method	128.8	175.7	165.5	85.7	90.0	167.5	186.5
Lower layer temperature	Quintiere's	26.3	27.7	28.0	21.1	25.2	31.5	36.1
	Emmons	18.6	17.4	18.1	17.4	21.1	20.9	25.9
	EOS	29.0	31.3	31.7	24.1	29.0	35.8	37.0
	Spatial averaging	30.0	33.1	33.4	24.5	29.5	37.9	37.7
	Janssens and Trans method	29.0	31.3	31.6	24.0	28.9	35.8	36.8

*many of the temperatures predicted by Emmons method for this thermocouple tree are negative and thus void of any physical meaning. However they are still shown to demonstrate the methods inability to predict upper layer temperatures from an integral identity.

Table A3-5 Interface height and zonal temperature predictions for centreline thermocouple tree located 900mm from front wall in front compartment

	Run	1	4	6	7
	Fire Size	112.2	55.36	168.14	112.11
Interface height prediction	Quintiere's	1.40	1.42	1.37	1.72
	Maximum slope	1.32	1.40	1.29	1.71
	N% - 10	0.00	3.27	1.87	N/A
	N% - 15	0.00	1.82	1.48	N/A
	N% - 20	0.00	0.63	1.09	N/A
Neutral plane height		1.01	1.01	0.99	0.84
Upper layer temperature	Quintiere's	200.7	129.2	260.3	300.5
	Emmons	205.6	144.6	263.7	845.5
	EOS	191.3	125.8	248.2	274.5
	Spatial averaging	192.0	125.7	248.6	275.7
	Janssens and Trans method	193.7	129.2	253.2	293.8
	Transport Terms	174.6	114.5	222.3	241.3
Lower layer temperature	Quintiere's	74.1	50.9	98.4	104.4
	Emmons	66.6	43.6	89.7	65.9
	EOS	72.5	51.4	95.8	109.4
	Spatial averaging	73.8	52.3	98.5	115.5
	Janssens and Trans method	71.4	53.6	97.8	109.1

Appendix 4 – Two layer profiles for corner temperature measurements

Figure A4-1 A4-6 show the zonal temperature predictions using five different methods and showing C-Fast predictions for the runs that were not shown in the results section (chapter 6)

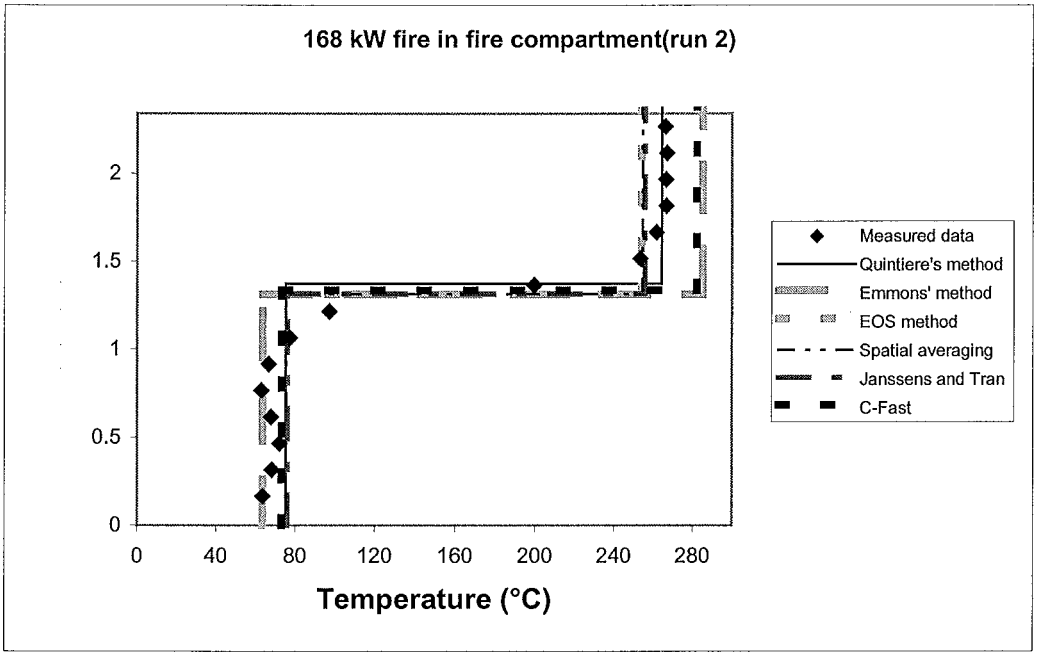

Figure A4-1 Comparison of averaging methods in fire compartment for 168kW fire (run 2)

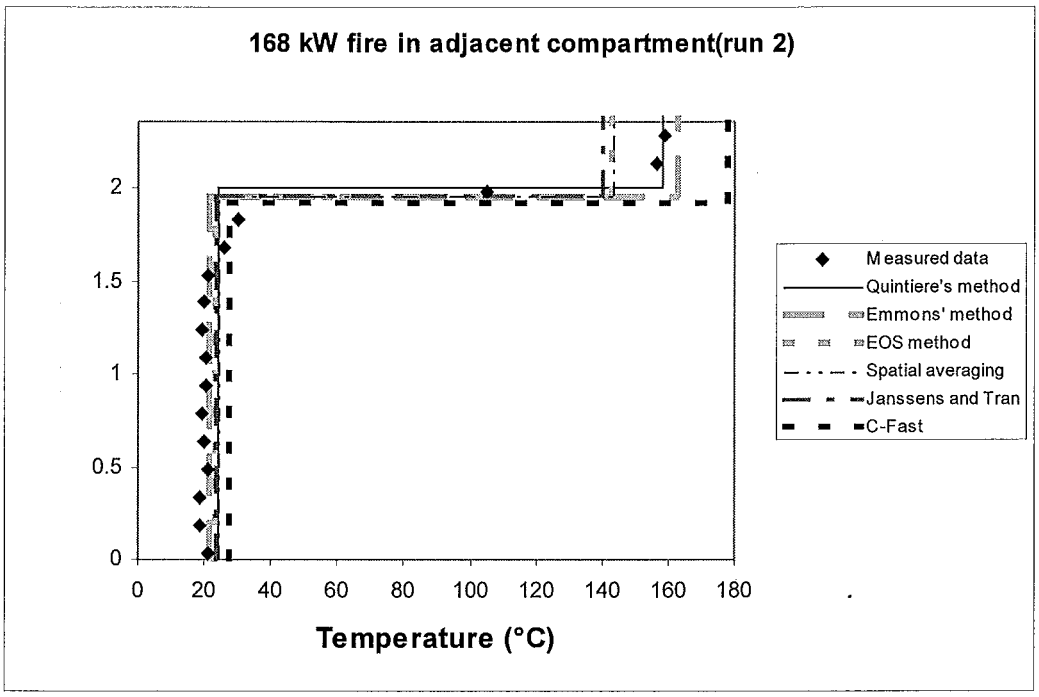

Figure A4-2 Comparison of averaging methods in adjacent compartment for 168kW fire (run 2)

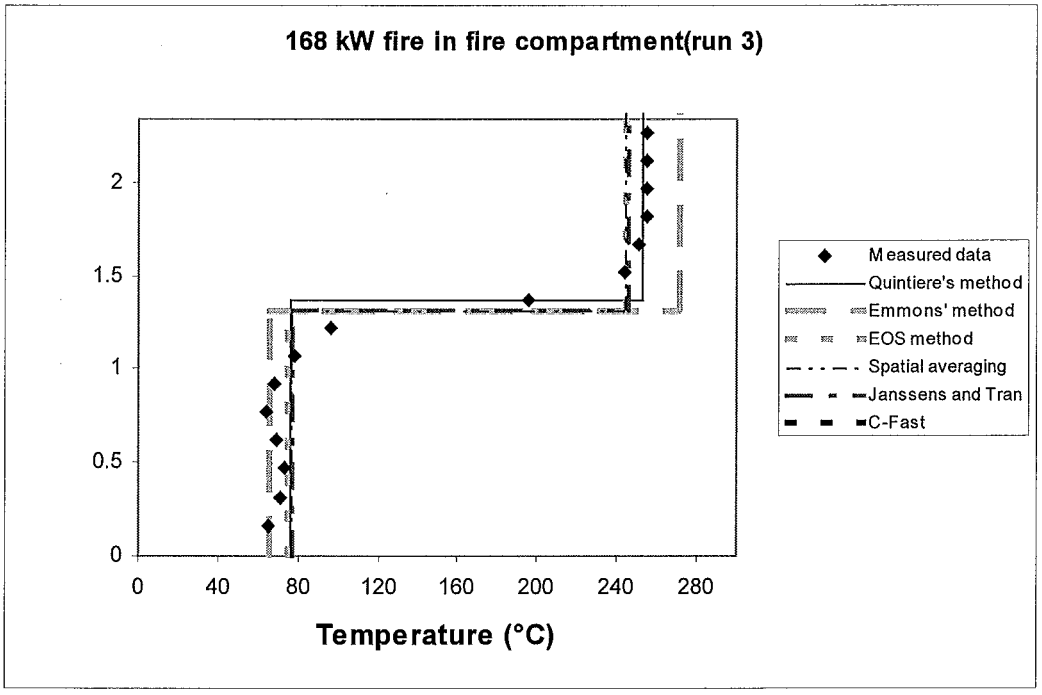

Figure A4-3 Comparison of averaging methods in fire compartment for 168kW fire (run 3)

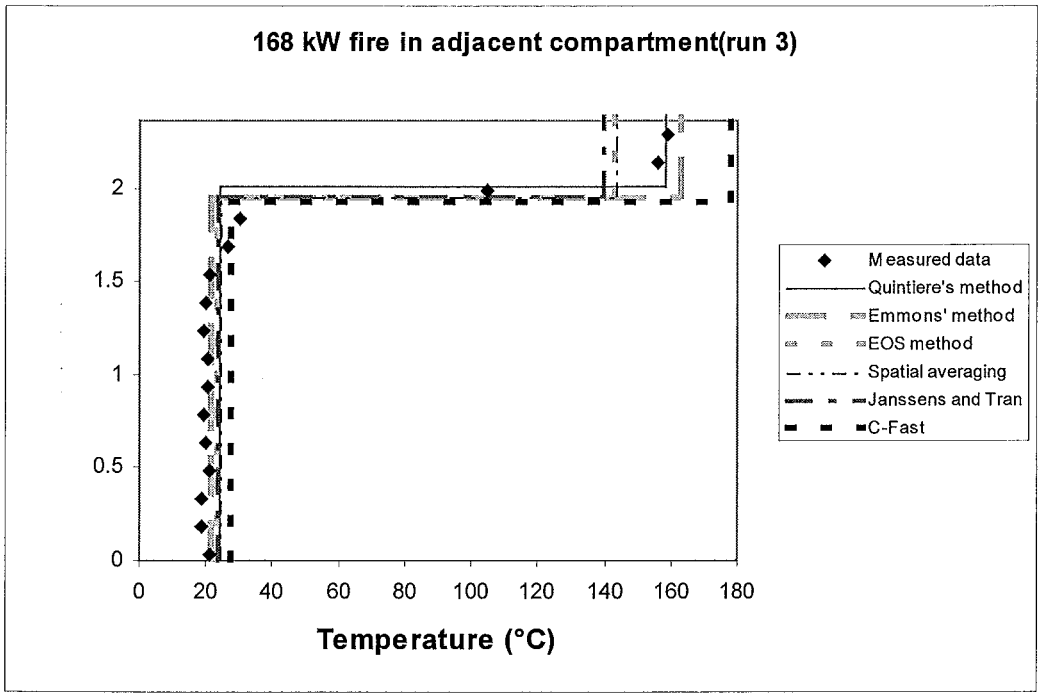

Figure A4-4 Comparison of averaging methods in adjacent compartment for 168kW fire (run 3)

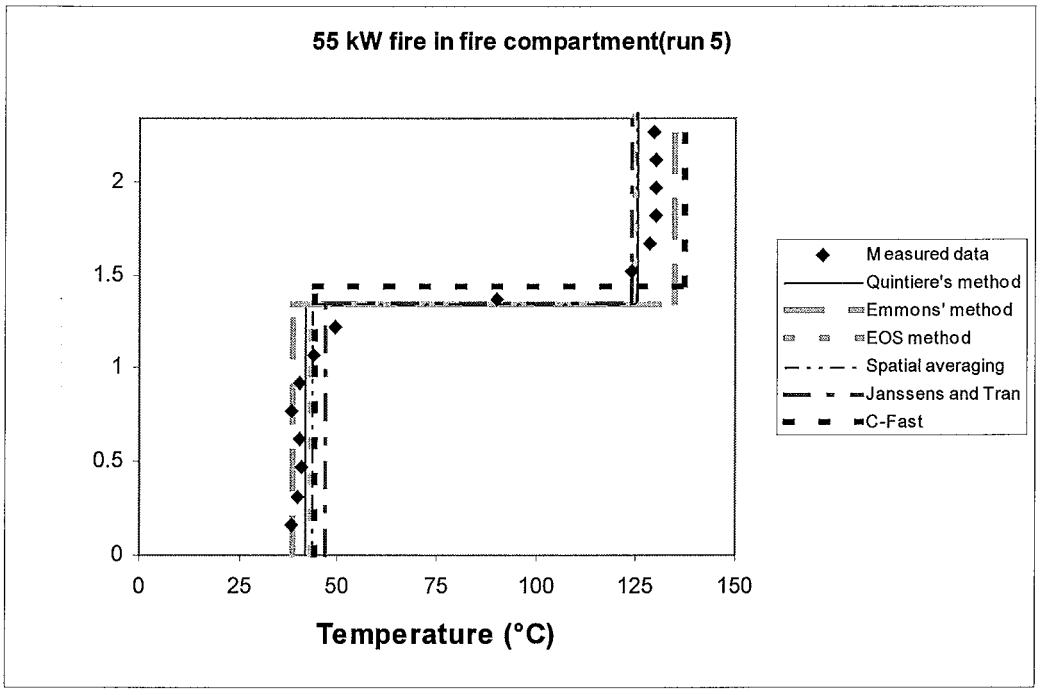

Figure A4-5 Comparison of averaging methods in fire compartment for 55kW fire(run 5)

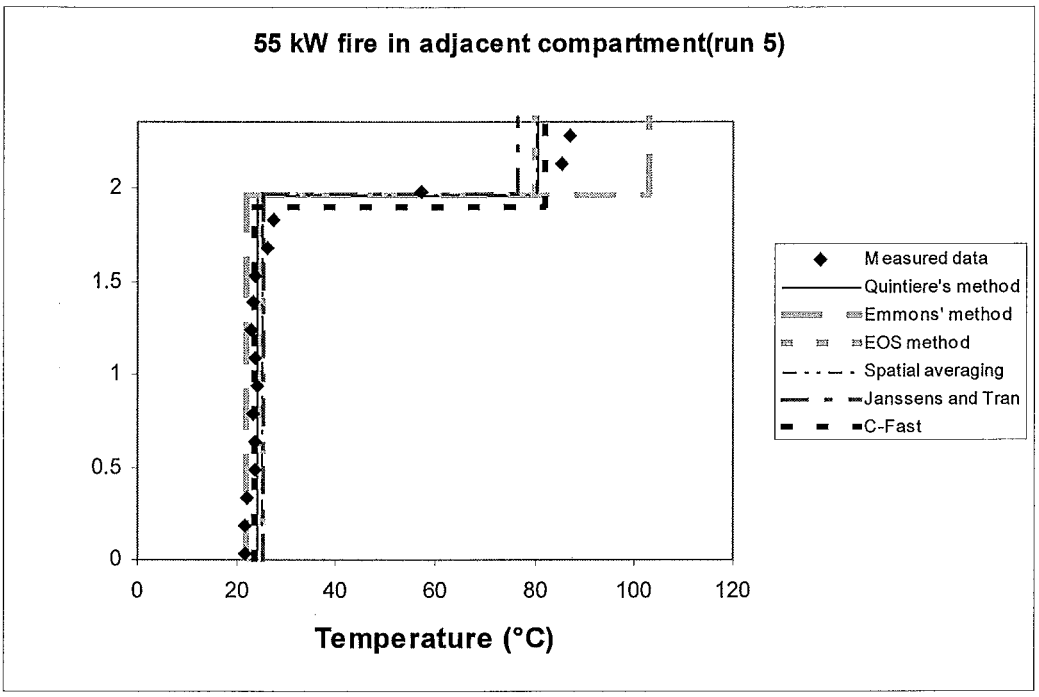

Figure A4-6 Comparison of averaging methods in adjacent compartment for 55kW fire (run 3)

Appendix 5 – Two layer profiles for centreline temperature measurements.

Fiigures A7 to A12 show the two layer temperature profiles predicted using 5 different temperature averaging methods for the centreline trees located 900mm and 2700mm from the front of the fire compartment and the centreline tree located 1800mm from the front of the adjacent compartment. The fire sizes shown are 55kW and 168kW. The results with a 112kW fire size can be seen in the results section (chapter 6)

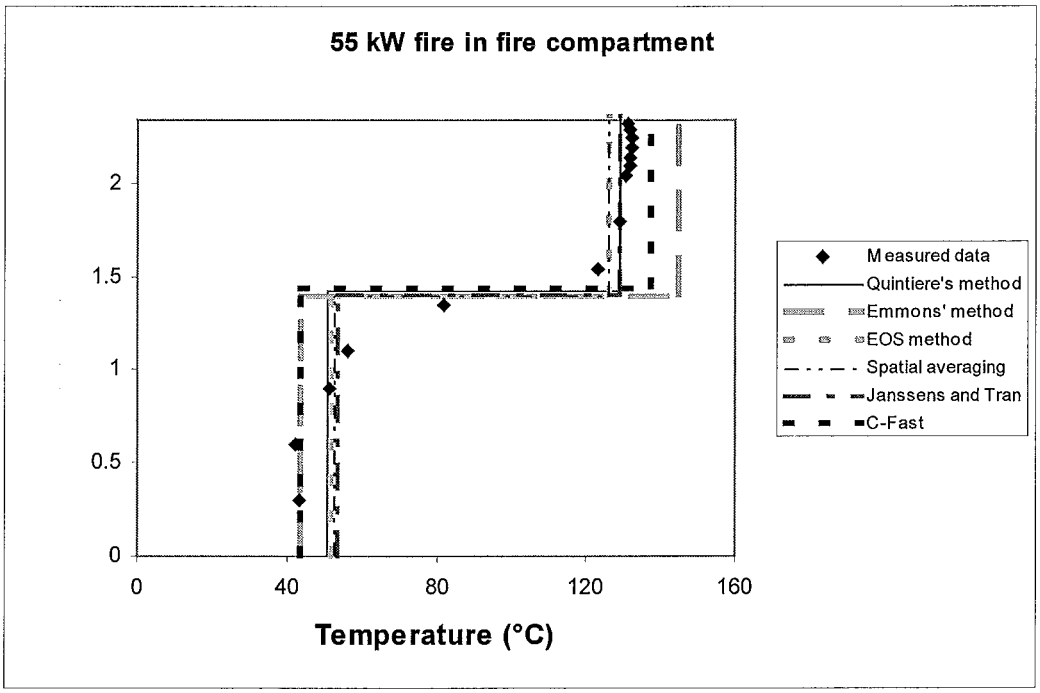

Figure A5-1 Comparison of averaging techniques using centreline thermocouple tree located 900mm from front in fire compartment during 112kW fire

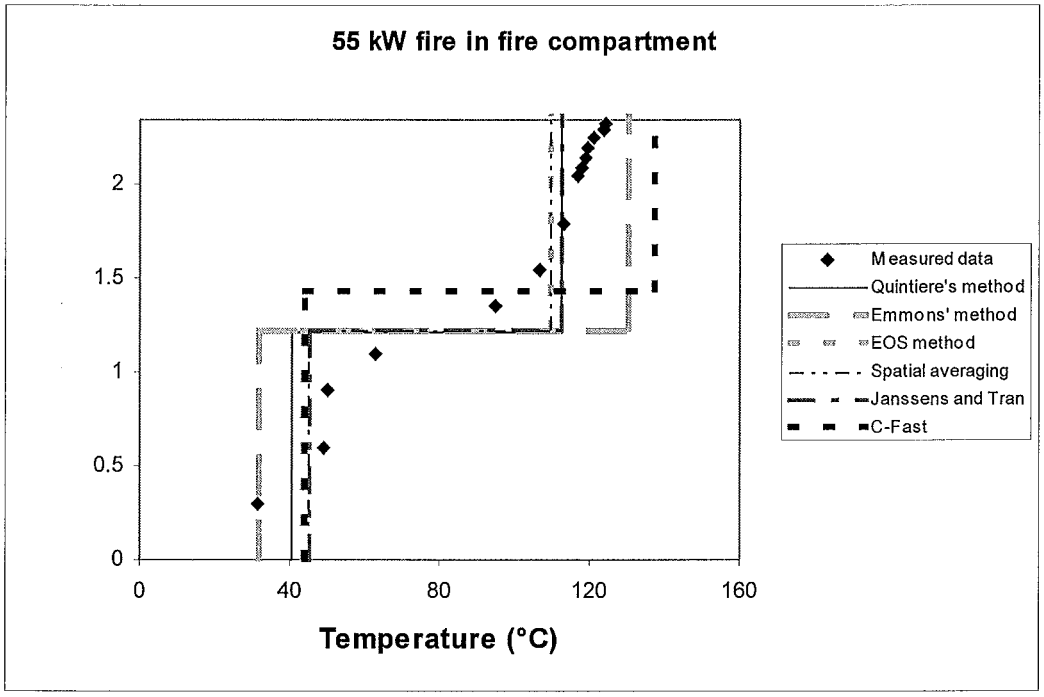

Figure A5-2 Comparison of averaging techniques using centreline thermocouple tree located 900mm from front in fire compartment during 112kW fire

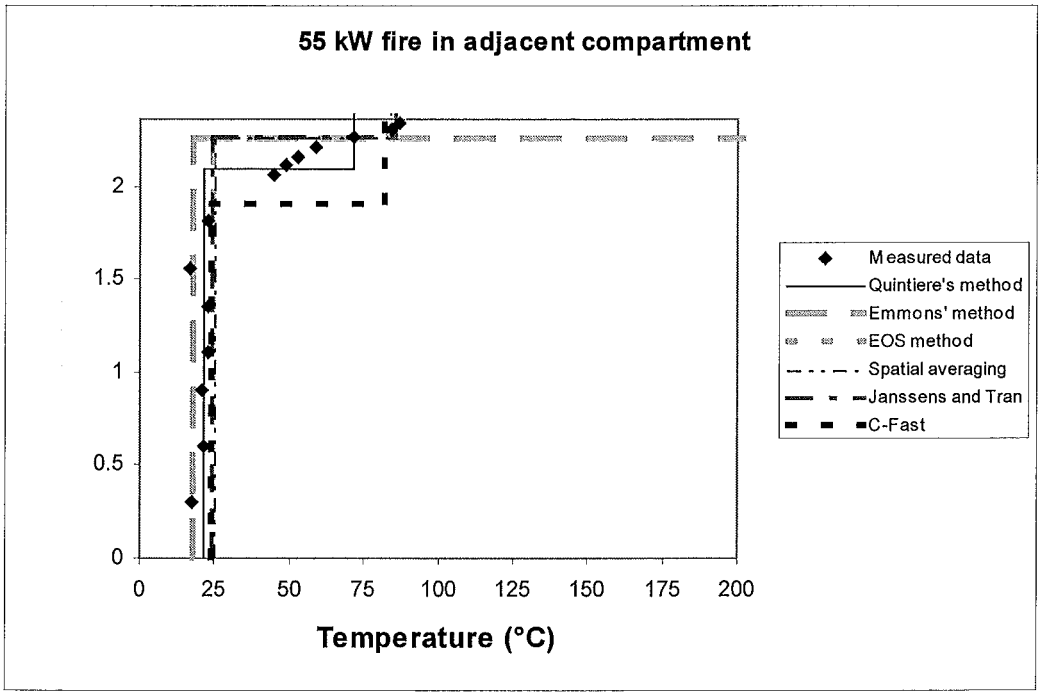

Figure A5-3 Comparison of averaging techniques using centreline thermocouple tree located 900mm from front in fire compartment during 112kW fire

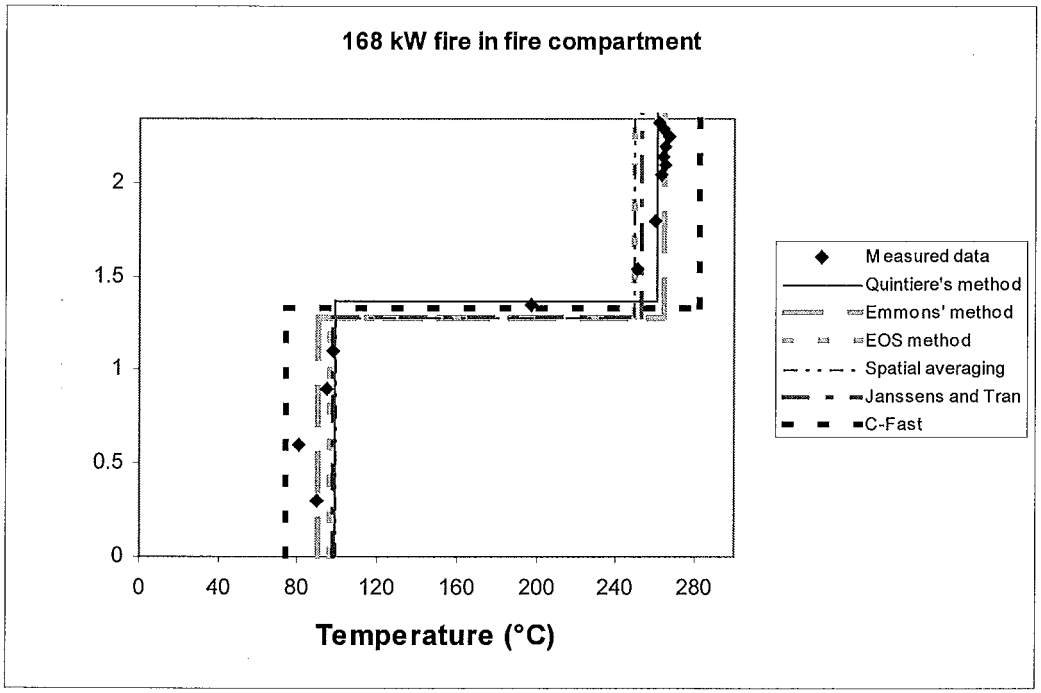

Figure A5-4 Comparison of averaging techniques using centreline thermocouple tree located 900mm from front in fire compartment during 112kW fire

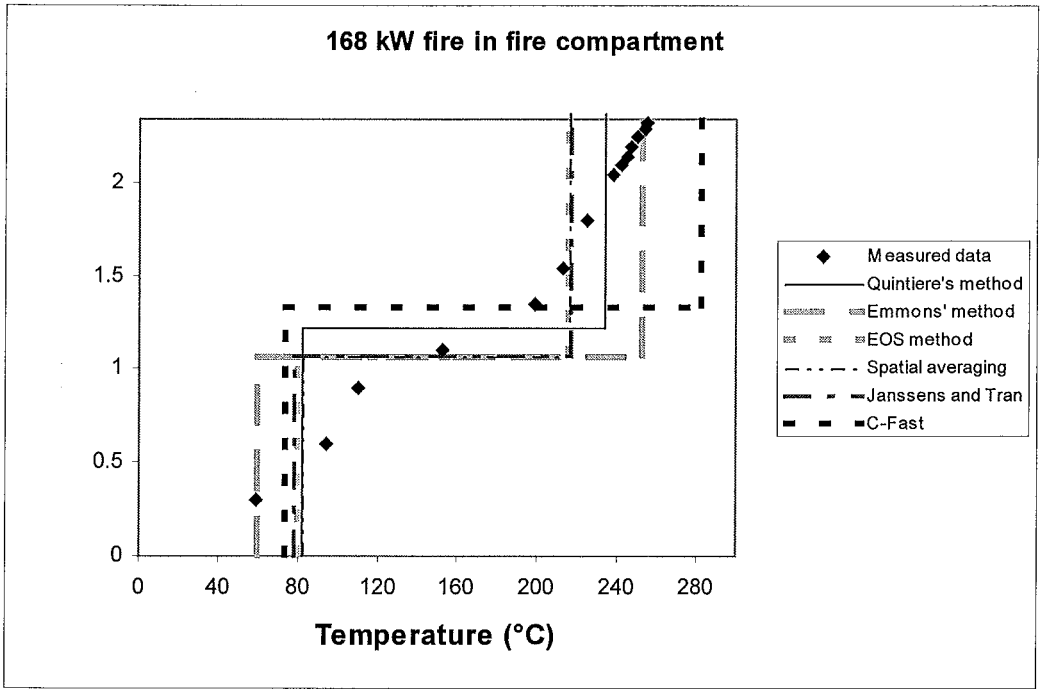

Figure A5-5 Comparison of averaging techniques using centreline thermocouple tree located 900mm from front in fire compartment during 112kW fire

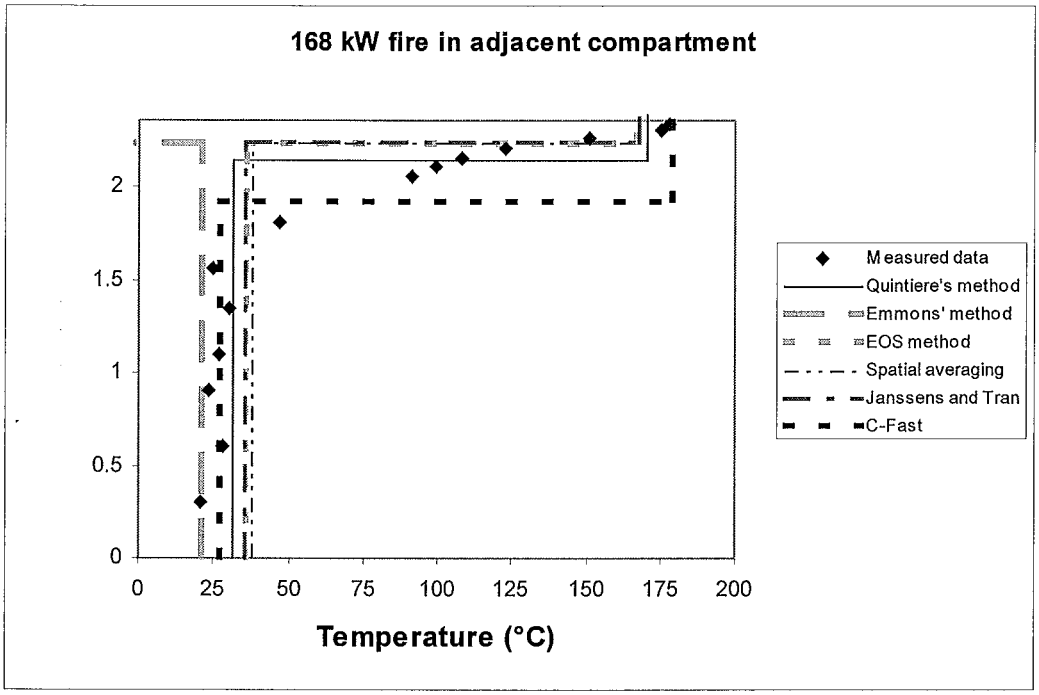

Figure A5-6 Comparison of averaging techniques using centreline thermocouple tree located 900mm from front in fire compartment during 112kW fire

Appendix 6 – Two layer profiles using interface layer method.

Figures A-14 to A-17 show the predicted two layer temperature profiles using the interface layer method for determining the interface heights used in the averaging techniques. Two fire sizes are shown 55kW, and 168kW. The graphs of the 112kW fire for both compartments are shown in the results section.

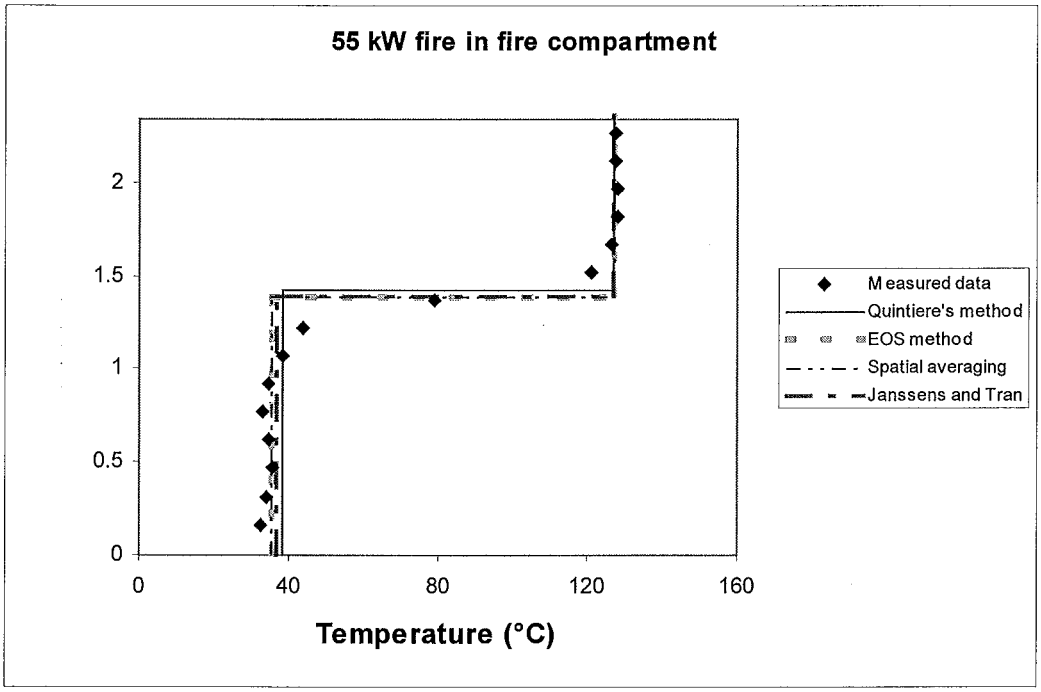

Figure A6-1 Temperature prediction based on an interface layer in fire compartment using corner thermocouple tree for 55kW fire..

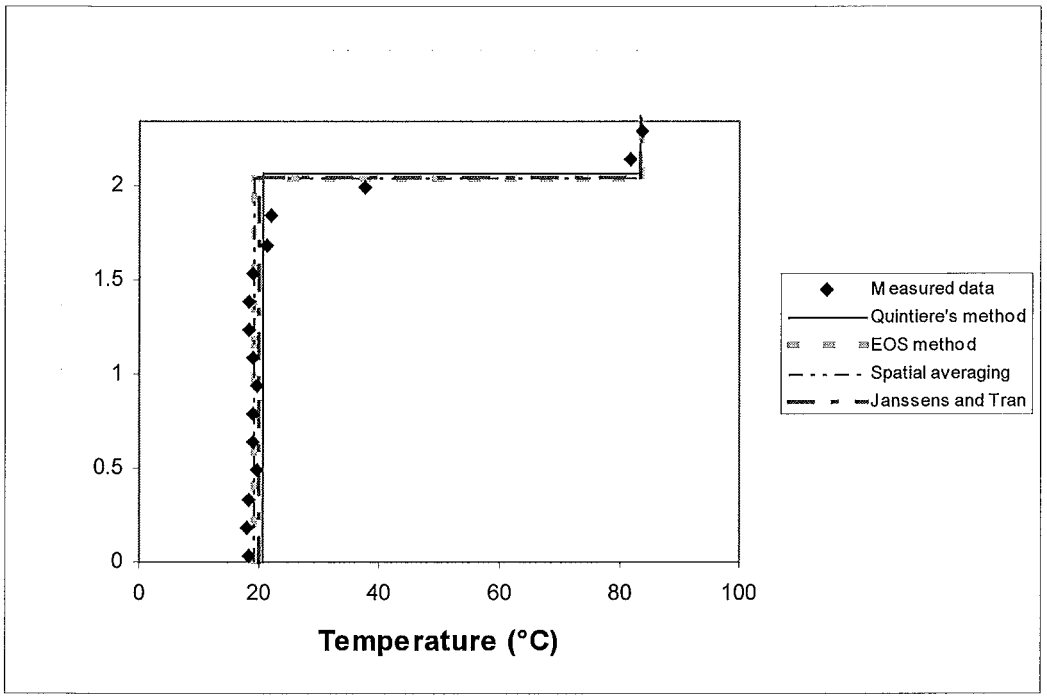

Figure A6-2 Temperature prediction based on an interface layer in the adjacent compartment using corner thermocouple tree for 55kW fire..

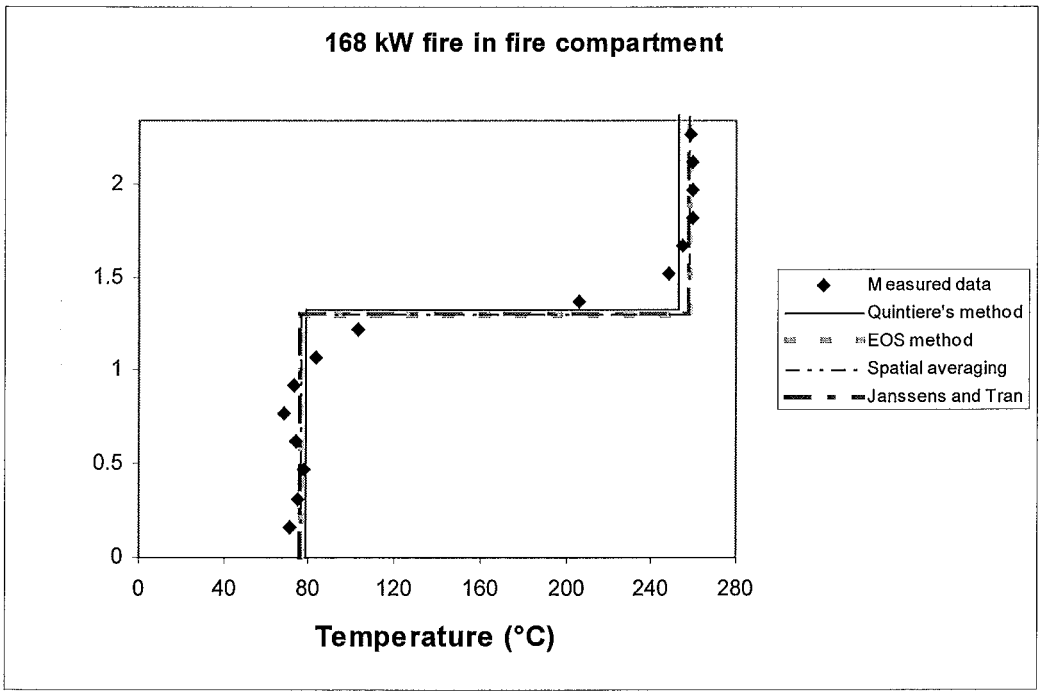

Figure A6-3 Temperature prediction based on an interface layer in the fire compartment using corner thermocouple tree for 168kW fire..

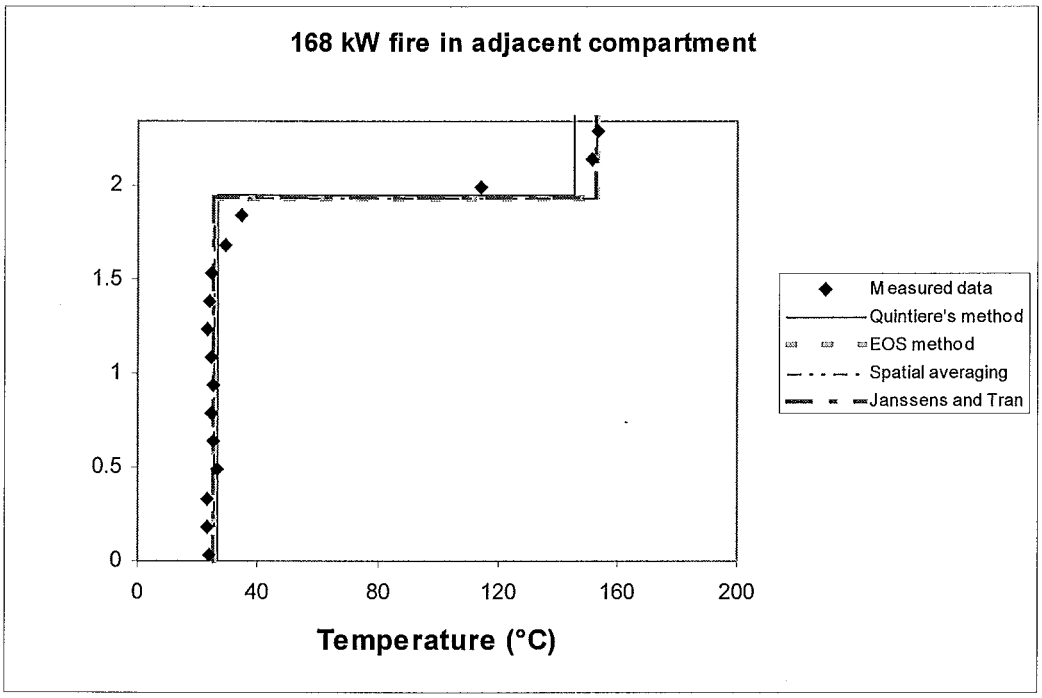

Figure A6-4 Temperature prediction based on an interface layer in the adjacent compartment using corner thermocouple tree for 168kW fire

FIRE ENGINEERING RESEARCH REPORTS

95/1	Full Residential Scale Backdraft	I B Bolliger
95/2	A Study of Full Scale Room Fire Experiments	P A Enright
95/3	Design of Load-bearing Light Steel Frame Walls for Fire Resistance	J T Gerlich
95/4	Full Scale Limited Ventilation Fire Experiments	D J Millar
95/5	An Analysis of Domestic Sprinkler Systems for Use in New Zealand	F Rahmanian
96/1	The Influence of Non-Uniform Electric Fields on Combustion Processes	M A Belsham
96/2	Mixing in Fire Induced Doorway Flows	J M Clements
96/3	Fire Design of Single Storey Industrial Buildings	B W Cosgrove
96/4	Modelling Smoke Flow Using Computational Fluid Dynamics	T N Kardos
96/5	Under-Ventilated Compartment Fires - A Precursor to Smoke Explosions	A R Parkes
96/6	An Investigation of the Effects of Sprinklers on Compartment Fires	M W Radford
97/1	Sprinkler Trade Off Clauses in the Approved Documents	G J Barnes
97/2	Risk Ranking of Buildings for Life Safety	J W Boyes
97/3	Improving the Waking Effectiveness of Fire Alarms in Residential Areas	T Grace
97/4	Study of Evacuation Movement through Different Building Components	P Holmberg
97/5	Domestic Fire Hazard in New Zealand	KDJ Irwin
97/6	An Appraisal of Existing Room-Corner Fire Models	D C Robertson
97/7	Fire Resistance of Light Timber Framed Walls and Floors	G C Thomas
97/8	Uncertainty Analysis of Zone Fire Models	A M Walker
97/9	New Zealand Building Regulations Five Years Later	T M Pastore
98/1	The Impact of Post-Earthquake Fire on the Built Urban Environment	R Botting
98/2	Full Scale Testing of Fire Suppression Agents on Unshielded Fires	M J Dunn
98/3	Full Scale Testing of Fire Suppression Agents on Shielded Fires	N Gravestock
98/4	Predicting Ignition Time Under Transient Heat Flux Using Results from Constant Flux Experiments	A Henderson
98/5	Comparison Studies of Zone and CFD Fire Simulations	A Lovatt
98/6	Bench Scale Testing of Light Timber Frame Walls	P Olsson
98/7	Exploratory Salt Water Experiments of Balcony Spill Plume Using Laser Induced Fluorescence Technique	E Y Yii
99/1	Fire Safety and Security in Schools	R A Carter
99/2	A Review of the Building Separation Requirements of the New Zealand Building Code Acceptable Solutions	J M Clarke
99/3	Effect of Safety Factors in Timed Human Egress Simulations	K M Crawford
99/4	Fire Response of HVAC Systems in Multistorey Buildings: An Examination of the NZBC Acceptable Solutions	M Dixon
99/5	The Effectiveness of the Domestic Smoke Alarm Signal	C Duncan

99/6	**Post-flashover Design Fires**	**R Feasey**
99/7	**An Analysis of Furniture Heat Release Rates by the Nordtest**	**J Firestone**
99/8	**Design for Escape from Fire**	**I J Garrett**
99/9	**Class A Foam Water Sprinkler Systems**	**D B Hipkins**
99/10	**Review of the New Zealand Standard for Concrete Structures (NZS 3101) for High Strength and Lightweight Concrete Exposed to Fire**	**M J Inwood**
99/12	**An Analytical Model for Vertical Flame Spread on Solids: An Initial Investigation**	**G A North**
99/13	**Should Bedroom Doors be Open or Closed While People are Sleeping? - A Probabilistic Risk Assessment**	**D L Palmer**
99/14	**Peoples Awareness of Fire**	**S J Rusbridge**
99/15	**Smoke Explosions**	**B J Sutherland**
99/16	**Reliability of Structural Fire Design**	**JKS Wong**
00/1	**Fire Spread on Exterior Walls**	**FNP Bong**
00/2	**Fire Resistance of Lightweight Framed Construction**	**PCR Collier**
00/3	**Fire Fighting Water: A Review of Fire Fighting Water Requirements (A New Zealand Perspective)**	**S Davis**
00/4	**The Combustion Behaviour of Upholstered Furniture Materials in New Zealand**	**H Denize**
00/5	**Full-Scale Compartment Fire Experiments on Upholstered Furniture**	**N Girgis**
00/6	**Fire Rated Seismic Joints**	**M James**
00/7	**Fire Design of Steel Members**	**K R Lewis**
00/8	**Stability of Precast Concrete Tilt Panels in Fire**	**L Lim**
00/9	**Heat Transfer Program for the Design of Structures Exposed to Fire**	**J Mason**
00/10	**An Analysis of Pre-Flashover Fire Experiments with Field Modelling Comparisons**	**C Nielsen**
00/11	**Fire Engineering Design Problems at Building Consent Stage**	**P Teo**
00/12	**A Comparison of Data Reduction Techniques for Zone Model Validation**	**S Weaver**
00/13	**Effect of Surface Area and Thickness on Fire Loads**	**H W Yii**

School of Engineering
University of Canterbury
Private Bag 4800, Christchurch, New Zealand

Phone 643 364-2250
Fax 643 364-2758